DESIGN, SYNTHESIS AND CHARACTERIZATION OF INDENOFLUORENE AND INDENOFLUORENONE DERIVATIVES

by

Tayebeh Hadizad, M.Sc.

A thesis submitted to

The Faculty of Graduate Studies and Research

In partial fulfillment of the requirements for the degree of

Doctor of Philosophy

The Department of Chemistry

Carleton University

Ottawa, ON Canada

March 2007

Your file Votre référence
ISBN: 978-0-494-33491-1
Our file Notre référence
ISBN: 978-0-494-33491-1

ABSTRACT

In the past decade, fluorene-based compounds (oligomers and polymers) have emerged as a very promising class of blue-light emitting materials for use in light emitting diodes. The electronic and optical properties arise from fluorene molecule's planarity. It is then hypothesized that the structurally related compound, indenofluorene, should have some unique electronic and optical characteristics, compared to the fluorenes, due to the presence of the three planarized phenylene rings and longer conjugation length. The overall objectives of this thesis include (i) to establish a new synthetic route to a series of indenofluorene derivatives and study their electrical and optical properties, (ii) to explore applications in organic thin-film transistors, organic light emitting diodes and photovoltaic cells and (iii) to design and synthesize a donor-acceptor type of polymers using indenofluorenone as an acceptor.

A new series of 2,6-disubstituted indenofluorenes containing thienyl, naphthyl and phenyl rings was successfully synthesized. A general route to indenofluorenes involves the Suzuki coupling reaction and the use of 2,6-dibromoindenofluorene as a key compound. The final products were obtained in high purity via vacuum sublimation. Among all, 2,6-diphenylindenofluorene formed single crystals during the sublimation and its structure was determined by X-ray crystallography. The potential of these conjugated indenofluorenes as new organic semiconductors was demonstrated by the light-emitting diode reaching a luminance of 1400 Cd/m^2 below 10 V.

A series of a donor-acceptor type of small molecules was designed and synthesized in which indenofluorenone was used as an acceptor. 2,6-Dibromoindenofluorenone was the key compound for the synthesis of this series, which

was successfully synthesized via three alternative routes. The UV absorption and PL emission of these indenofluorenone compounds showed a significant red shift compared with indenofluorene derivatives.

The polymerization of two dibromide monomers, 2,5-bis(4-bromophenyl)terephthalate and 2,5-dibromoterephthalate with 9,9-dioctylfluorene-2,7-bis(trimethyleneborate) and 4,4`-bis(4,4,5,5-tetramethyl-1,3,2-dioxaborolane-2-yl)- N-hexyldiphenylamine afforded a series of four polymers with moderate to high molecular weight. Post-polymerization treatment with concentrated sulfuric acid led to the formation of indenofluorenone derivatives of the polymers, which displayed a red shift in their absorption and emission spectra.

ACKNOWLEDGMENTS

I would like to express my gratitude to my supervisor, Dr. Wayne Wang whose expertise, stimulating suggestions, encouragement and patience, added considerably to my graduate experience and also provided a good basis for the present thesis.

My warm thanks are due to Dr. Jane Gao and all the colleagues in the laboratory. Over the past four and a half years, during the journey of Ph.D. study, I made many good friends whose support and help made this journey possible. Specially, I would like to thank Jidong Zhang, Yuxing Cui, Shidi Xun, Xianzhen Li, Xianguo Wu, Xun Sun, Gaetan LeClair, Wendy Hao, Ying Xiong, Hongding Tang, Majid Rastegar, Erin Todd, Cristina Badarau, Andrew Beaudin, Yaowen Bai, and Naiheng Song.

I would also like to thank the dedicated support staff of Chemistry Department of Carleton University. Among them, my special thanks go to Keith Bourque, Tony O'Neil and Jim Logan. As well, I extend my sincere appreciation to the CNS secretarial staff Sheila Thayer and Marilyn Stock for their support.

Lastly, and most importantly, I wish to thank all my family members for providing a loving and caring environment throughout my entire life. I thank my lovely mother who has been offering her constant support and encouragement and also my late father who had always motivated me to pursue graduates studies. Without them, I would not have finished this thesis. I thank my dear brother who has always been source of all kinds of support particularly during the thesis work and writing. Finally, I would like to offer special thanks to my late sister who had suffered from a lung cancer during her last

year of life but chose not to disclose it to me earlier so as not to affect my Ph.D. studies. To this wonderful family of mine, hereby, I dedicate this thesis.

Table of Contents

List of Tables

List of Figures

List of Schemes

List of Symbols and Abbreviations

OLED	Organic light-emitting device
AlQ3	Tris(8-hydroxyquinolinolato) aluminum
PPV	Polyphenylenevinylene
HTL	Hole-transport layer
ETL	Electron-transport layer
HOMO	Highest occupied molecular orbital
LUMO	Lowest unoccupied molecular orbital
OVPD	Organic vapor phase deposition
SMS	Semiconductor-metal-semiconductor
PBTs	Permeable-base transistors
ITO	Indium-tin oxide
PEDOT/PSS	Poly(3,4-ethylenedioxythiophene)-poly(styrene)
NPB	N,N′-diphenyl-N,N′-bis-(1-naphthyl)-1,1′-biphenyl-4,4′-diamine
DEQ	N,N′-diethylquinacridone
RGB	Red-Green-Blue
$Pd(PPh_3)_4$	Terakis(triphenylphosphine)Palladium(0)
$Pd(OAc)_2$	Palladium acetate
IR	Infrared spectroscopy
MS, HRMS	Low and high-resolution mass spectroscopy
NMR	Nuclear magnetic resonance
DSC	Differential Scanning Calorimetry

EI	Electron impact
ORTEP	Oak Ridge thermal ellipsoid plot
TGA	Thermogravimetric analysis
T_d	Decomposition temperatures
T_c	Crystallization temperature.
DME	1,2-Dimethoxyethane
TLC	Thin layer chromatography
TCE	Tetrachloroethane
NMP	N-Methyl-2-pyrolidinone
TFTs	Thin-film transistors
CV	Cyclic voltammetry
CuPc	Copper phthalocyanine
C60	Fullerene
PBD	2-(4-biphenylyl)-5-phenyl-1,3,4-oxadiazole
UV- Vis	Ultra violet- Visible
PL	Photoluminescence
EL	Electroluminescence
I_E	Emitter current
I_C	Collector current
DMF	Dimethylformamide
λ	Wavelength
E_g	Band gap
Φ	Quantum yield

$\Im$	Integrated area of emission peak
AFM	Atomic force microscope
PMMA	Poly(methyl mathacrylate),
D-A	Donor-Acceptor
EDOT	3,4-(Ethylenedioxythiophene)
ESI	Electrospray ionisation
DABCO	1,4-Diazabicyclo[2,2,2]octane
THF	Tetrahydrofuran
TBPBr	Tetrabutylphosphonium bromide
TBABr	Tetrabutylammonium bromide
T_g	Glass transition temperatures
T_m	Melting point
E_{OX}	Oxidation potential
E_{red}	Reduction potential

List of Publications

1. Hadizad, T.; Zhang, J.; Wang, Z. Y.; Gorjanc, T. C.; Py, C. *Org. Lett.* **2005**, *7*, 795.
2. Hadizad, T.; Zhang, J.; Yan, D.; Wang, Z. Y.; Serbena, J. P. M.; Meruvia, M. S.; Hummelgen, I. A. *J. Mater. Sci: Mater. Electron.* Accepted: 25 October **2006**.
3. Py, C.; Gorjanc, T. C.; Hadizad, T.; Zhang, J.; Wang, Z. Y. J. *Vac. Sci. Technol. A.* **2006**, *24*, 654.
4. Serbena, J. P. M.; Hummelgen, I. A.; Hadizad, T.; Wang, Z. Y. *Small* **2006**, *2*, 372.

Chapter I

Introduction

I.1. Organic Light-Emitting Diodes

Organic electroluminescence (EL) is the electrically driven emission of light from non-crystalline organic materials. In 1965, it was discovered that single crystals of anthracene could be made to emit light when provided with proper electrodes and external bias.[1] The first organic light-emitting devices (OLED) failed to attract attention because they required very high operating voltages. Difficulties of producing large anthracene single crystals also made them unsuitable for practical applications. In the next two decades, devices based on evaporated amorphous anthracene films were demonstrated,[2] but their light output decayed in a few minutes. In 1987, a team in Kodak fabricated a high performance device using the double-layer organic light-emitting diodes.[3] The device structure was based on tris(8-hydroxyquinoline) aluminum (AlQ3), an emitter and electron transport material, and a hole transport material (tertiary amine). This device was made by the combination of modern thin film deposition techniques (vacuum evaporation of organic small-molecules) and a metallic cathode on a conductive substrate to give moderately low bias voltages, and half-life of hundreds of hours.[4] Soon after, a variety of organic materials had been developed as luminescent materials including small molecular systems and π-conjugated polymers. In 1990, the Cambridge group announced the observation of electroluminescence in a single-layer device of polyphenylenevinylene (PPV).[5] These two developments opened the door for a new technology of organic light-emitting devices. The two directions of small molecule and polymer based OLEDs, in many respects, developed independently. But recently, the gap between them has significantly narrowed and it seems that both approaches are feasible for practical applications.

The basic structure of an organic EL device consists of one or more organic thin films (total thickness of less than 0.2 μm) deposited in between two electrodes, at least one of which is transparent. The simplest device configuration, consisting of a typical electrode/emitter/electrode sandwich structure, is depicted in Figure I.1.

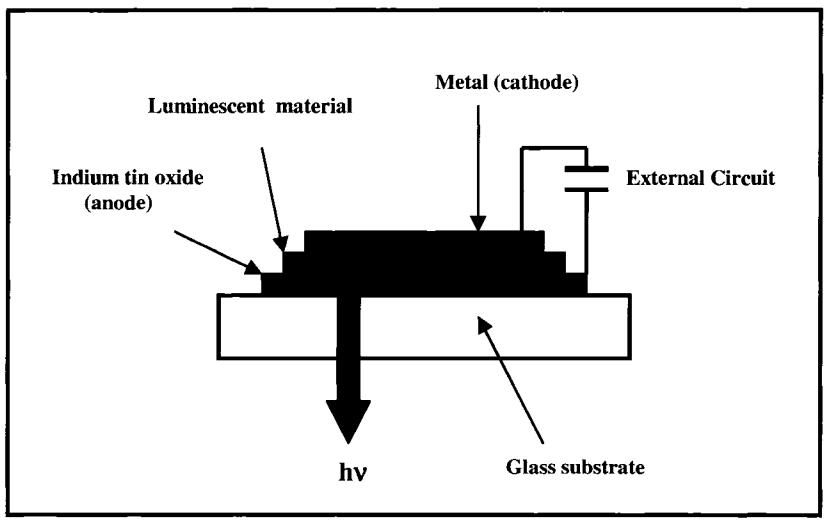

Figure I.1. Structure of a simple device configuration for an organic LED

In a basic two-layer OLED structure, one organic layer is specifically chosen to transport holes and the other organic layer is specifically chosen to transport electrons. The interface between the two layers provides an efficient site for the recombination of the injected hole-electron pair and resultant electroluminescence.

The typical cell structure for a multiplayer OLED device is: an anode (indium tin oxide on glass substrate) / a hole-transporting layer / a light-emitting layer / an electron transporting layer / a cathode (a low work function metal). For most designs, the electron transporting compound is also the emitter. When an electrical potential difference is applied between the anode and the cathode, injection of holes occurs from the anode (positive electrical potential) into the hole-transport layer (HTL), while electrons are

injected from the cathode (negative electrical potential) into the electron-transport layer (ETL).[6] The injected holes and electrons migrate toward the oppositely charged electrode until they meet. The energetic electrons can drop into the holes, which release their excess energy as light, which is emitted from the light-transmissive anode and substrate.[7]

In order to facilitate hole-injection from the HTL into the ETL, the heterojunction should be designed. The HOMO of the HTL should be slightly above that of the ETL, so that holes can readily enter into the ETL, while the LUMO of the ETL has to be significantly below that of the HTL, so that electrons will be trapped in the ETL.

Although inorganic materials have dominated the field of electroluminescence in the last twenty-five years, the organic materials attracted more attention because of their high photoluminescence quantum yields and excellent color gamut.[5] Both small molecules and polymer-based organic devices have been investigated, but polymer-based devices have the advantage of simple fabrication by spin coating methods.[8] While small molecule devices are usually fabricated by thermal evaporation techniques in vacuum such as "organic vapor phase deposition (OVPD)", in a low cost useful for large scale deposition of small molecules.[9]

The design of EL materials for used in OLEDs is critical to device performance. Charge injection and transport are the limiting factors in determining operating voltage and luminance efficiency. In OLEDs, the hole current is limited by injection, and the electron current is strongly influenced by the presence of traps owing to metal-organic interactions. The energy barrier for injection of electrons has been controlled by employing an efficient electron-injecting metal as the cathode and the use of appropriate surface treatments of anodes.[10] In order to lower the operation voltage of the devices, an

specific attention should be paid to match the work functions of the electrodes and either the highest occupied molecular orbital (HOMO) or the lowest unoccupied molecular orbital (LUMO) of the layer materials.[11] The charge mobility as well as charge blocking capabilities of the materials are also very important for the effective recombination of electrons and holes for a high quantum yield in the device.[12]

A high purity for all materials is essential in order to have a good device performance since impurities quench the excitons. The stability of the devices can be improved by stripping off oxygen and moisture.[13]

The device operational lifetime is also one of the most critical performance characteristics for OLEDs to be considered since continuous operation of OLEDs generally leads to a steady loss of efficiency and a gradual rise in bias voltages.

I.2. Organic Transistors

In addition to OLED application, organic-based transistors in various architectures are constantly aimed for performance improvement, since transistors are largely used in current switching and amplifying electronic devices. One transistor architecture potentially favorable for fast switching was proposed more than 40 years ago,[14, 15] but initially suffered from low performance and associated complex production technology. These semiconductor-metal-semiconductor (SMS) devices presented an important advantage allowing construction in vertical architecture, by simply stacking the device active layers, envisaging larger device integration and lower paths for charge carriers transit between device emitter and collector, or emitter and base. The all-inorganic SMS devices were developed and at least three derivatives are currently

investigated: metal-base transistors, permeable-base transistors and static-induction transistors, which differ by the absence/presence and dimensions of pinholes in the metallic base.[16]

SMS transistors are conceptually simple, comprising a thin metal base located between two semiconductors layers, the emitter and collector. Despite being conceptually simple, their fabrication remains a challenge, requiring sophisticated techniques such as ultrahigh-vacuum deposition and annealing.

In permeable-base transistors (PBTs), charge-carrier transfer between emitter and collector occurs mainly through small openings in the base layer rather than by ballistic transport across the base, as is the case in metal-base transistors. In the conventional (inorganic) PBT, the base is a metal and the potential of the base controls the current flow between emitter and collector.

I.3. Hole-injection and Hole-transport Materials

In order to minimize the barriers for charge injection, the work function of the electrode should be as close as possible to the energy levels of the organic layer. The hole-injection contact requires a metal of high work function to match with the HOMO of the organic material. A high work function material, typically transparent and conductive tin doped indium oxide (In_2O_3) (ITO), deposited on a glass substrate serves as the anode to facilitate hole-injection while permitting light to escape the device. The work function of the ITO varies from 4.5 to 5.0 eV, and is strongly depending on its exact stoichiometry and on the methods of surface treatment.[17] Oxidation of the ITO surface by O_2 plasma have been used to increase the work function and reduce the carrier injection energy

barrier, even though the highest work function achieved for ITO (5.0 eV) is still lower than most of the HOMO of hole-transport materials. A layer of material with higher work function than ITO, which reduces the energy barrier in-between ITO/HTL, is therefore beneficial to enhance the charge injection at the interfaces.[17] One of the widely used materials for promoting hole-injection is poly(3,4-ethylenedioxythiophene)-poly(styrene) known as PEDOT/PSS.[18] This aqueous gel dispersion as hole-injection layer can smooth the ITO surface, reducing the probability of electrical shorts, decreasing the turn-on voltage and prolonging the operation lifetime of the device.[19]

Another approach to improve the hole injection is the evaporating of a thin layer of insulating materials between the ITO and emissive layer which acts as a barrier for electrons causing the accumulation of electrons at the emissive layer-insulator interface.[20] The high electron density enhances the electric field at that interface narrowing the barrier for hole-injection.

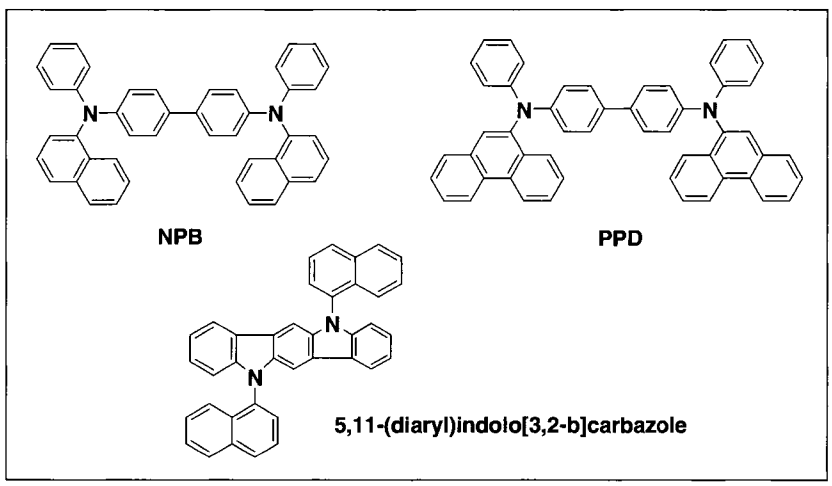

Figure I.2. Example of hole-transport materials

Aromatic amines have been found to be excellent hole-transport materials (HTM). One of the most widely used HTM in OLED is N,N′-diphenyl-N,N′-bis-(1-naphthyl)-

1,1′-biphenyl-4,4′-diamine (NPB) (Figure I.2). The reason for its popularity is that it can be easily be sublimed for device manufacturing, but its low T_g may affect its morphological stability at high operating temperature.[21] Since heat treatment of organic multi-layers has been found to cause an interdiffusion between organic layers in OLEDs, therefore, using materials with high thermal and morphological stabilities is critical. It has been reported that, by increasing the number of π-electrons and decreasing the rotational moment of the molecule by introducing the bulky moieties, the thermal stability of the molecule will increase (PPD, Figure I.2). Carbazole derivatives have also been widely used as HTMs since they are electron rich and most of them have high T_g, such as 5,11-(diaryl)indolo[3,2-b]carbazole (Figure I.2). In general, such electron rich materials with low oxidation potential can effectively be used as HTM.

I.4. Electron-injection and Electron-transport Materials

Matching the LUMO level of materials for electron injection requires the use of low work function metals. The alkali metals such as Cs and Rb have the lowest value of work function (below 2.2 eV), but their low melting points and instability make them very difficult to be used as an appropriate cathode. Other metals such as Ca, Mg, and Ba with the work functions of lower than 2.7 eV are also used as the cathode in OLEDs. The work functions of these metals are low enough to be matched for green and red emitter materials, but they produce a high heterojunction for the blue emitters,[22] while it is not easy to handle these metals due to facile oxidations. A simple and more commonly used way to reduce the limitation of electron injection is, to introduce a thin layer of fluorides

based on alkali or alkaline earth metals like LiF and CsF. By far, the most useful metal is found to be Al due to its air-stability, even though it has high work function of 4.28 eV.[22]

To date, the most widely used electron-transport material in OLEDs is tris(8-hydroxyquinolato)aluminum (III) (AlQ_3) because of being thermally and morphologically stable to be evaporated as thin films. But, it has also some disadvantages such as low quantum efficiency and electron mobility. It has been found that the mobility of AlQ_3 will be increased as the deposition rate decreased. To improve the quantum efficiency, thermal stability and thin layer morphology of AlQ_3, some structural modifications have been applied. It was reported that, tris(5-hydroxymethyl-8-quinilinolato)aluminum (AlQ_3) can form a more uniform amorphous thin film than AlQ3 due to the intermolecular hydrogen bond formation.[23]

In addition to metal chelates, a large number of n-type organic semiconductors have been reported for use in OLEDs as electron-transport materials. Thiophene derivatives, (oligothiophene and polythiophene) and perfluorinated *p*-phenylenes are amongst the most widely used n-type semiconductors for OLED. In general, such electron-deficient materials with low reduction potential can effectively be used as ETM.

I.5. Organic Fluorescent Materials

For multicolor display applications, the light-emitting diodes with three basic colors red, green, and blue are needed. Full color LED displays can be constructed in different ways. The first method is filtering white light for a specific color. It is a simple way but wastes energy due to generation of unwanted color. The second strategy is applying different bias potentials to LEDs. Some materials tend to emit different colors

depending on the operation potential, but it is not easy to control the light intensity and the emission color at the same time.[24] The last way of making a full color LED is using efficient dyes to convert colors. Conversion of blue light with the short wavelength to green or red having longer wavelength is possible while green or red cannot be converted to blue. Using this method, the blue light emitters alone may be used to generate all colors.[24]

I.5.1. Green Emitters

The green fluorescent materials with long lifetime stability and good device performances were amongst the first to be successfully demonstrated. One of the best green emitters is known as C-545T which belongs to the highly fluorescent group of coumarin (Figure I.3). It is believed that the p-orbital of nitrogen connected to the carbon number 7 overlaps with the π-orbitals of phenyl rings resulting more effective conjugation length and increasing the relative quantum yield. The structural modification of the compound caused the higher luminance efficiency. Another notable green emitter is N,N′-diethylquinacridone (DEQ) which is known to be thermally stable in the device operation[25] (Figure I.3).

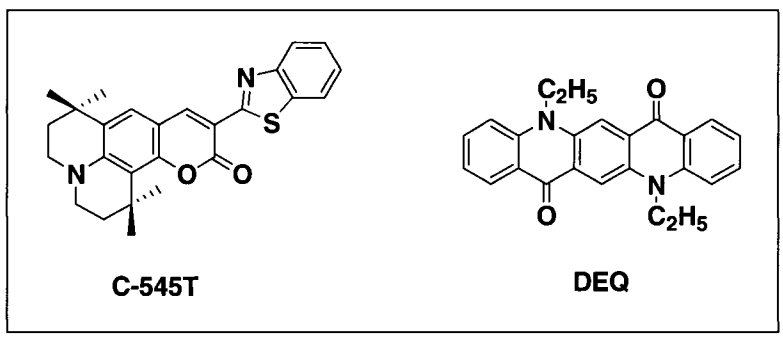

Figure I.3. Example of green fluorescent materials

I.5.2. Red Emitters

Among the RGB compounds used in OLED, red emitters still need to be improved due to their moderate efficiency. In order to have a pure red emitter, the band gap of the molecules should decrease significantly. There are several powerful approaches to construct the narrow-band gap systems. One way is the copolymerization of aromatic and *o*-quinoid units.[26] It is believed that the combination of monomer segments with different electronic structures can lower the band gap through the relaxation of bond length alternation. Another approach to design such systems is the alternation of strong electron-donating and electron-withdrawing segments at regular arrangements along the conjugated backbone.[27] In this case the mixture of monomer segments with higher HOMO and lower LUMO can reduce the band gap due to the intrachain charge transfer. While, the interaction of the donor-acceptor units enhances the double bond character between the repeating units preventing the twisted arrangement of the molecule.[28] It is well known that the extension of conjugated length in compounds will also decrease the band gap significantly, shifting the emission wavelength towards the red. The most common electron donating groups are amines, thiophene and pyrrole since they are electron rich while ketone, cyano and nitro groups are the best candidates as electron acceptor. It should be mentioned that all three methods to decrease the band gap of molecules could be applied in both small molecules and polymers.

I.5.3. Blue Emitters

The blue light-emitting materials are still far away from specifications required by full color displays due to low efficiency, wide band gap, high oxidation potential and low

electron affinities.[29] Because of these features, polymeric blue-light emitting devices usually face charge injection difficulties. One method to achieve blue emission is through the use of a dopant. To do so it is necessary to select or design an appropriate blue host material. Many hole transport materials such as NPB and PPD described previously, are capable of emitting in the blue. In order to enhance the EL efficiency and maintain the purity of the blue emission, insertion of a hole blocking layer in device often becomes necessary.

The fluorophores for blue color emission consist of chemical structures like phenyl, or fluorene, or heterocycles such as thiophene, pyridine and furan. These fluorophores are either used in small molecules or polymers (either backbone or side chain).

I.6. Fluorene-based Emitters

In the past decade, fluorene-based conjugated polymers have emerged as a very promising class of blue-light emitting compounds for use in PLEDs because of their high photoluminescence and electroluminescence quantum efficiencies, good film forming, thermal stability, good solubility and facile functionalization at the C-9 position of fluorine.[30] However, the disadvantages of polyfluorenes, such as aggregation and/or excimers formation in the solid states, insufficient color stability, and high energy barrier for hole injection, limit their application in polymer LEDs.[31] It is believed that, the color instability "a tailed emission band at long wavelengths (> 500 nm) during device fabrication",[30] and reduced efficiency are attributed to the undesired interchain

aggregation. On the other hand, the methylene group of the fluorene may lower the chemical stability of the molecule due to oxidation or photooxidation.[32]

In the attempt of tuning the physical properties of polyfluorenes by molecular structure modification, one has to face the problem that the only possibility of functionalization is at the C-9 position, and any other position of the fluorene unit is very difficult to perform functional chemical reactions. It is found that the C-9 aryl substituents are significantly beneficial in improving the morphological stability and thermal stability.[33] The substituted alkyl chains at position 9 render no change in emission spectrum but improve the solubility of the polymer in organic solvents.

Copolymerization of fluorene with various aryls allows for tunability of electronic properties and enhances thermal stability. For example, copolymers of fluorene and anthracene are highly resistant against heat, while fluorene-triarylamine copolymers demonstrate high charge carrier mobilities.[31] Alternating copolymer of fluorene and carbazole showed complete blue shift and improved hole-transporting capabilities due to the interruption of the main chain conjugation by the presence of the carbazole units[30] (Figure I.4, A). The same properties was observed in copolymer of fluorene and oxadiazole[34] (Figure I.4, B), while the copolymer of fluorene and thieno-[3,2-b]thiophene exhibited a pure green emission[35] (Figure I.4, C).

Fluorene is a rigid and planar molecule, due to the methylene group bridging the 2,2´-positions of the biphenyl. The electronic and optical properties arise from its planarity while the rigidity improves the thermal stability by prohibiting free rotation around the 1-1´ bond of the biphenyl.[21] Therefore, it is conceivable that the structurally related compound, indenofluorene, should have some unique electronic and optical

characteristics, compared to the fluorene, due to the presence of the three planarized phenylene rings and longer conjugation length.

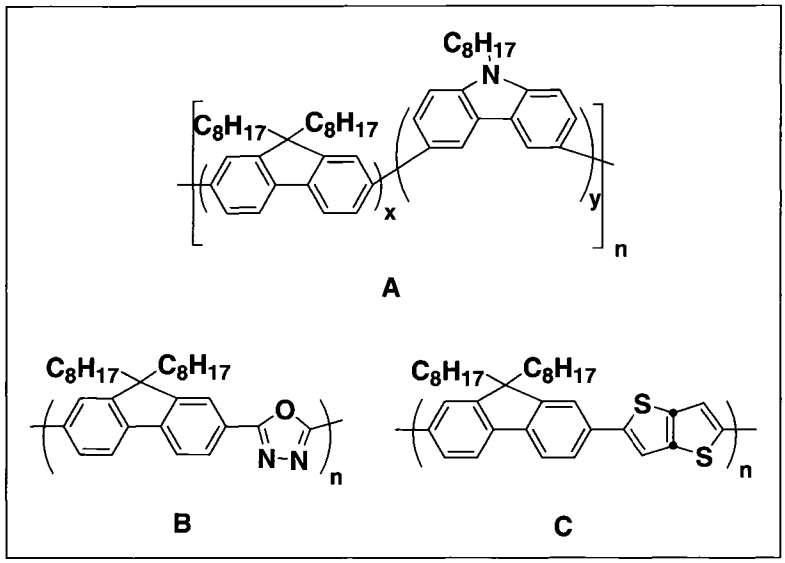

Figure I.4. Example of fluorene-based polymers

I.7. Synthetic Routes to Indenofluorenes

There are several possible synthetic routes to indenofluorenes. These include Stille Coupling,[36] Suzuki coupling,[36] Yamamoto reaction,[36] Grignard reaction[36] and Friedel-Crafts condensation.[37,38] Due to the poor solubility in common organic solvents, the most appropriate method for derivatization of indenofluorene as well as polymerization, was found to be Suzuki coupling. This approach, in addition to others, is discussed in further details.

I.7.1. Stille Coupling

The Stille reaction is the first method to prepare the derivatized indenofluorenes. This approach involves the palladium-catalyzed reaction of 2,6-dibromoindenofluorene and organostannane derivatives (Scheme I.1).

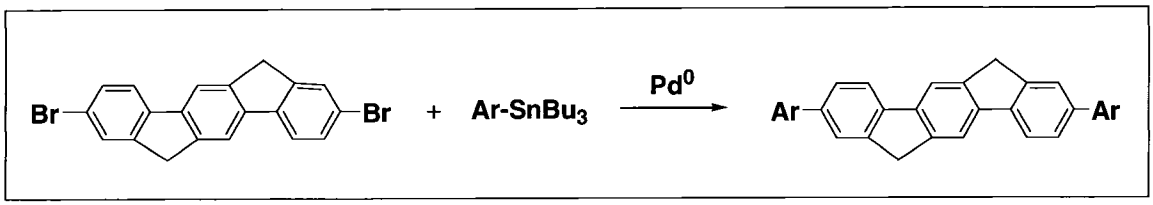

Scheme I.1. Synthesis of 2,6-disubstituted indenofluorenes using the Stille reaction

The original mechanism proposed by Stille, included four steps: oxidative addition, transmetalation, cis-trans isomerization and reductive elimination.[39] This initial mechanism has been progressively modified and it is found that the transmetalation step is the main rate-determining step. A catalytic cycle for the Stille reaction is shown in Figure I.5.

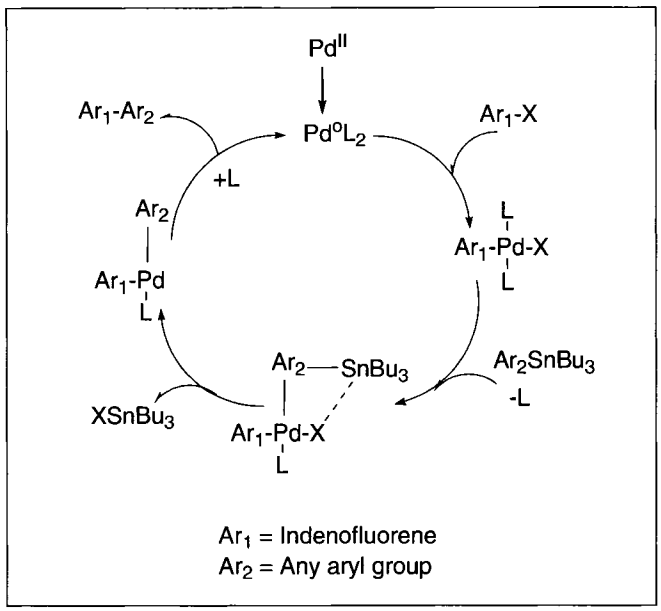

Figure I.5. Catalytic cycle of the Stille reaction

The first step in this catalytic cycle is the reduction of the palladium catalyst to the active Pd(0) species. The oxidative addition of the organohalide gives a cis intermediate which rapidly isomerizes to the trans intermediate. Transmetallation with

the organostannane compound gives the second intermediate. Finally the reductive elimination produces the desired product and re-generates the active Pd(0) species.

I.7.2. Suzuki Coupling

The second synthetic route leading to indenofluorene derivatives is Suzuki coupling.[40, 41] It is a palladium-catalyzed cross-coupling of organoboronic acids or esters with 2,6-dibromoindenofluorene (Scheme I.2). This method is among the most powerful and versatile synthetic methods for carbon-carbon bond formation.

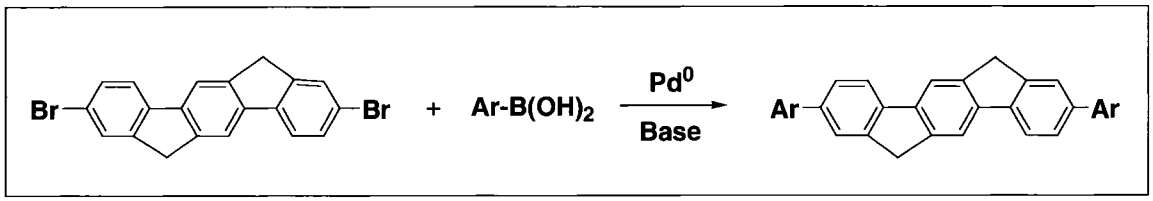

Scheme I.2. Synthesis of 2,6-disubstituted indenofluorenes by the Suzuki coupling

Since organoborons are highly electrophilic, but the organic groups on boron are weakly nucleophilic, therefore, the presence of a negatively charged base such as sodium or potassium ethoxide or hydroxide has been found to be essential to increase the nucleophilicity of the organic group and facilitate its transfer to the adjacent positive center.

Like the Stille reaction, a general catalytic cycle for the Suzuki cross-coupling reaction involves oxidative addition, transmetalation and reductive elimination steps. In oxidative addition step, halide compounds are added to the palladium(0) complex to afford a stable organo-palladium(II) intermediate. This intermediate then undergoes a transmetallation with the boronate compound from which the desired product is expelled by reductive elimination, regenerating the palladium(0) catalyst. As it was mentioned in

section I.7.1, transmetallation is also a rate-determining step in the Suzuki coupling reaction.

I.7.3. Yamamoto Reaction

The Yamamoto reaction known as nickel-catalyzed polycondensation, has only been used to synthesize polyindenofluorene[42] (Scheme I.3). This method involves nickel-mediated coupling of two dibromo monomers. Homopolymers and random polymers can be made by this method. Since both starting materials bear bromo units, this is not a suitable way for the syntheses of small molecules (2,6-disubstituted indenofluorene) due to the formation of various by-products.

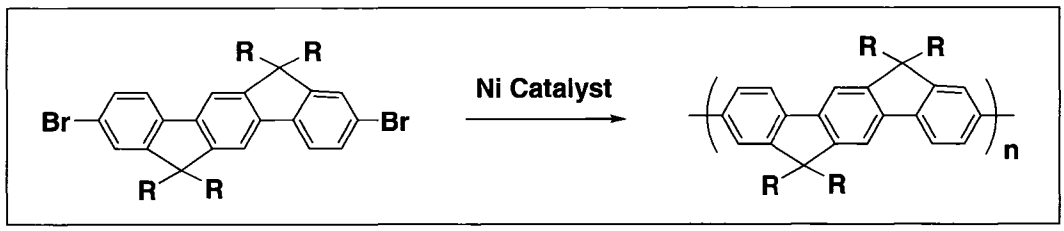

Scheme I.3. Synthesis of polyindenofluorene by the Yamamoto reaction

I.7.4. Grignard Reaction

Another synthetic route leading to indenofluorene derivatives is the Grignard reaction.[43] In this method, a C-C bond could form via a palladium complex-catalyzed cross coupling reaction of the Grignard reagent of an aryl bromide with 2,6-dibromoindenofluorene (Scheme I.4).

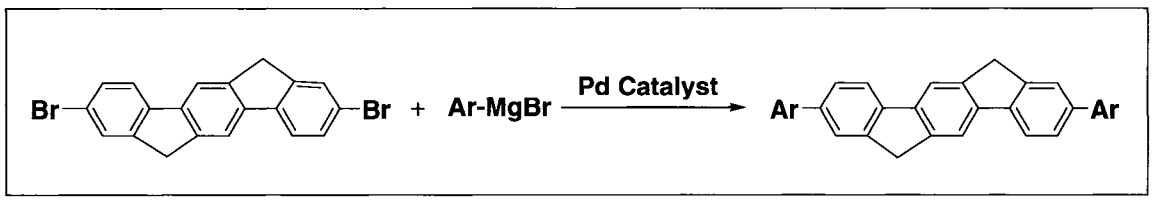

Scheme I.4. Grignard reaction route to 2,6-disubstituted indenofluorenes

I.7.5. Friedel-Crafts Condensation

Indenofluorene derivatives may also be obtained by the Friedel-Crafts condensation of 1,4-xylene with cyclohexane derivatives and $AlCl_3$.[37] Catalytic dehydrogenation of the product followed by oxidation with $KMnO_4$, cyclization in concentrated sulfuric acid and reduction, produces the final product (Scheme I.5). It should be mentioned that, the application of this method is limited due to the availability of starting materials.

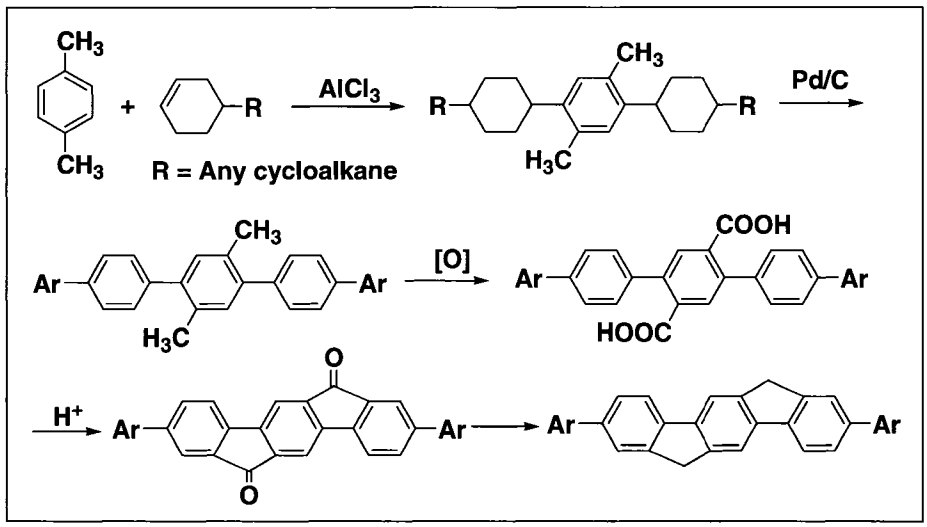

Scheme I.5. Use of Friedel-Crafts reaction in construction of 2,6-disubstituted indenofluorenes

I.8. Fluorenone Derivatives

Fluorene-based polymers such as polyfluorenes and polyindenofluorenes are of great interest as potential blue-emitting materials in applications such as LEDs. These materials show efficient blue or blue-green emission in solution with emission color red-shifting as the chain rigidity increases. However, the blue emission in the solid state is unstable, due to the rapid appearance of long-wavelength emission band.[42] These were

assigned to aggregation of the polymer chains, but Moses and his group[44] presented comprehensive evidence that the low energy emission band originates from emissive fluorenone defects formed by oxidation at the methylene bridge rather than from aggregation or excimer formation.

Having identified the role of fluorenone defects in the polyfluorenes, two opportunities emerge: stabilization of the blue emission from polyfluorenes by excluding the formation of fluorenone defects and taking advantage of the fluorenone defect for creating materials with stable green emission or stable n-type materials.[45] The presence of electron-withdrawing carbonyl group in 9-position of fluorene may increase the oxidation potential and may also reduce the reduction potential of the molecule, making it a candidate for n-type conductor use.

There have been very few reports on the synthesis of fluorenone derivatives. Sieber and his group prepared the indenofluorenone derivatives via a Friedel-Crafts condensation of fluorene and benzoyl chloride derivatives and $AlCl_3$[46] (Scheme I.6). This method is limited to the synthesis of a few alkyl substituted indenofluorenones.

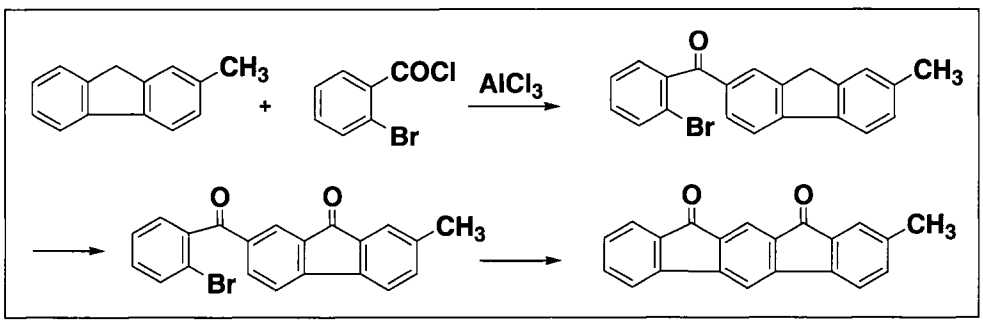

Scheme I.6. Synthesis of indenofluorenone by Friedel-Crafts method

The first polyfluorenone was prepared by Uckert et al. as an insoluble polymer using a method that involves the soluble blue emitting polyketal derivative of fluorene, followed by deketalisation in the solid state with dichloroacetic acid vapour.[47, 48] The

polymer showed orange-red emission with the LUMO level of –3.3 eV which was a promising candidate for use as an electron transporting material.

The random polymer of fluorene and fluorenone made by Moses et al. demonstrated that the blue emission of polyfluorene reduced significantly as the fluorenone concentration was increased[44] while the green emission became more intense. This means that, the energy transfer to and charge carrier trapping on fluorenone defects are responsible for the color degradation of polyfluorenes.

With all this evidence revealing that fluorenone could be an appropriate n-type material for use in LEDs, it is expected that an extra carbonyl group (indenofluorenone) will increase the electron withdrawing properties of the molecule even more.

I.9. Research Hypothesis and Directions

Molecular engineering points at designing new materials with specific properties appropriate for technological applications. However, to succeed in engineering such new materials, a complete understanding of the relationship between the chemical structure and properties is necessary. The properties that can be tuned through molecular design are the energy levels of valence and conduction bands and the energy gap. The valence and conduction band levels govern the p and n dupability and the doped state stability of the materials. The energy gap is strictly related to the electrical and optical properties.

Generally speaking, a proper substitution with strong electron donors or electron acceptors on the aromatic units produces appreciable variations on energy levels, affecting both HOMO and LUMO levels of the molecule. There are several useful approaches to construction of the narrow-band gap systems. One way to lower the band

gap of the material is to increase the conjugation length. Alternation of strong donor and acceptor moieties at regular arrangements in the repeating units is another approach to tuning the band gap. The donor-acceptor system can also be realized in small molecules.

Most organic materials are p-type, which accept and transport holes better than electrons, but n-type materials are needed for use in n-type transistors, as the electron-accepting components in devices, and to increase the efficiency of LEDs by improving electron injection and transport.

Fluorene-based conjugated compounds (oligomers and polymers) as blue emitters have the advantages of high photoluminescence and electroluminescence quantum efficiencies, thermal and chemical stability. The electronic and optical properties arise from fluorene molecule's planarity. It is expected that the structurally related compound, indenofluorene, should have some unique electronic and optical characteristics, compared to fluorenes, due to the presence of the three planar phenylene rings and longer conjugation length.

It is thus hypothesized that, by incorporation of aromatic rings such as thienyl, naphthyl and phenyl at both ends of indenofluorene, the conjugation length of the resulting compounds would increase, leading to the decreased band gap and light emission at longer wavelengths.

It is further hypothesized that the presence of strongly electronegative substituents such as fluorine and cyano groups on the aromatic rings mentioned above, would lower the LUMO level of the molecules, affording appropriate electron-accepting and -transporting compounds that could be used in transistors as n-type semiconductor materials as well as in OLEDs as electron transport materials.

A number of different synthetic routes are available for the syntheses of indenofluorene derivatives that are mainly functionalized at the 9,9′-positions with the alkyl groups. Each one is unique, but not general enough to allow for the synthesis of a series of structurally related indenofluorenes for probing the structure-property relationships. Therefore, a general synthetic route to a new series of indenofluorene derivatives with aryl groups at the terminal 2,6-position is proposed (Figure I.6).

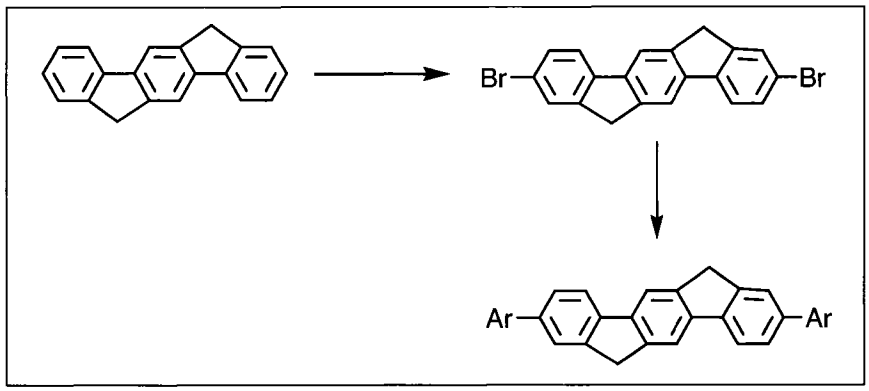

Figure I.6. Proposed synthetic route to indenofluorene derivatives

A logical extension to the work is to construct the narrow-band gap systems. To do so, the donor-acceptor system based on indenofluorenone is chosen in both small molecules and polymers. The presence of such an electron-withdrawing group is expected to reduce the reduction potential, making it a good candidate as n-type semiconductor. It is expected that extra carbonyl groups (indenofluorenone) increase the electron-deficient nature of the molecule. Therefore, a series of donor-acceptor type molecules (small molecules and polymers) based on the indenofluorenone as an acceptor is proposed and a general synthetic route starting from indenofluorenone is proposed (Figure I.7).

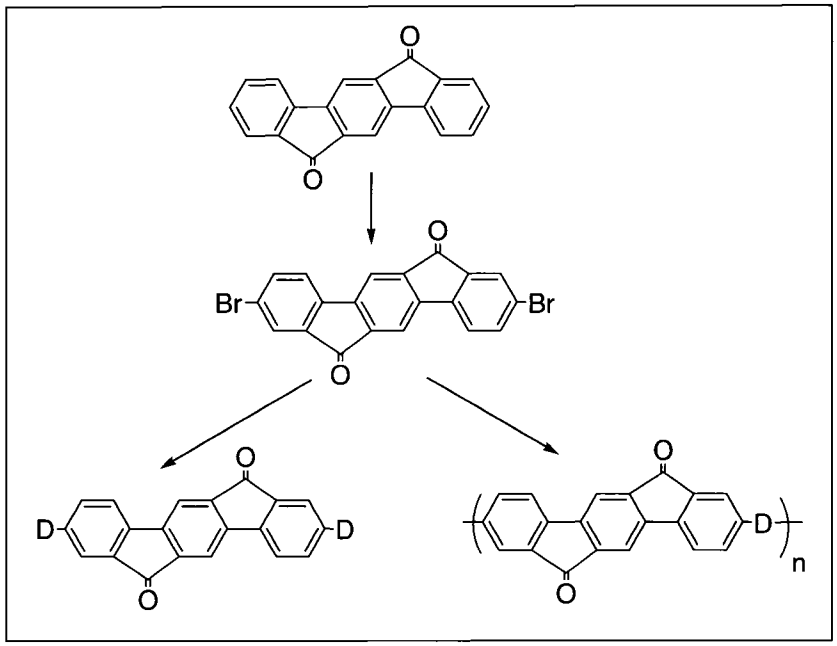

Figure I.7. Proposed synthetic route to indenofluorenone derivatives in small molecules (left) and polymers (right)

Therefore, the overall objectives of this thesis are:

(1) to establish a synthetic route to a series of indenofluorene derivatives,

(2) to study the electrical and optical properties of indenofluorene derivatives,

(3) to synthesize a new series of donor-acceptor compounds and polymers using indenofluorenone as an acceptor,

(4) to correlate the molecular structures with the optical and electronic properties,

(5) to explore applications in organic thin-film transistors and organic light-emitting diodes.

References

1. Helfrich, W.; Scheider, W. G. *Phys. Rev. Lett.* **1965**, *14*, 229.
2. Vincett, P. S.; Barlow, W. A. Hann, R. A.; Roberts, C. G. *Thin Solid Films* **1982**, *94*, 171.
3. Tang, C. W.; VanSlyke, S. A. *Appl. Phys. Lett.* **1987**, *51*, 913.
4. Tang, C. W.; VanSlyke, S. A.; Chen, C. H. *J. Appl. Phys.* **1989**, *65*, 3610.
5. Burroughes, J. H.; Bradley, D.D.C.; Brown, A.R.; Marks, R. N.; Mackay, K.; Friend, R.H.; Burns, P.L.; Holmes, A.B. *Nature* **1990**, *347*, 539.
6. Kraft, A.; Grimsdale, A. C.; Holmes, A. B. *Angew. Chem. Int. Ed.* **1998**, *37*, 402.
7. Segura, J. L. *Acta Polym.* **1998**, *49*, 319.
8. Baldo, M. A.; Kozlov, V. G.; Burrows, P. E.; Forrest, S. R.; Ban, V. S.; Koene, B.; Thompson, M. E. *Appl. Phys. Lett.* **1997**, *71*, 3033.
9. Forrest, S. R.; Burrows, P. E.; Stroustrup, A.; Strickland, D.; Ban, V. S. *Appl. Phys. Lett.* **1996**, *68*, 1326.
10. Braun, D.; Heeger, A. J. *Appl. Phys. Lett.* **1991**, *58*, 1982.
11. Gustafsson, G.; Treacy, G. M.; Cao, Y.; Klavetter, F.; Colaneri, N.; Heeger, A. J. *Synth. Met.* **1993**, *55-57*, 4123.
12. Greenham, N. C.; Moratti, S. C.; Bradley, D. D. C.; Friend, R. H.; Holmes, A. B. *Nature* **1993**, *365*, 628.
13. Berntsen, A.; Weijer, P.; Croonen, Y.; Liedenbaum, C.; Vleggaar, J. *Phillips J. Res.* **1998**, *51*, 511.
14. Atalla, M.; Khang, D. *IEEE Trans. Electron. Dev.* **1962**, *ED-9*, 507.
15. Geppert, D. V. *Proc. IRE* **1962**, *50*, 1527.

16. Ng, K. K. *Complete Guide to Semiconductor Devices*, Wiley, New York **2002.**

17. Patel, N. K.; Cina, S.; Burroughes, J. H. *IEEE J. Selected Top. Quantum Electron.* **2002**, *8*, 346.

18. Groenendaal, L. B.; Jonas, F.; Freitag, D.; Pielartzik, H.; Reynolds, J. R. *Adv. Mater.* **2000**, *12*, 481.

19. Brown, T. M.; Kim, J. S.; Friend, R. H.; Cacialli, F.; Daik, R.; Feast, W. J. *Appl. Phys. Lett.* **1999**, *75*, 1679.

20. Murata, K.; Cina, S.; Greenham, N. *Appl. Phys. Lett.* **2001**, *79*, 1193.

21. Loy, D. E.; Koene, B. E.; Thompson, M. E. *Adv. Funct. Mater.* **2002**, *12*, 245.

22. Bernius, M. T.; Inbasekaran, M.; O`Brien, J.; Wu, W. *Adv. Mater.* **2000**, *12*, 1737.

23. Yin, S.; Hua, Y.; Chen, S.; Yang, X.; Hou, Y.; Xu, X.; *Synth. Met.* **2000**, *111*, 109.

24. Virgili, T.; Lidzey, D. G.; Bradley, D. D. C. *Adv. Mater.* **2000**, *12*, 58.

25. Murata, H.; Merritt, C. D.; Inada, H.; Shirota, Y.; Kafafi, Z. H. *Appl. Phys. Lett.* **1999**, *75*, 3252.

26. Kitamura, C.; Tanaka, S.; Yamashita, Y. *Chem. Mater.* **1996**, *8,* 570.

27. Chen, M. X.; Perzon, E.; Robisso, N.; Jonsson, S. K. M.; Andersson, M. R.; Fahlman, M.; Berggren, M. *Synth. Met.* **2004**, *146*, 233.

28. Ajayaghosh, A. *Chem. Soc. Rev.* **2003**, *32*, 181.

29. Yang, W.; Huang, J.; Liu, C.; Niu, Y.; Hou, Q.; Yang, R.; Cao, Y. *Polymer* **2004**, *45*, 865.

30. Lu, J.; Tao, Y.; D`iorio, M.; Li, Y.; Ding, J.; Day, M. *Macromolecules* **2004**, *37*, 2442.

31. Liu, B.; Yu, W. L.; Lai, Y. H.; Huang, W. *Macromolecules* **2000**, *33*, 8945.

32. Li, Y.; Ding, J.; Day, M.; Tao, Y.; Lu, J.; D`iorio, M. *Chem. Mater.* **2004**, *16*, 2165.

33. Wong, K. T.; Chien, Y. Y.; Chen, R. T.; Wang, C. F.; Lin, Y. T.; Chiang, H. H.; Hsieh, P. Y.; Wu, C. C.; Chou, C. H.; Su, Y. O.; Lee, G. H.; Peng, S. M. *J. Am. Chem. Soc.* **2002**, *124*, 11576.

34. Ding, J.; Day, M.; Robertson, G.; Roovers, J. *Macromolecules* **2002**, *35*, 3474.

35. Lim, E.; Jung, B. J.; Shim, H. K. *Macromolecules* **2003**, *36*, 4288.

36. Clayden, J.; Greeves, N.; Warren, S.; Wothers, P. *Organic Chemistry*, Oxford, Chapter 48.

37. Deuschel, W. *Helv. Chim. Acta.* **1951**, *34*, 2043.

38. Chardonnens, L.; Laroche, B.; Sieber, W. *Helv. Chim. Acta.* **1974**, *57*, 585.

39. Stille, J. K. *Angew. Chem. Int. Ed. Engl.* **1986**, *25*, 508.

40. Hu, N. X.; Aziz, H.; Jain, P.; Popovic, Z. D. *US Pat. 6562485*, **2003**.

41. Jacob, J.; Sax, S.; Piok, T.; List, E. J. W.; Grimsdale, A. C.; Mullen, K. J. Am. *Chem. Soc.* **2004**, *126*, 6987.

42. Setayesh, S.; Marsitzky, D.; Mullen, K. *Macromolecules* **2000**, *33*, 2016.

43. Abbotto, A.; Bradamante, S.; Facchetti, A.; Pagani, G. A. *J. Org. Chem.* **1997**, *62*, 5755.

44. Gong, X.; Moses, D.; Heeger, A.; Xiao, S. *Synth. Met.* **2004**, *141*, 17.

45. Gong, X.; Moses, D.; Heeger, A. J. *J. Phys. Chem.* **2004**, *108*, 8601.

46. Chardonnens, L.; Laroche, B.; Sieber, W. *Helv. Chim. Acta.* **1974**, *57*, 585.

47. Uckert, F.; Tak, Y. H.; Mullen, K.; Bassler, H. *Adv. Mater.* **2000**, *12*, 905.

48. Becker, S.; Ego, C.; Grimsdale, A. C.; List, E. J. W.; Marsitzky, D.; Pogantsch, A.; Setayesh, S.; Leising, G.; Mullen, K. *Synth. Met.* **2002**, *125*, 73.

Chapter II

Synthesis and Characterization of Indenofluorene Derivatives

II.1. Introduction

Fluorene derivatives are known to have excellent performance characteristics including high thermal and chemical stability, good fluorescence quantum yield and intense blue emission properties. These compounds are being widely used as hole-transporting materials in organic light emitting diodes (OLEDs). Significant efforts have been made to tune the light-emitting color of fluorene derivatives to a longer wavelength in order to be used as electron-transporting compounds as well as emissive layer other than blue. One way to achieve this goal is to increase the conjugation length of fluorene. Therefore, indenofluorene and its derivatives can be good choices for this purpose due to their longer conjugation length in comparison with fluorene. Since indenofluorene derivatives are designed for use in transistors and as an emitter layer in OLEDs, a simple and reproducible synthetic route to indenofluorenes is required. Due to its poor solubility in common organic solvents, direct derivatization of indenofluorene has not been reported.

As mentioned in Chapter one, there are four major methods to prepare indenofluorene derivatives: Stille coupling,[1] Grignard reaction,[1] Friedel-Crafts condensation[2,3] and Suzuki coupling.[1] Considering the advantages and disadvantages of these methods, Suzuki coupling is the best choice for the preparation of indenofluorene derivatives.

II.1.1. An overview of Suzuki Cross-Coupling Reaction

Palladium-catalyzed cross-coupling of organoboronic acids with aryl bromides, iodides, or triflates, known as the Suzuki reaction, is among the most powerful and

versatile synthetic methods for carbon-carbon bond formation.[1] The scope of the reaction is broad and the additional advantages of this method are being largely unaffected by the presence of water, tolerating a broad range of functionality and yielding nontoxic byproducts.[4] Since a variety of organoboran derivatives are now available, stable in air and inert to various functional groups, a number of studies on transition-metal-catalyzed cross-coupling reactions of organoboronic acids have been reported.

Organoboron compounds are highly electrophilic, but the organic groups on boron are weakly nucleophilic, therefore limiting the use of organoboron reagents for the ionic reactions.[5] The coordination of a negatively charged base to the boron atom has been recognized to be an efficient method of increasing its nucleophilicity to transfer the organic group on boron to the adjacent positive center.

A general catalytic cycle for the cross-coupling reaction of organometallics involves oxidative addition, transmetalation and reductive elimination steps. Each step also involves further processes such as ligand exchange.

Oxidative addition of halide compounds to the palladium(0) complex affords a stable palladium(II) intermediate. Potential ligands that do not have a lone pair or filled π type orbital are still able to interact with transition metal complexes but only by breaking a σ bond. It is called oxidative addition because the formal oxidation state of the transition metal will raise from, for example, M(0) to M(II) in the process.[1] Since the oxidative addition step is very slow, alkyl halides having β-hydrogen rarely tolerate this step and may undergo to β-hydride elimination. This is usually rate-determining step in catalytic cycle. The relative reactivity of halides is I > Br > Cl and aryl halides activated

by the electron-withdrawing groups are usually more reactive to the oxidative addition than those bearing electron-donating groups.

A wide range of palladium(0) catalysts can be used for this method. The most commonly used catalyst is $Pd(PPh_3)_4$, while $Pd(OAc)_2$ with phosphine ligands are also very efficient due to their stability to air and readily reducability to the active Pd(0) complexes.[6]

The palladium(II) intermediate generated in the oxidative addition step then undergoes a transmetallation with the boronate compound from which the product is expelled by reductive elimination, regenerating the palladium(0) catalyst. The transmetallation step in the Suzuki coupling will be markedly accelerated by additional base such as sodium or potassium ethoxide or hydroxide leading to the borate directly via a more nucleophilic complex. A general catalytic cycle for Suzuki coupling is shown below (Figure II.1).

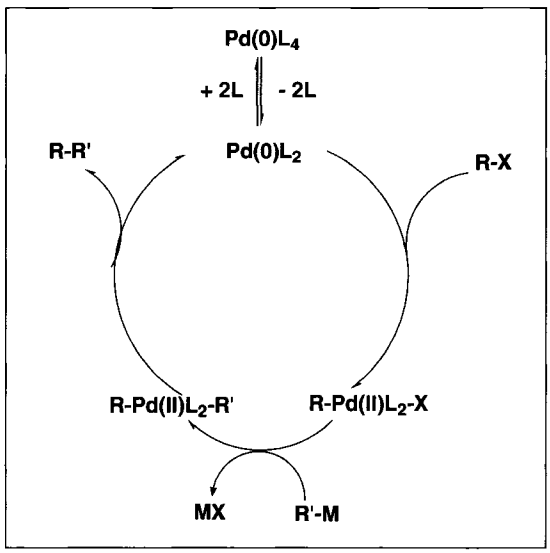

Figure II.1. Catalytic cycle of Suzuki coupling reaction

II.1.2. Design of synthetic routes to indenofluorene derivatives

Proposed synthetic routes to the synthesis of a series of indenofluorene derivatives are shown in Figure II.2. Based on the availability of starting materials, two major synthetic routes were designed. In the first route, 4-aryl-substituted phenyl boronic acid will react with dibromoterephthalic acid by the Suzuki coupling reaction to provide 4-aryl-substituted diphenylterephthalic acid. A cyclization reaction and subsequent reduction are required to obtain the final product. This approach is only applicable to a limited number of 2,6-disubstituted indenofluorenes, since a few aryl boronic acids are commercially available.

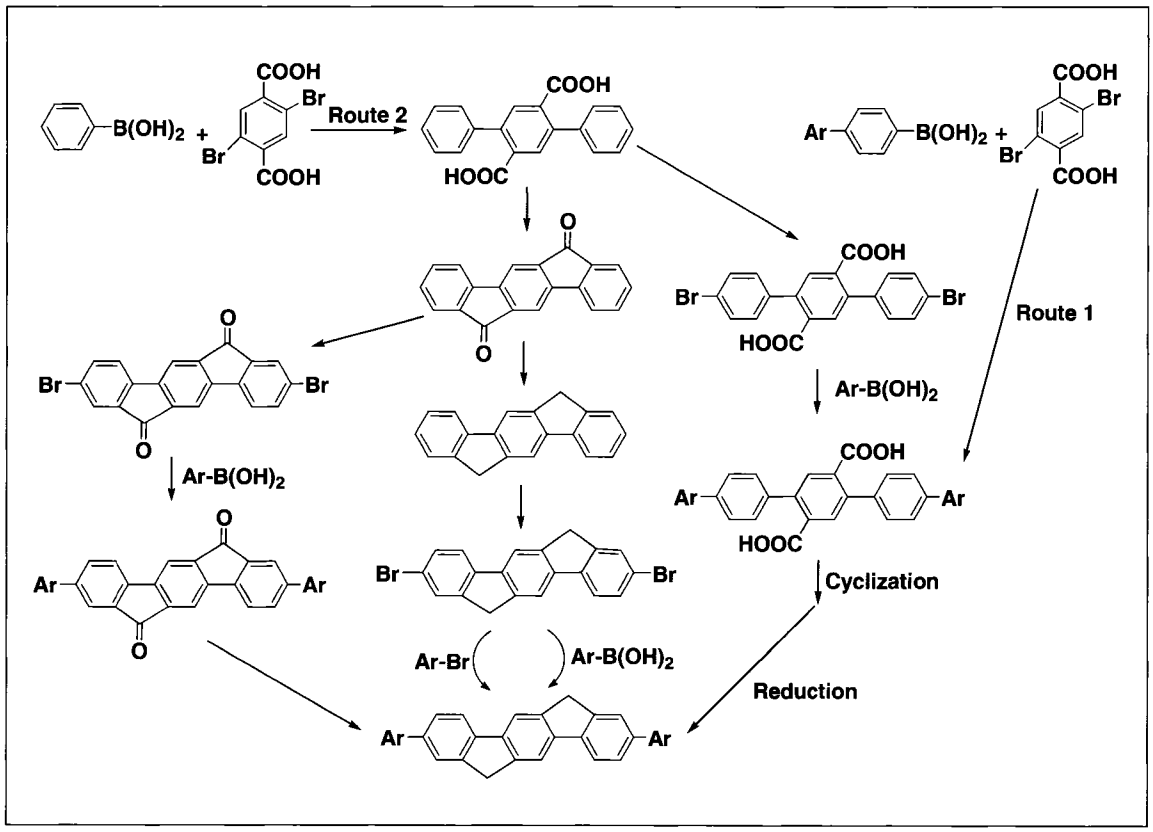

Figure II.2. Proposed synthetic routes to indenofluorene derivatives

To overcome to this problem, a more general route is then proposed (Route 2, Fig. II.2). Phenylboronic acid and dibromoterephthalic acid will first react to provide a key

intermediate, diphenylterephthalic acid, to which the bromine group can be introduced in two ways. In the first path, a bromination reaction is to be carried out on the intermediate, followed by aryl substitution, cyclization and reduction to produce the final product. The second path involves the ring closure, followed either direct bromination or reduction and then bromination. Introduction of the aryl groups by the Suzuki-Coupling reaction will then be carried out (Figure II.2).

As it is shown in Figure II.2, one of the key reactions in all synthetic routes is the cyclization reaction. This reaction usually proceeds in concentrated sulfuric acid or in Eaton's reagent (phosphorus pentoxide, 7.7 wt. % solution in methanesulfonic acid).[7] In some cases, the reaction may fail in concentrated sulfuric acid due to insufficient activation of the carboxylic acid to generate the corresponding acylium ion.[8]

Reduction of two carbonyl groups to the methylene units was the next reaction to be considered. One option is the conversion of the strong C=O bond to a weaker C-S bond that can easily be reduced over Raney nickel catalyst. In this method the carbonyl group will be converted to thioacetals using a dithiol with a Lewis acid catalyst. Freshly prepared Raney nickel and hydrogen will reduce the thioacetal.

The second method to reduce the carbonyl group is the Clemmensen reduction. In this method zinc amalgam will be used together with concentrated hydrochloric acid. Zinc metal in acid provides electrons to reduce the carbonyl bond. The Clemmensen reduction is good for the compounds sensitive to base.

The third method that is slightly more vigorous is known as the Wolff-Kishner reduction. It is suitable for compounds sensitive to acid and is driven by the elimination of nitrogen gas from a hydrazone in the presence of a strong base.[9]

II.2. Synthesis of 2,6-diphenylindenofluorene

A multi-step synthetic route was taken for the synthesis of 2,6-diphenylindenofluorene.

II.2.1. Synthesis of 2,5-Bis(4-biphenyl)terephthalate

Compound **II-2** was made in two steps from commercially available 2,5-dibromoterephthalic acid, the acid was first esterified by methanol to give 2,5-dibromoterephthalate (**II-1**). A Suzuki coupling between compound **II-1** and 4-biphenylboronic acid afforded 2,5-bis(4-biphenyl)terephthalate (**II-2,** 91.5%) (Scheme II.1).

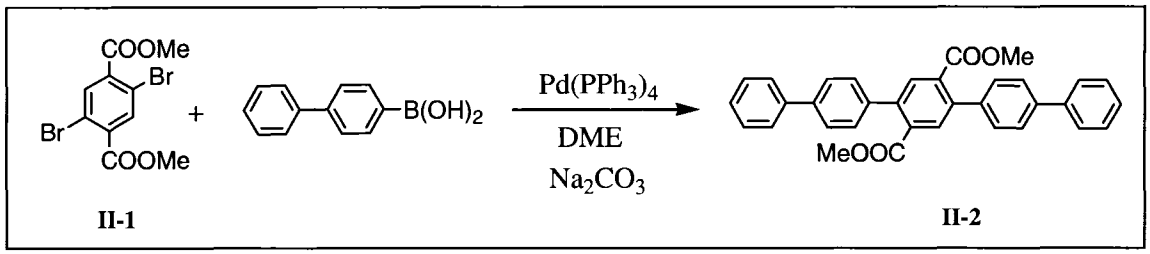

II-1 II-2

Scheme II.1. Synthesis of 2,5-bis(4-biphenyl)terephthalate (**II-2**)

It should be mentioned that the conversion of 2,5-dibromoterephthalic acid to the ester derivative is required for this reaction. After several attempts, the reaction did not proceed with the acid derivative of compound **II-1**. Thus an additional step was added, namely, esterification of 2,5-dibromoterephthalic acid to compound **II-1** which was easily used for Suzuki reaction.

II.2.2. Cyclization (conversion of two ester groups to ketones)

As it has been mentioned before, synthesis of 2,6-diphenylindenofluorene is performed in three major steps, a Suzuki coupling followed by a cyclization of product from the first step in acidic condition (Scheme II.2). Two strong acids were tried for this

purpose, concentrated sulfuric acid and Eaton's reagent (phosphorus pentoxide, 7.7 wt. % solution in methanesulfonic acid). In the case of 2,5-bis(4-biphenyl)terephthalic acid, the reaction failed in concentrated sulfuric acid. The failure might be due to insufficient activation of carboxylic acid to generate the corresponding acylium intermediate.[8] Diphenylindenofluorenone (**II-4**) was successfully obtained by reacting the precursor (**II-3**) with Eaton's reagent in a high yield (99.7 %). It gave a very low yield when the cyclization reaction was applied on compound **II-2**. Therefore, an additional step was added, which was the conversion of compound **II-2** to its acid derivative (**II-3**).

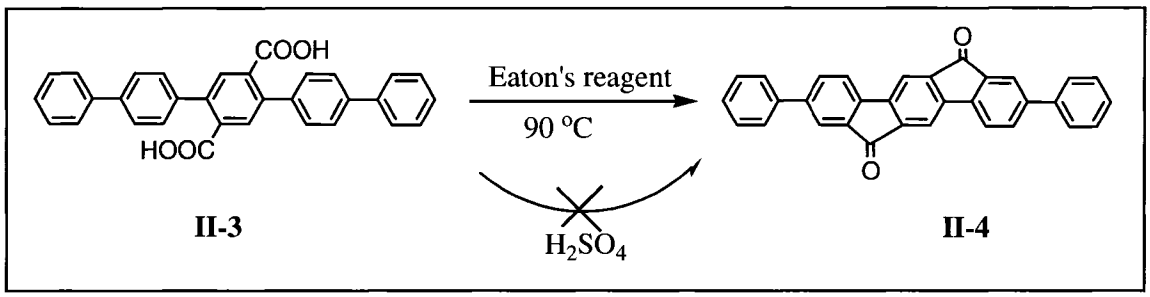

II-3 **II-4**

Scheme II.2. Synthesis of 2,6-diphenylindenofluorenone

In the cyclization step, firstly the lone pairs of the hydroxyl group will be protonated by the acid, which only strong acids are powerful enough to protonate this group.

These protonated hydroxyl groups (even a small percentage) then increase the rate of substitution reaction enormously, because of being converted to an extremely powerful electrophile and being ready to be attacked by even a weak nucleophile. Once the oxygen atom of OH group is protonated, it becomes a much better leaving group. The result of this step is a reactive acylium ion, which readily re-forms the C=O bond by a nucleophilic attack of double bond on the phenyl ring (Figure II.3). Elimination of one

proton from the same phenyl ring re-generates the aromatic structure. Therefore acid plays another powerful role again by the elimination of proton (Figure II.3).

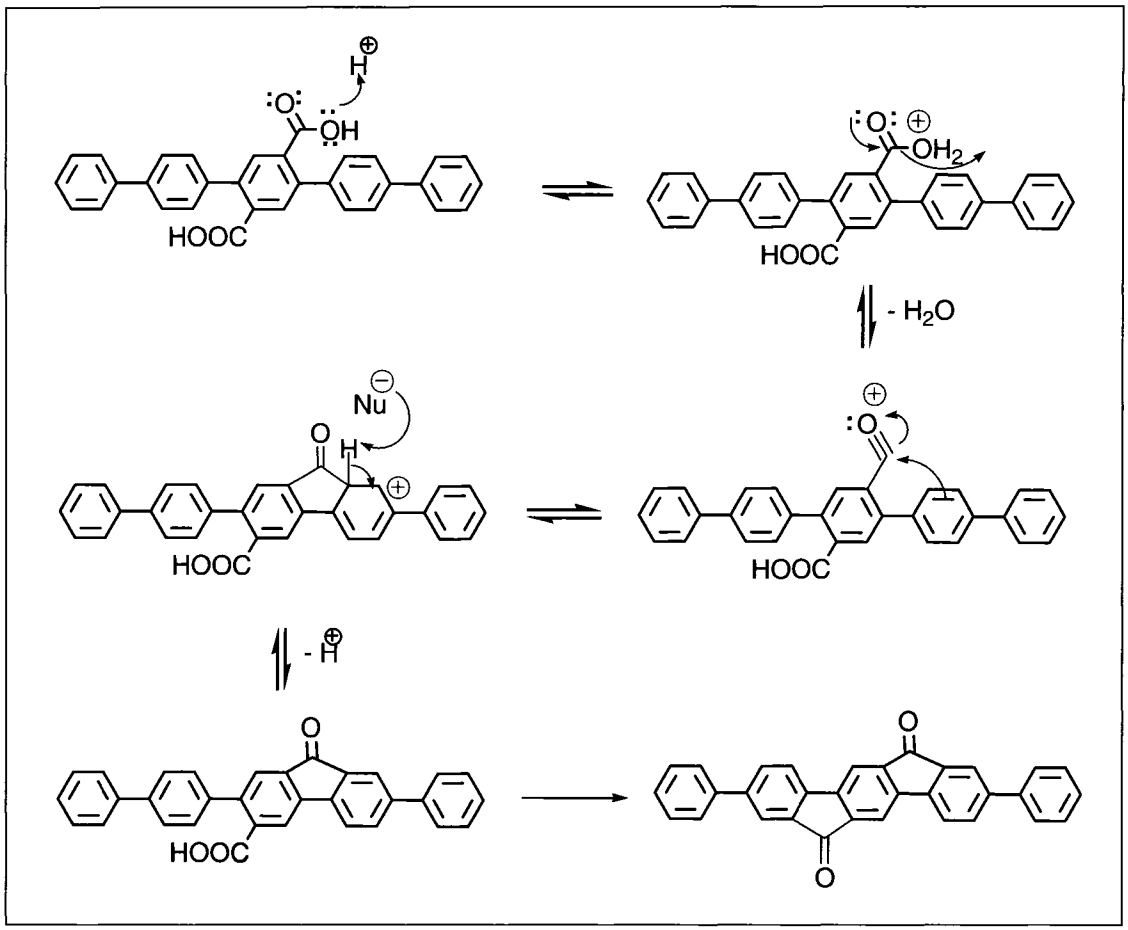

Figure II.3. Mechanism for the acid-catalyzed cyclization

II.2.3. Reduction (Wolff- Kishner reaction)

As it was mentioned previously, synthesis of 2,6-diphenylindenofluorene was terminated by a reduction of the carbonyl groups to the methylene units (Scheme II.3). There were few options to remove the carbonyl groups and among all, the Wolff-Kishner reaction was found the simplest method since compound **II-4** is not sensitive in basic condition at high temperature.

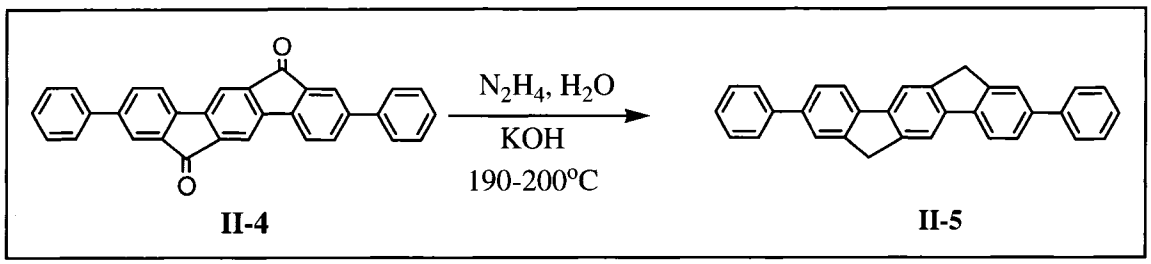

II-4 **II-5**

Scheme II.3. Conversion of the ketone to the methylene group

The ketone groups of 2-6-diphenylindenofluorenone were reduced to the corresponding methylene units using the Wolff-Kishner method in 57% yield.

II.3. Synthesis of 2,6-disubstituted indenofluorenes

II.3.1. Synthesis of indenofluorene

As it was seen in section II.2.1, for the synthesis of 2,6-diphenylindenofluorene one of the starting materials was 4-biphenylboronic acid which provides one phenyl ring as the substitution unit at both ends of indenofluorene. Therefore to have a series of indenofluorene derivatives using the same synthetic procedure, the boronic acid compound requires to have the end unit of goal substituent group. Since not all kinds of boronic acids are commercially available, a few more steps are needed to prepare the starting materials. To avoid these extra steps in the synthetic route and have an easier and general method for a series of indenofluorene derivatives, synthesis of 2,6-dibromoindenofluorene as a key starting compound for the series was designed. This new synthetic route was performed in five steps starting with a Suzuki coupling on 2,5-dibromo-*p*-xylene and phenyl boronic acid followed by an oxidation step using potassium permanganate in aqueous pyridine to yield 2,6-diphenylterephthalic acid[10] (**II-7**). Cyclization in concentrated sulfuric acid and the subsequent Wolff-Kishner reduction afforded indenofluorene (**II-9**) with an overall yield of 78.2% (Scheme II.4). These

known procedures were slightly modified to accommodate the larger scale needed and all the compounds were characterized by the spectroscopic means.

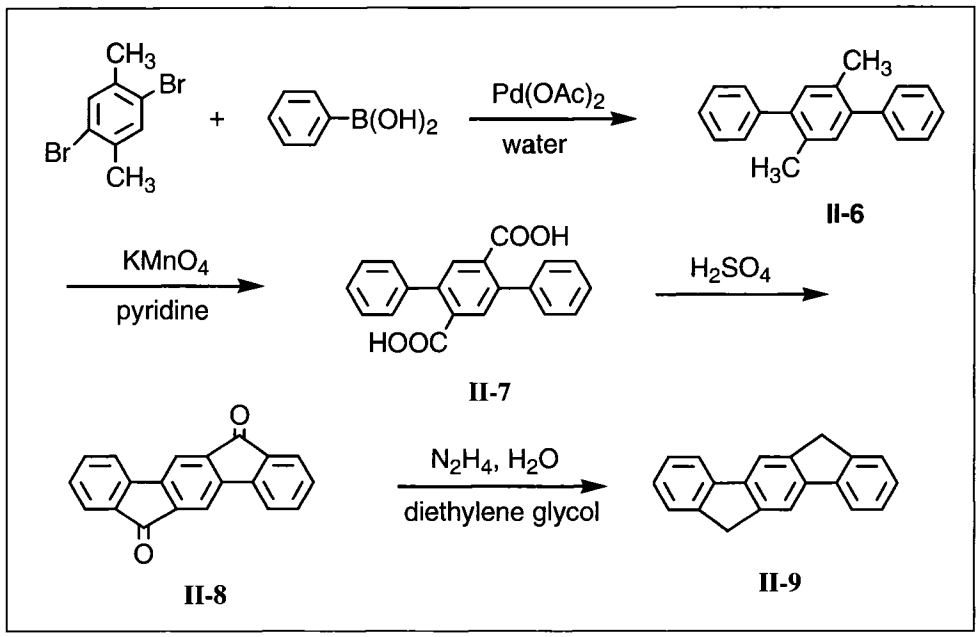

Scheme II.4. Synthetic route to indenofluorene (**II-9**)

It is also possible to start with a Suzuki coupling with 2,5-diiodo-1,4-xylene and 4-bromophenyl boronic acid to yield 2,5-bis(4-bromophenyl)-1,4-xylene. This compound that already carries bromine unites will be oxidized with the same method mentioned above. Closing step followed by the reduction of carbonyl group will give the key compound (2,6-dibromoindenofluorene). This route also includes five steps that will be described in following chapter in more details.

II.3.2. Bromination of indenofluorene

Three major methods can be used to brominate indenofluorene: a) bromine with mercuric oxide[11,12], b) alumina-supported copper(II) bromide[13,14] and c) electrophilic substitution on aromatic ring using bromine. The first method that goes through a free

radical pathway[15] has the advantage of being nontoxic because no hydrogen bromide is evolved during the reaction.[16] On the other hand, there is a possibility of bromination of two methylene groups with moderate yield. Using concentrate sulfuric acid can facilitate this reaction towards the brominated aromatic ring but there is no advantage over the conventional methods of electrophilic bromination. Aromatic hydrocarbons also react with copper(II) bromide supported by alumina under heterogeneous conditions in nonpolar solvents. The main disadvantage of this method is the difficulties in separation of product from alumina. It has been found that the simplest and more convenient method for bromination of indenofluorene is the electrophilic substitution (Scheme II.5).

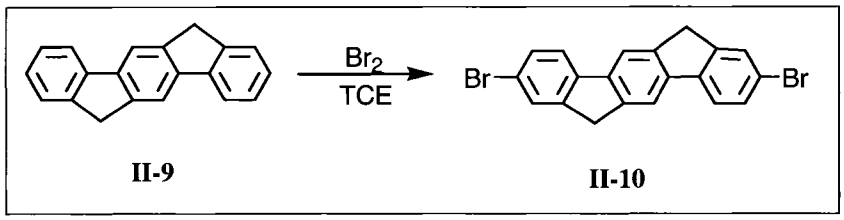

Scheme II.5. Synthesis of 2,6-dibromoindenofluorene as key compound

The position of the bromo group in compound **II-10** was confirmed by the crystal structure of one of the final products that will be described later in this chapter. However, mechanism of the reaction and number of resonance structures indicates that the orientation of electrophilic group like Br^+ is towards the *para* position. In principal, an activating group like phenyl ring directs *ortho* and *para* simply because it activates the *ortho* and *para* position much more than it does the *meta*. Therefore, there is a possibility of *ortho* substitution as well but since bromine is a very bulky element, the possibility of this direction is much less than *para* position.

II.3.3. Substitution of indenofluorene

Now that the key compound was synthesized and characterized, making a library with a series of 2,6-disubstituted indenofluorene was planed. To reach this goal, Suzuki coupling could be the best choice. As it was mentioned, the structure and reactivity of both starting materials affect on reaction, therefore, in some cases this synthetic route may not be a good choice. The Stille reaction can be another method, which allows to the coupling of the same dibromo compound with an organostannane material.

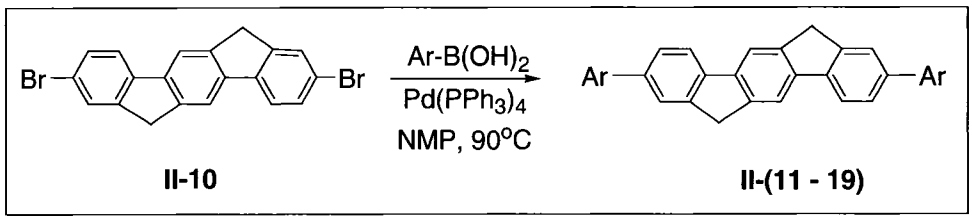

Scheme II.6. Substitution of aryl groups

The choice of substrates for both the Suzuki coupling and Stille reaction is limited to aryl, heteroaryl, vinylic, and benzylic halides, as the presence of an sp^3 carbon in β position carrying one hydrogen, rapidly results in β-hydride elimination because the oxidative addition step is slow. On the other hand, organoboron compounds bearing strongly electrophilic groups will stabilize the nucleophilic "ate" complex formed in transmetallation step, leading to either a very low yield or failure of the coupling.[1]

Table II.1. The results from the Suzuki reaction

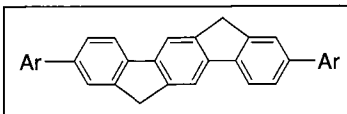	**Aryl group**	**Reaction Condition**	**Yield (%)**
II-11		90 °C, 24 h	51.7
II-12		100 °C, 24 h	44.3
II-13		90 °C, 24 h	19.8
II-14	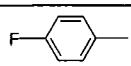	90 °C, 24 h	16.3
II-15	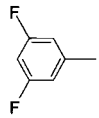	100 °C, 24 h	27.6
II-16	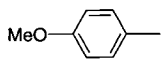	100 °C, 24 h	7.0
II-17	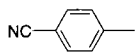	100 °C, 24 h	17.5
II-18		90 °C, 24 h	7.0
II-19	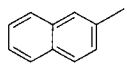	90 °C, 24 h	8.0

The general procedure for Suzuki coupling was the same as before, starting with the arylbromide mixed with the organoboron compound and catalyst stirring under inert gas (Scheme II.6). Solvent was then added and heated up to dissolve all the starting materials and base was the last to be added and heating was continued for appropriate time. Vacuum sublimation was the only way to purify all the products since none of them were soluble in common organic solvents. The results are summarized in Table II.1.

II.4. Characterization of indenofluorene derivatives

Characterizations of indenofluorene derivatives and all the intermediates were performed using infrared (IR), low and high-resolution mass spectroscopy (MS, HRMS), nuclear magnetic resonance (NMR), when solubility allowed, and crystallography. The melting points of all final products were measured by Differential Scanning Calorimetry (DSC).

II.4.1. Infrared Spectroscopy

Infrared spectroscopy is a powerful method to distinguish between the compounds with specific functional groups like a carbonyl units. This method can be used to identify a compound and to investigate the composition of a sample. As for the characterization of indenofluorenes, the only characteristic bond is C=C in aromatic ring that lies in all of them. It is expected that the peaks corresponds to the ring stretch absorption occur in pair at around 1600 cm^{-1} and 1475 cm^{-1} based on the structure of molecule.[17] From the infrared spectrum of all indenofluorene derivatives the presence of this peak can be observed (Table II.2).

Since the C-X absorption appears at very low frequency, it is difficult to determine the presence of halide in a compound using only infrared spectroscopy.

The peak related to the stretch of C≡N group occurs near 2250 cm^{-1} in medium intensity, but in the case of aromatic nitriles, this peak shifts to a lower frequency, near 2230 cm^{-1} due to conjugation with aromatic rings. This phenomenum can be clearly observed in the IR spectrum of compound **II-17**.

Table II.2. Characteristic IR peaks for indenofluorene derivatives

Compound	Characteristic IR peaks (cm^{-1})
II-5 or **II-11**	1595, 1485 (C=C aromatic)
II-12	1593, 1489 (C=C aromatic)
II-13	1593, 1489 (C=C aromatic)
II-14	1595, 1472 (C=C aromatic), 1224, 1121 (C-F aromatic)
II-15	1593, 1467 (C=C aromatic), 1228, 1115 (C-F aromatic)
II-16	1603, 1498 (C=C aromatic)
II-17	1602, 1491 (C=C aromatic), 2227 (C≡N nitrile)
II-18	1595, 1493 (C=C aromatic)
II-19	1595, 1493 (C=C aromatic)

Infrared spectroscopy was the best method to identify compounds **II-4** and **II-5** from the first synthetic route used for the synthesis of 2,5-diphenylindenofluorene due to the structural differences between two compounds. It was very important to convert all the ketone groups to methylene units. Compound **II-4** contains two ketone groups and has a strong peak at 1708 cm^{-1}. This peak is completely disappeared in the infrared spectrum of compound **II-5** (Figure II.4).

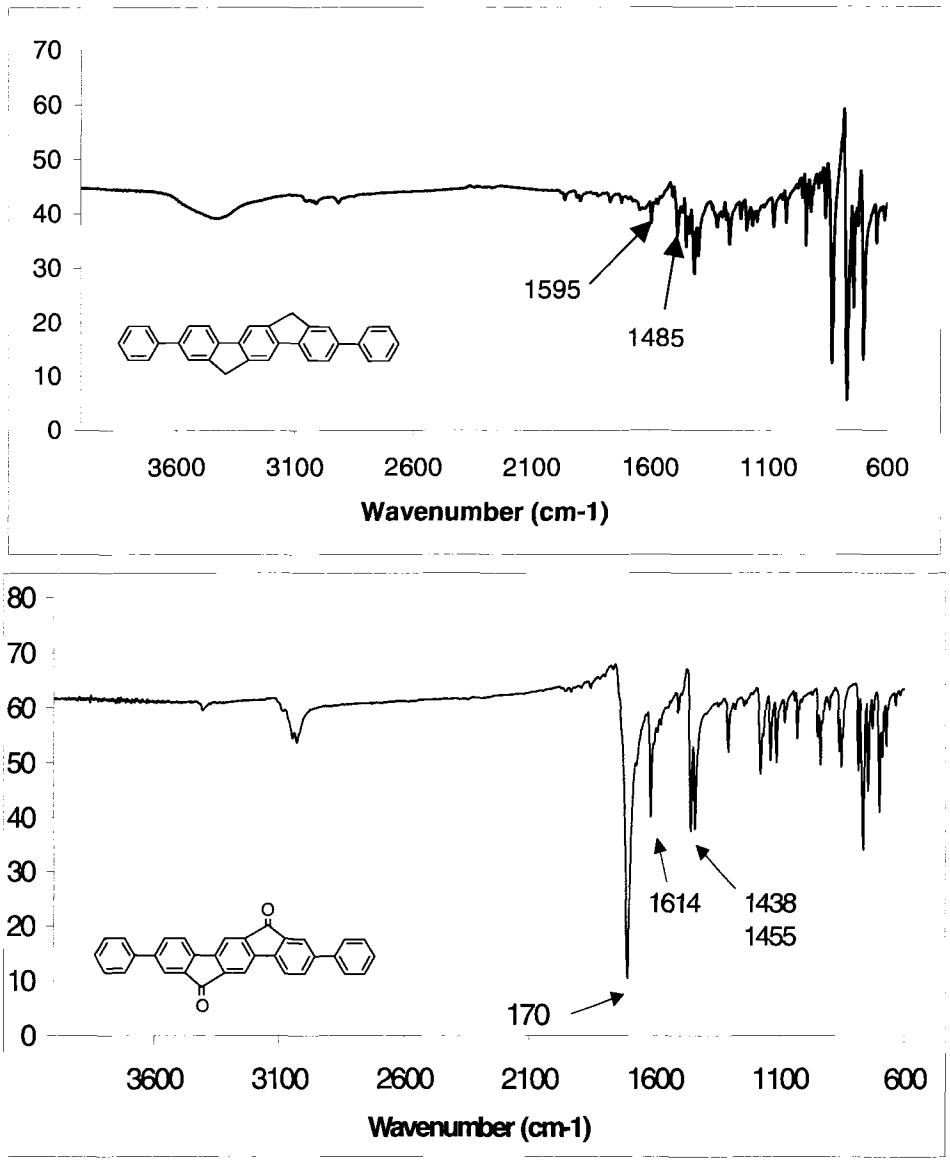

Figure II.4. Infrared spectra of compounds **II-4** and **II-5**

II.4.2. Mass Spectroscopy

Due to the poor solubility in common organic solvents, characterization of indenofluorene derivatives is limited to the mass spectroscopy. From the mass spectroscopy not only the mass of an unknown compound can be identified but also the isotopic composition of elements in a molecule as well as the structure of a compound by observing its fragmentation can be determined.

Due to the stability of the molecular ion of indenofluorene derivatives, electron impact (EI) technique is used in mass spectroscopy. In this method a high energy beam of electrons is used to remove an electron from the organic molecule to form a radical cation ($M^{+\cdot}$), known as the molecular ion, which can then fragment to give other smaller pieces. The fragment ions may either be radical cations or carbocations, depending on the nature of the fragments. With a high precision the weight of this ion is the actual molecular weight of the original molecule because it is only missing one electron. For example, in mass spectrum of 2,6-diphenylindenofluorene the most intense peak corresponds to molecular ion at *m/e* 406 (Figure II.5).

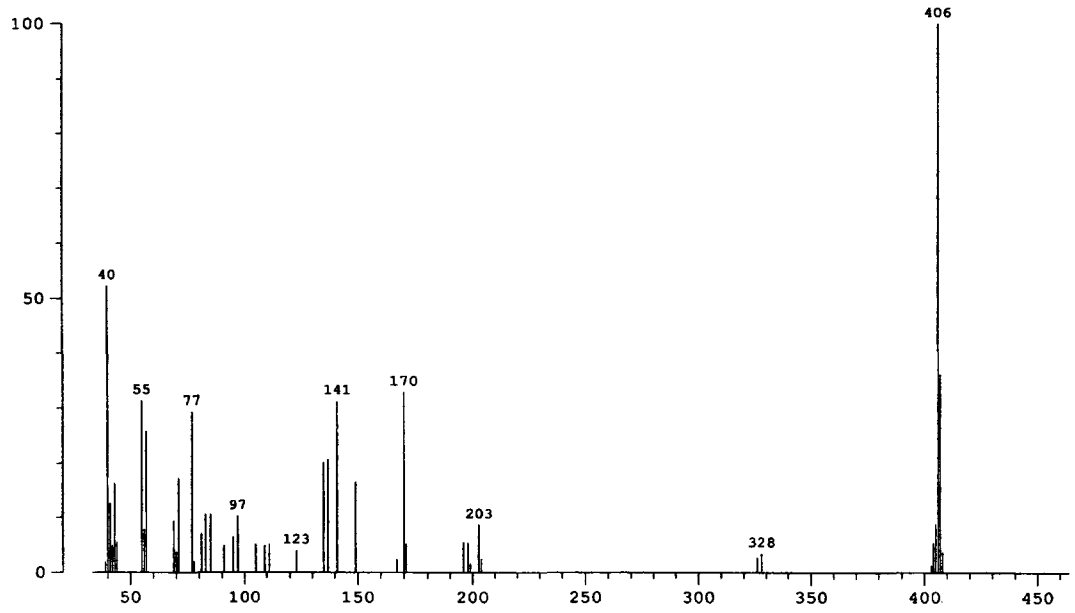

Figure II.5. Mass spectrum of 2,6-diphenylindenofluorene (**II-11**)

Since a mass spectrometer separates and detects ions of slightly different masses, it easily distinguishes different isotopes of a given element. This is manifested most dramatically for compounds containing bromine. Since bromine has two isotopes with the natural abundance of ^{81}Br which is 98.0% that of ^{79}Br, the *M+2* peak with the intensity

almost equal to the intensity of molecular ion peak becomes very significant to identify if the molecule contains one bromine atom. In the case of two bromine atoms in molecule a quite distinct *M+4* peak will be observed. In this case, the intensity of *M+4* peak is almost equal to molecular ion peak while the intensity of *M+2* peak rises twice due to the alternative possibility of presence of each isotope in molecular structure. These phenomena can be observed in mass spectrum of 2,6-dibromoindenofluorene (**II-10**) and the ratio of peaks confirms the presence of two bromines in molecular structure (Figure II.6).

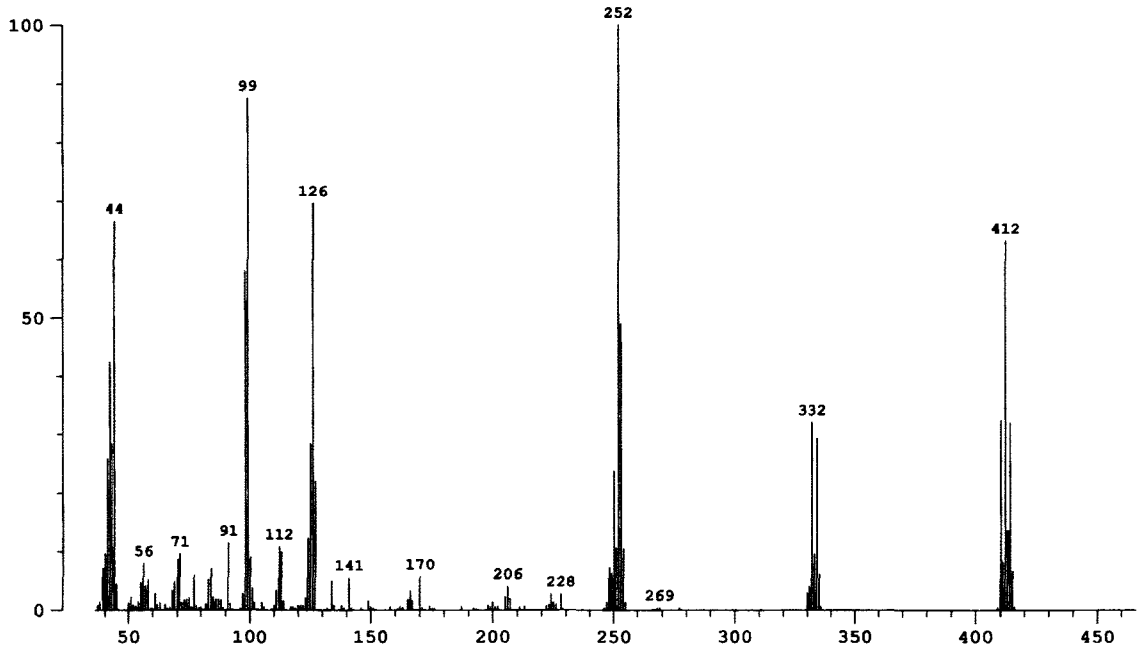

Figure II.6. Mass spectrum of 2,6-dibromoindenofluorene **(II-10)**

Molecular ion peak appeared at *m/e* 410 while *m/e* 412 indicates the *M+2* (twice intensity of molecular ion) and *M+4* peak is observed at *m/e* 414 (equal intensity with molecular ion).

The molecular ion peaks for indenofluorene derivatives are presented in Table II.3.

Table II.3. Molecular ion peaks for indenofluorene derivatives

Compound	Molecular formula	Molecular mass (intensity %)
II-4	$C_{32}H_{18}O_2$	434 (100)
II-5 or **II-11**	$C_{32}H_{22}$	406 (100)
II-10	$C_{20}H_{12}Br_2$	410 (43.1)
II-12	$C_{28}H_{18}S_2$	418 (100)
II-13	$C_{28}H_{18}S_2$	418 (100)
II-14	$C_{32}H_{20}F_2$	442 (100)
II-15	$C_{32}H_{18}F_4$	478 (100)
II-16	$C_{34}H_{26}O_2$	466 (24.6)
II-17	$C_{34}H_{20}N_2$	456 (100)
II-18	$C_{40}H_{26}$	506 (100)
II-19	$C_{40}H_{26}$	506 (4.8)

II.4.3. X-ray Crystallographic Study

Since indenofluorene derivatives are not soluble in any common organic solvents, single-crystal X-ray diffraction study is the best method to deduce the details of molecular structure if compounds form an appropriate single crystal. There are three different methods for crystallization of small molecules, diffusion gradient, concentration

through evaporation and sublimation. Due to poor solubility of indenofluorene derivatives, sublimation was the only choice to make the crystals.

The X-ray structure of 2,6-diphenylindenofluorene is presented in Figure II.7. The molecular structure exhibits a torsion angle of 29.6° for C(10)-C(9)-C(11)-C(16). This result reveals that the total structure of molecule is not planar, therefore the conjugation of molecule will be affected even though it has been reported that the torsion angles below 30° dose not affect the conjugation of molecules. Since a small band gap resulted from high conjugation length depends on planarity of molecules, changes in torsion angle can affect absorption and emission of these compounds. The position of two phenyl groups in both ends of the molecule reveals the selective bromination of indenofluorene, while mass spectroscopy could only show the presence of two bromo units in molecular structure but not the exact position. The X-ray diffraction analysis also corroborated the structure of other eight compounds in the series. The results confirmed the successful bromination and coupling reactions.

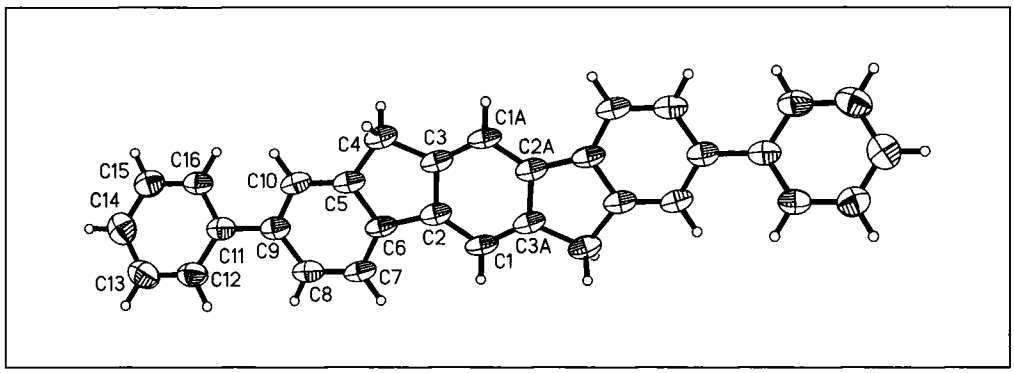

Figure II.7. ORTEP structure of 2,6-diphenylindenofluorene

II.4.4. Thermal Property

Since indenofluorene derivatives are to be used in OLEDs and transistors, their thermostability is one of the major factors needed to be determind. Thermogravimetric analysis (TGA) is a method in which the changes in the weight (mass) of a sample as a function of temperature and/or time can be measured and differential scanning calorimetry (DSC) measures the energy absorbed or released by a sample as a function of temperature or time. When thermal transition occurs in the sample, DSC provides a direct calorimetric measurement of the transition energy at the temperature of the transition. Therefore it can be an appropriate method to measure the melting point of compounds in endothermic phase transition from solid to liquid and the crystallization temperature of compounds when they undergo exothermic processes from liquid to solid.

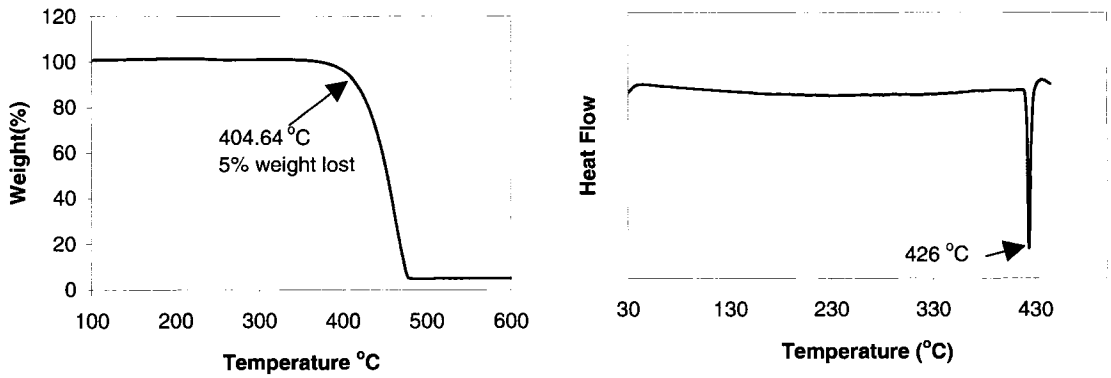

Figure II.8. TGA (left) and DSC traces (right) of 2,6-diphenylindenofluorene

Due to its high accuracy for measuring both endothermic and exothermic phase transitions, DSC was used to determine the melting points of indenofluorene derivatives. Melting points of the products were in the range of 337-426 °C. The decomposition temperatures (T_d), as assessed by the onset temperature of 5% weight loss by TGA,

occurred in the range of 374-423 °C under nitrogen atmosphere (Table II.4). The results of TGA analysis were in good accordance with the DSC results, as 5% weight loss of 2,6-diphenylindenofluorene was at 404 °C under nitrogen atmosphere. The DSC revealed the melting transitions at 426 °C for this compound (Figure II.8). The high melting point (above 360 °C) is also observed for the other indenofluorene derivatives (Table II.4). Among all, compounds **II-(14-15)** and **II-(17-18)** were crystallized upon cooling.

Table II.4. Thermal stability of indenofluorene derivatives

Compound	Melting Point (T_c,°C)[a]	Decomposition Temperature (°C)[b]
II-11	426	404
II-12	362	409
II-13	NA	410
II-14	392 (338)	379
II-15	397 (385)	358
II-16	NA	423
II-17	389 (380)	NA
II-18	337 (281)	NA
II-19	NA	347

[a] DSC analysis under N_2 at a heating rate of 10 °C/min, T_c is the crystallization temperature.
[b] Temperature for 5% weight loss, as assessed by TGA under N_2 at a heating rate of 20 °C/min.

II.5. Conclusion

The synthesis of a series of nine aryl-substituted indenofluorenes containing thienyl, naphthyl and phenyl rings was successfully performed. A general route to indenofluorenes involves the use of 2,6-dibromoindenofluorene as a key compound. By

vacuum sublimation the final products were obtained in high purity. The indenofluorene derivatives were fully characterized by mass and infrared spectroscopies. Among all, 2,6-diphenylindenofluorene formed single crystals during the sublimation and its structure was determined by X-ray crystallography. The X-ray results also confirm the selective bromination of indenofluorene at the 2 and 6 positions and thus the positions of the two aryl groups in indenofluorene derivatives.

II.6. Experimental Section

Materials and Measurments

All starting materials and reagents were purchased from Aldrich Canada Inc. unless otherwise stated. All reagents were used as received without further purification. All the final products were purified by sublimation (Carbolite, CTF 12/65/550). Infrared measurements were performed on a Varian 1000 FT-IR Scimitar series. ^{1}H NMR and ^{13}C NMR were measured by a Bruker AMX-400 spectrophotometer, respectively. Melting points of all final products were recorded on Differential Scanning Calorimetry (DSC) on DSC Q100 Instrument at a heating rate of 10 ^{o}C/min under nitrogen. Decomposition temperature of products were measured on Thermogravimetric Analyzer (TGA) on TGA 2950 CE Instrument at a heating rate of 20 ^{o}C/min. The University of Ottawa Mass Spectroscopy Center performed mass spectral analysis. X-ray diffraction analysis was also done in University of Ottawa. The measurement was made on a Bruker SMART 1K CCD diffractometer with graphite monochromated MoKα (0.71073 Å) radiation. The data was collected at a temperature of 205(2) K and the structure was solved by direct methods and expanded by Fourier techniques using SHELXTL. All non-hydrogen atoms

were refined anisotropically. Hydrogen atoms were included in idealized positions and not refined. Data were merged and corrected for beam inhomogeneous and absorption using SADABS.

Synthesis of dimethyl 2,5-dibromoterephthalate (II-1)

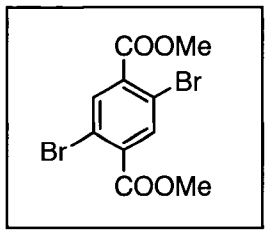

A 250 mL, one-necked, round-bottomed flask equipped with a condenser and magnetic stirrer was charged with dibromoterephthalic acid (10.0 g, 30.0 mmol), methanol (150 mL) and sulfuric acid (2.5 mL). After being refluxed for 5 h, the reaction mixture was cooled to room temperature. The white solid (10.5 g, 96%) was collected after filtration and dried at 60 °C in a vacuum oven overnight. Crystallization was done using dichloromethane/methanol. Mp: 140 °C (DSC); ^{1}H NMR (DMSO-d_6, 400 MHz) δ_H 8.08 (s, 2 H), 3.87 (s, 6 H); ^{13}C NMR (DMSO-d_6, 100 MHz) δ_C 164.25, 135.95, 135.26, 118.95, 53.00.

Synthesis of dimethyl 2,5-bis(4-biphenyl)terephthalate (II-2)

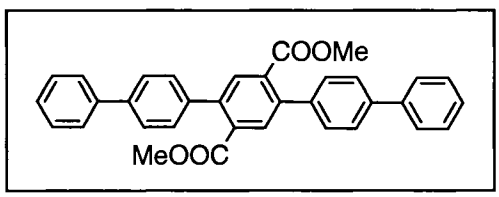

An argon-flashed, three-necked, round-bottomed flask was charged with 2,5-dibromoterephthalate (3.860 g, 10.0 mmol), 4-biphenylboronic acid (5.400 g, 27.0 mmol)

and $Pd(PPh_3)_4$ (0.193 g, 0.2 mmol). 1,2-Dimethoxyethane (DME, 250 mL) was then added while the mixture was stirred under argon, followed by addition of a solution of Na_2CO_3 (12.4 g dissolved in minimum volume of water). The progress of the reaction was followed by TLC using ethyl acetate / hexane (2/3, V/V) as eluent. After being heated at 90 °C for 24 h it was then cooled to room temperature. The precipitate was filtered, washed with water and dried at 60 °C in a vacuum oven. After sublimation, the white solid was obtained: 5.000 g (91.5%); Mp: 275 °C (DSC); MS (EI, *m/z*): 498 (M^+, 100%); ^1H NMR (DMSO-d_6, at 330 °K, 400 MHz) δ_H 7.81 (s, 2H), 7.76-7.71 (m, 8H), 7.50-7.45 (m, 8H), 7.40-7.35 (m, 2H), 3.67 (s, 6H).

Synthesis of 2,5-bis(4-biphenyl)terephthalic acid (II-3)

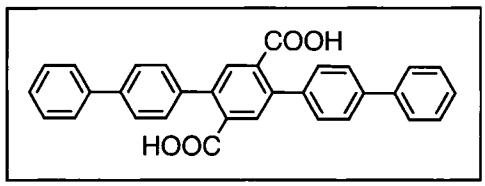

In a two-necked, round-bottomed flask 2.000 g (4.0 mmol) of **II-2** was mixed with 300 mL of DME and the reaction mixture was heated up to 90 °C. Sodium hydroxide solution (60 mL, 10%) was then added in different portions and heating was continued for overnight. It was cooled to room temperature and filtered to remove insoluble particles. The reaction solution was poured into hydrochloric acid solution (20%) and put in ice bath for 30 min. The white solid was filtered and washed with water. Recrystallization from dimethoxy ethane (DME) gave white crystals (1.860 g) in 98.5% yield. Mp: 375 °C (DSC); ^1H NMR (DMSO-d_6, 400 MHz) δ_H 13.23 (s, 2H), 7.78 (s, 2H), 7.75 (d, 8H, J=9.8 Hz), 7.55-7.49 (m, 8H), 7.40 (dd, 2H, J=15.4 Hz). ^{13}C NMR (DMSO-

d_6, 100 MHz) δ_C 168.83, 139.57, 139.38, 139.20, 138.63, 134.26, 131.01, 129.04, 128.95, 127.64, 126.67, 126.61.

Synthesis of 2,6-diphenylindenofluorenone (II-4)

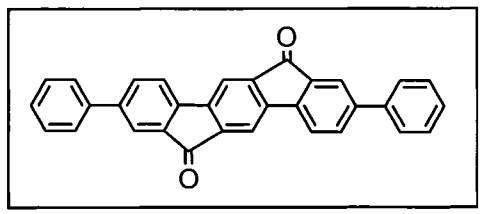

A three-necked flask connected to a condenser was charged with compound **II-3** (1.900 g, 4.0 mmol). After being 15 min under argon gas, the Eaton's reagent (65 mL) was added and the reaction mixture was heated up to 90 °C for 4 h. It was then cooled to room temperature and poured into ice. The reddish solid was collected by filtration, washed with water and dried at 80 °C in vacuum oven. The product was further purified by vacuum sublimation to give red crystals (1.750 g, 99.7%); Mp: 400 °C (DSC); MS (EI, *m/z*): 434 (M^+, 100%); HRMS calcd. for $C_{32}H_{18}O_2$: 434.13068, found: 434.13206; IR (KBr): 1707.7 (C=O) cm^{-1}.

Synthesis of 2,6-diphenylindenofluorene (II-5)

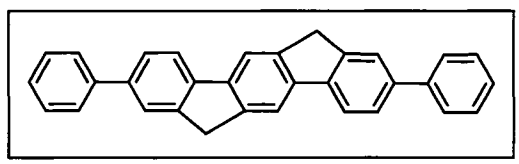

A modified Wolff-Kishner reduction was used to synthesis 2,6-diphenylindenofluorene. In a two-neck flask connected to a reflux condenser, 230 mL of commercial diethylene glycol and 10.2 g (180.0 mmol) of potassium hydroxide were

placed. The mixture was heated until the potassium hydroxide melted (140 °C) and went into solution. It was then cooled to about 80 °C and 2,6-diphenylindenofluorenone (3.000 g, 6.9 mmol) and 23 mL (23.2 g, 460.0 mmol) of 98% hydrazine monohydrate were added. The reaction mixture was heated up to 195-200 °C for 48 h. At the end of the heating period the reaction mixture was cooled and was then poured into 600 mL of hydrochloric acid (20%), stirred for a while and put in ice bath for 30 min. The light green solid was filtered, washed with water and dried at 80 °C in vacuum oven. The final product was then purified by vacuum sublimation to give yellow crystals (1.600 g, 57.2%); Mp: 426 °C (DSC); MS (EI, *m/z*): 406 (M^+, 100%).

Synthesis of 2,5-diphenyl-1,4-xylene (II-6)

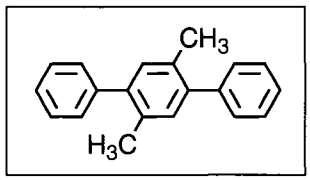

To a 100 mL flask flushed with argon and equipped with a rubber septum and a stirring bar, 2,5-dibromo-1,4-xylene (5.000 g, 18.9 mmol), phenylboronic acid (5.075 g, 41.6 mmol), palladium (II) acetate (0.009 g, 37.8×10^{-3} mmol), potassium carbonate (13.1 g, 94.7 mmol) and tetrabutyl ammonium bromide (n-Bu_4NBr, 12.2 g, 37.9 mmol) were placed. Water (42 mL) was added through a syringe and the resulting suspension was vigorously stirred under argon for 30 min. The reaction mixture was then heated up to 70 °C for 2 h, all the times under argon. After cooling to room temperature, it was diluted with some more water and extracted with toluene. The organic layer was dried over $MgSO_4$, filtered and the solvent was evaporated. The residue was purified by washing

with potassium hydroxide (KOH) solution and checked by TLC using hexane/toluene (4/1) as eluent to give pure product as white powder (4.820 g, 98.6%).

Synthesis of 2,5-diphenylterephthalic acid (II-7)

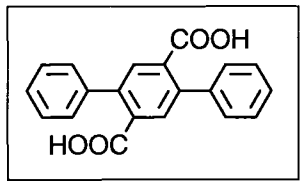

To a mixture of 2,5-diphenyl-1,4-xylene (5.000 g, 19.4 mmol) and potassium permangenate (14.4 g), 100 mL of pyridine and 10 mL of water were added and the reaction mixture was heated to reflux. After about one hour reflux, the color of reaction mixture turned brown showing that all the potassium permangenate went into the reaction and more reagent was needed. Each 30 min, some potassium permangenate and water was added and reflux was continued for overnight. It was then filtered hot and washed with boiled water. All the pyridine and some of the water were evaporated using rotary evaporator and the PH of mixture changed to 2.0 by addition of concentrated hydrochloric acid. The pure white powder was filtered and dried at 50 ^{o}C in a vacuum oven (5.640 g, 91.5%). IR spectrum approved the product and the purity of it was checked by TLC (methanol as a solvent).

Synthesis of indenofluorenone II-8

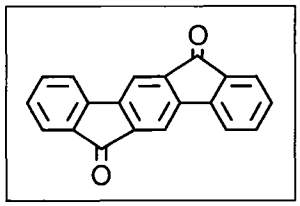

In an erlen mayer equipped with an stirring bar, the 2,5-diphenylterephthalic acid (2.000 g, 6.3 mmol) was dissolved in 100 mL of concentrated H_2SO_4. The dark green solution was stirred for two hours at room temperature. It was then poured in a big portion of ice very slowly. After about 30 min, the purple product was filtered and washed with cold water. The solid was then stirred in a concentrated potassium carbonate solution (this step needs more caution) for a few hours, filtered and purified by potassium hydroxide solution and washed with water several times, filtered again and dried at 100 ^{o}C in vacuum oven to give purple powder (1.700 g, 95.8%); IR: 1707 (C=O) cm^{-1}.

Synthesis of indenofluorene II-9

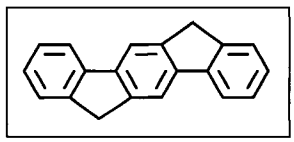

Indenofluorene was synthesized by the Wolff-Kishner reduction of indenofluorenone (**II-8**). In a one-necked, round-bottomed flask, 3.000 g of indenofluorenone (10.6 mmol) was suspended in 65 mL of diethylene glycol. Potassium hydroxide (9.7 g) and hydrazine monohydrate (10.5 mL) were added and the purple reaction mixture was heated at 190 ^{o}C for 48 hours. It was then cooled to room temperature and poured in HCl solution (PH=2). The yellow precipitate was filtered,

washed with more water and dried in vacuum oven to give the crude product (3.200 g). The product was purified by vacuum sublimation (2.112 g, 78.2%).

Synthesis of 2,6-dibromoindenofluorene (II-10)

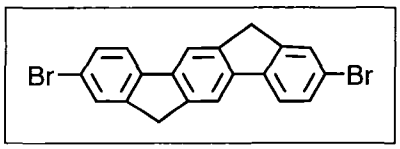

In a three-necked, round-bottomed flask (150 mL) equipped with a condenser and stirring bar, 120 mL of tetrachloroethane (TCE) was added to indenofluorene (1.000 g, 3.9 mmol) and heated up to 80 °C to dissolve all starting materials. It was then cooled down to room temperature and Br_2 (0.500 g, 9.8 mmol) diluted in small portion of TCE, was added dropwise. The reaction mixture was stirred at room temperature for overnight. The yellow solid was filtered and dried (1.240 g, 76.5%). Vacuum sublimation had been applied for further purification; MS (EI, *m/z*): 412 (M^+, 100%); Mp: 346 °C (DSC).

Synthesis of 2,6-diphenylindenofluorene (II-11)

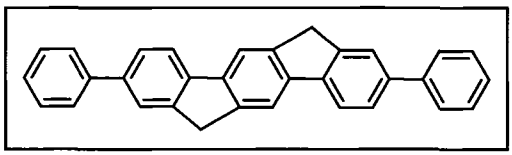

To a mixture of 2,6-dibromoindenofluorene (0.100 g, 2.4×10^{-1} mmol), phenylboronic acid (0.074 g, 0.6 mmol) and terakis(triphenylphosphine)palladium(0) (0.039 g) was added 20 mL of NMP and the reaction mixture was heated up to 90 °C. It was stirred for one hour under argon and then a solution of 0.515 g sodium carbonate was added and heating was continued for overnight. It was then cooled to room temperature

and crude product was poured in water, filtered, washed with more water and dried. Vacuum sublimation was used to purify the final product. The yellow solid was obtained and checked by mass spectroscopy that shows the high purity of compound (0.051 g, 51.7%); Mp: 426 °C (DSC); MS (EI, *m/z*): 406 (M^+, 100%).

Synthesis of 2,6-bis(2-thienyl)indenofluorene (II-12)

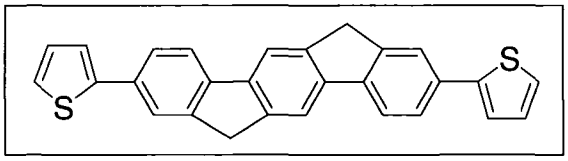

Dibromoindenofluorene **II-10** (1.000 g, 2.4 mmol), 2-thiopheneboronic acid (0.930 g, 7.3 mmol) and tetrakis(triphenylphosphine)palladium(0) (0.386 g, 3.3×10^{-1} mmol) were dissolved in 1-methyl-2-pyrrolidinone (NMP) (200 mL) at 90 °C. Argon was bubbled through this reaction solution for one hour to remove dissolved oxygen. To the reaction solution was added an aqueous solution of sodium carbonate (5.150 g) and the mixture was heated at 100 °C for overnight all the times under argon environment. The resulting precipitates were filtered, washed with water and dried. The yellow solid product was then purified by vacuum sublimation (0.450 g, 44.3%); Mp: 362 °C (DSC); MS (EI, *m/z*): 418 (M^+, 100%); HRMS calcd. for $C_{28}H_{18}S_2$: 418.08499, found: 418.08347.

Synthesis of 2,6-bis(3-thienyl)indenofluorene (II-13)

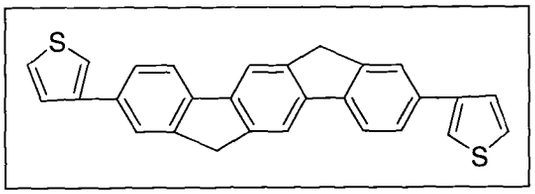

Dibromoindenofluorene (0.100 g, 2.4×10^{-1} mmol), 3-thiophenboronic acid (0.093 g, 7.3×10^{-1} mmol) and terakis(triphenylphosphine)Palladium(0) (0.039 g) were placed in a three-necked, round-bottomed flask. Then the solvent (NMP, 20 mL) was added and the reaction mixture was heated up to 90 °C. After one hour stirring under argon, a solution of 0.515 g sodium carbonate was added and heating was continued for overnight. After cooling to room temperature, the crude product was filtered, washed and dried. Vacuum sublimation was applied to purify the final product. The yellow solid was obtained and checked by Mass spectroscopy that shows the high purity of compound; (0.020 g, 19.8%); MS (EI, *m/z*): 418 (M^+, 100%).

Synthesis of 2,6-bis(4-fluorophenyl)indenofluorene (II-14)

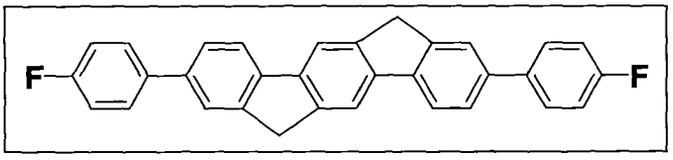

The same procedure of compound **II-11** had been used to synthesize this product. Dibromoindenofluorene **II-10** (0.150 g, 3.6×10^{-1} mmol), 4-fluorophenylboronic acid (0.127 g, 0.9 mmol) and terakis(triphenylphosphine)Palladium(0) (0.058 g) were dissolved in 30 mL of NMP at 90 °C under argon atmosphere. To this reaction solution an aqueous solution of sodium carbonate (0.772 g) was added and the reaction was heated up to 100 °C for overnight. It was then cooled to room temperature, filtered and

washed with water and dried. The final product was purified by vacuum sublimation to yield the yellow solid (0.026 g, 16.2%); Mp: 392 °C (DSC); MS (EI, *m/z*): 442 (M^+, 100%).

Synthesis of 2,6-bis(3,5-difluorophenyl)indenofluorene (II-15)

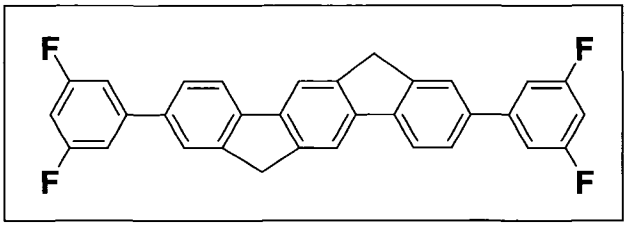

The reaction procedure and the ratio of starting materials were the same as for **II-14**. Dibromoindenofluorene **II-10** (0.150 g, 3.6×10^{-1} mmol), 3,5-difluorophenylboronic acid (0.144 g, 0.9 mmol) and terakis(triphenylphosphine)Palladium(0) (0.058 g) were dissolved in 30 mL of NMP. A solution of sodium carbonate (0.800 g) was then added under argon followed by heating up to 100 °C for overnight. Crude product was filtered, washed and dried. The product was purified by vacuum sublimation as a yellow solid (0.048 g, 27.6%); Mp: 397 °C (DSC); MS (EI, *m/z*): 478 (M^+, 100%).

Synthesis of 2,6-bis(4-methoxyphenyl)indenofluorene (II-16)

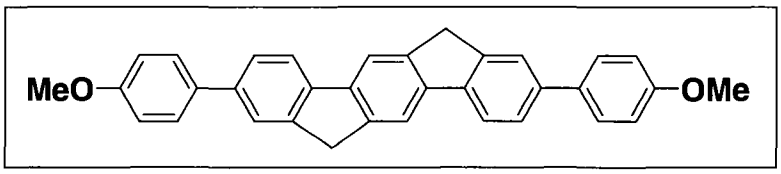

Dibromoindenofluorene (0.150 g, 3.6×10^{-1} mmol) was used to react with 4-methoxyphenylboronic acid (0.138 mg, 0.9 mmol) in the presence of terakis(triphenylphosphine)Palladium(0) (0.058 g). The rest of the reaction condition was

the same as **II-12**. The reaction yield was too low after vacuum sublimation. The mass spectrum of light yellow product showed high purity. MS (EI, *m/z*): 466 (M^+, 100%). HRMS calcd. for $C_{34}H_{26}O_2$: 466.19328, found: 466.19482.

Synthesis of 2,6-bis(4-cyanophenyl)indenofluorene (II-17)

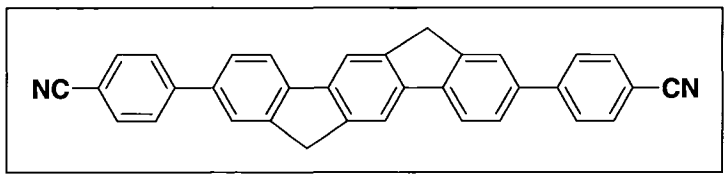

Dibromoindenofluorene (0.150 g, 3.6×10^{-1} mmol) was reacted with 4-cyanophenylboronic acid (0.134 g, 0.9 mmol) in the presence of 0.058 g terakis(triphenylphosphine)Palladium(0), 0.772 g of sodium carbonate and 30 mL of NMP under argon at 100 °C. After washing and drying the crude product it was vacuum sublimated to have the pure yellow solid (0.029mg, 17.5%). Mass spectroscopy confirmed the product (EI, *m/z*): 456 (M^+, 100%).

Synthesis of 2,6-bis(1-naphthyl)indenofluorene (II-18)

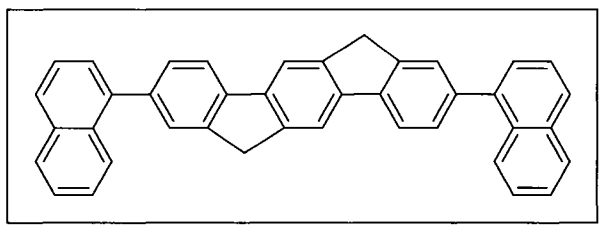

The reaction procedure was exactly the same as for **II-11**. The dark orange solid was 0.013 g (7%); MS (EI, *m/z*): 506 (M^+, 100%).

Synthesis of 2,6-bis(2-naphthyl)indenofluorene (II-19)

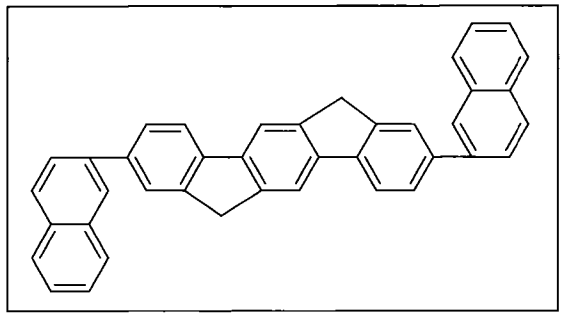

Dibromoindenofluorene (0.150 g, 3.6×10^{-1} mmol) was reacted with 2-naphthaleneboronic acid (0.157 g, 0.9 mmol) under the Suzuki coupling reaction. The reaction condition and the ratio of starting materials were the same as for **II-11**. Vacuum sublimation was used to purify the product. The yellow solid was 0.015 g (8.2%) with high purity. Product was characterized by low and high resolution mass spectroscopy. MS (EI, *m/z*): 506 (M^+, 100%); HRMS calcd. for $C_{40}H_{26}$: 506.20345, found: 506.20217.

References

1. Clayden, J.; Greeves, N.; Warren, S.; Wothers, P. *Organic Chemistry*, Oxford, Chapter 48.
2. Deuschel, W. *Helv. Chim. Acta.* **1951**, *34*, 2043.
3. Chardonnens, L.; Laroche, B.; Sieber, W. *Helv. Chim. Acta.* **1974**, *57*, 585.
4. Wallow, T. I.; Novak, B. M. *J. Org. Chem.* **1994,** *59*, 5034.
5. Suzuki, A.; Brown, H. C. *Organic Syntheses Via Boranes. Volume 3. Suzuki Coupling.* Aldrich Chemical Company, Inc. **2003**.
6. Miyaura, N.; Suzuki, A. *Chem. Rev.* **1995**, *95*, 2457.
7. Patai, S. *The Chemistry of the Quionoid Compounds*, John Wiley & Sons, London-New York- Sydney- Toronto, **1974**. 136.

8. Seong, M. R.; Kim, J. N. *Bulletin of the Korean Chemical Society.* **1999,** *20,* 1249.

9. Morrison, R. T.; Boyd, R. N. *Organic Chemistry.* Fourth edition. Allyn and Bacon, Inc. 1**983**.

10. Merlet, S.; Birau, M.; Wang, Z. Y. *Org. Lett.* **2002**, *4*, 2157.

11. Hassan, J.; Gozzi, C.; Schulz, E.; Lemaire, M. *J. Organomet. Chem.* **2003,** *687,* 280.

12. Miller, L. L.; Yu, Y. *J. Org. Chem.* **1995,** *60*, 6813.

13. Kodomari, M.; Satoh, H.; Yoshitomi, S. *J. Org. Chem.* **1988,** *53*, 2093.

14. Ranger, M.; Rondeau, D.; Leclerc, M. *Macromolecules* **1997,** *30*, 7686.

15. Bunce, N. J. *Can. J. Chem.* **1972,** *50*, 3109.

16. Afzal Khan, S.; Munawar, M. A.; Siddiq, M. *J. Org. Chem.* **1988,** *53*, 1799.

17. Pavia, D. L.; Lampman, G. M.; Kriz, G. S. *Introduction to spectroscopy.* Third edition. Harcourt College Publishers, **2001**.

Chapter III

Electronic and Optical Properties of Indenofluorene Derivatives

III.1. Introduction

Conjugated aromatic compounds are potential candidates as organic semiconductors for use in thin-film transistors (TFTs) and light-emitting diodes (LEDs). By incorporation of strongly electronegative substituents such as fluorine[1] and cyano groups[2] into certain aromatic molecules, some important n-type compounds have been obtained for TFT applications. To develop organic LED devices (OLEDs) with uniform luminescence, saturated color, and low driving voltages, many materials factors must be considered, such as emission efficiency, color purity, carrier mobility, thermal and chemical stability, and processability (for vapor-phase deposition).[3]

Among those organic semiconductors known for transistor and OLED applications, the fluorene-based compounds,[4] oligomers,[5] and polymers[6] have received most attention, owing to their unique properties, availability, and processability. Since the substituted fluorenes are known to have relatively high band gaps and low HOMO levels, they are stable to photo- and electro-oxidation and the related devices have shown high on/off ratios with good aging characteristics.[7]

Fluorene is a rigid and planar molecule, due to the methylene bridging unit at the 2,2′-positions of the biphenyl moiety, with high thermal stability.[8] Since its electronic and optical properties arise from its planar biphenyl moiety, it is conceivable that the structurally related compound, indenofluorene, should have some unique electronic and optical characteristics, attributable to a planar, longer conjugated *p*-terphenyl moiety.

A new series of indenofluorene derivatives (nine compounds) with aryl groups at the terminal 2,6-position were synthesized and the chemical structure of the compounds were confirmed (Chapter II). Due to the extended conjugation length, the band gaps of

the resulting compounds are expected to decrease, leading to the emission of light at longer wavelengths. The potential applications of such compounds are in OLEDs and transistors as emitter layers. On the other hand, it was expected that by the insertion of the strong electronegative units such as fluorine and cyano groups in molecular structure, the LUMO level of the compounds would decrease, resulting the n-type materials to be used in LEDs as electron transport components. Therefore, the objective of current chapter is to correlate the relationship between the extended conjugation lengths of the compounds and their optical and electronic properties.

III.2. Electronic Properties

III.2.1. Electrochemical Study

Among all nine compounds mentioned in Chapter II, the electrochemical behavior of compounds **II-(11-13)** was tested and the energy levels were determined using the data from cyclic voltammetry and absorption spectra.[9] Table III.1 summarizes the oxidation potentials derived from the cyclic voltammograms of the compounds. However, like many conjugated organic compounds, the electrochemical processes were not reversible, since no reduction peaks were observed. This means that the reduction states of the compounds are not stable.

The highest occupied molecular orbital (HOMO) of the compounds were calculated using the onset potential of the oxidation waves. By calculating with the HOMO-LUMO band gaps measured from the absorption spectra, the LUMO levels of the compounds were determined (Table III.1). Among these three compounds, **II-13** is the weakest p-type material due to the lowest HOMO, while its LUMO level makes it a

suitable n-type compound. The highest HOMO level of compound **II-12** reveals that it can be used as p-type material better than the other two.

Table III.1. Electrochemical properties of Compounds **II-(11-13)**

Compound	E_{ox} (V)[a]	HOMO (eV)	E_g (eV)[b]	LUMO (eV)
II-11	0.82	5.30	3.30	2.00
II-12	0.55	5.10	3.10	2.00
II-13	1.18	5.80	3.20	2.60
II-11 (Film)	0.78	5.17	3.00	2.17

[a] Redox potential versus NHE; Performed in propylene carbonate containing 0.1M $LiClO_4$
[b] Optical band gap

The electrochemical characteristics of compound **II-11** in thin film are displayed in Table III.1. The thin film was prepared by vacuum deposition of 2,6-diphenylindenofluorene on ITO and the CV was measured in 0.1M solution of $LiClO_4$ in acetonitrile. The oxidization process occured at 0.78 V (Figure III.1) and the HOMO level was calculated from the on-set potential of the peak. The higher HOMO level of the compound **II-11** in thin film compared to the solution corresponds to the well-packed film which causes the higher conjugation length. This result is in agreement with the lower optical band gap observed for the thin film.

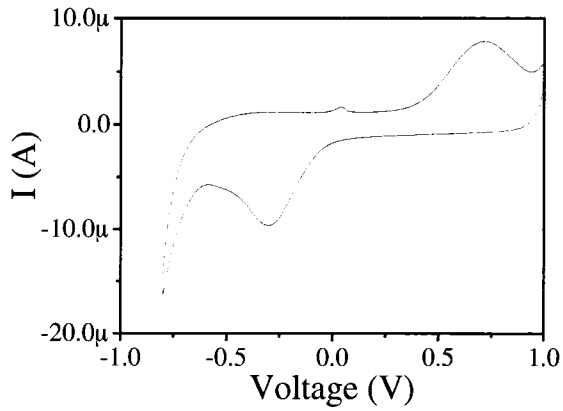

Figure III.1. Cyclic voltammogram of 2,6-diphenylindenofluorene thin film in 0.1M solution of $LiClO_4$ in acetonitrile

III.2.2. Transistor Characteristics

III.2.2.1. OLED Devices

In order to determine that compound **II-11** is either a p-type or an n-type semiconductor, the single-layer devices with the configuration of ITO/**II-11**/A1 and ITO/**II-11**/Au were fabricated. The I~V characteristic of former device showed a diode behavior, while a resistant behavior was observed in the latter device.

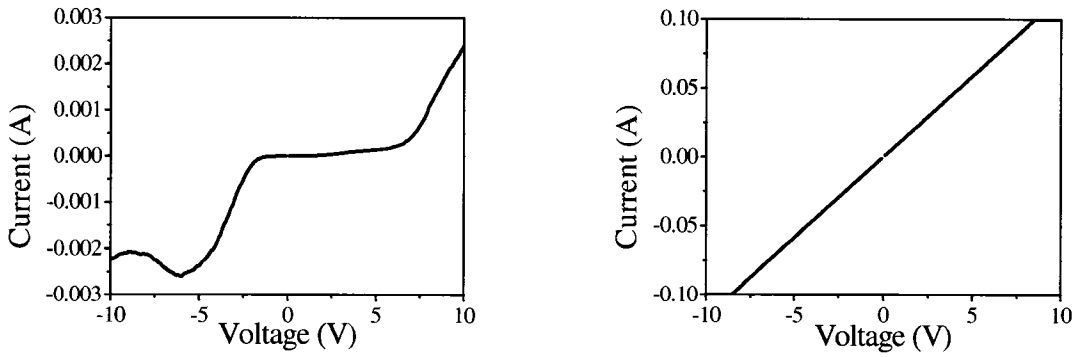

Figure III.2. Single-layer diodes of compound **II-11**. ITO/**II-11**/Al (left) and ITO/**II-11**/Au (right)

This means that compound **II-11** can form junction with Al and ohm contact with Au, which is the performance of p-type semiconductor (Figure III.2). To confirm these observations the double-layer devices of ITO/**II-11**/C60/Al and ITO/**II-11**/CuPc/Au were fabricated. The same results were obtained with these two devices which reveal that, the compound **II-11** can form junction with C60 and ohm contact with CuPc, the typical characteristic of p-type semiconductor (Figure III.3).

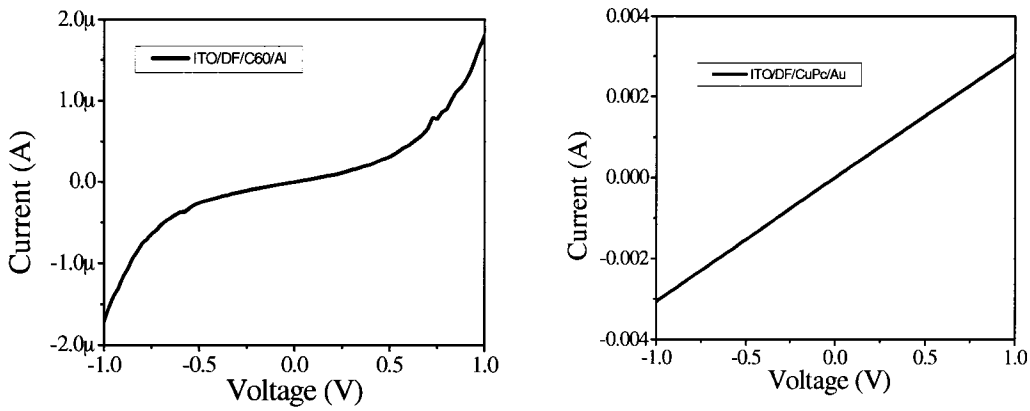

Figure III.3. Double-layer diodes of compound **II-11**. ITO/**II-11**/C60/Al (left) and ITO/**II-11**/CuPc/Au (right)

The electroluminescence properties of compound **II-12** were tested in the following OLED structure: ITO/**II-12** (500 Å)/PBD (500 Å)/LiF (15 Å)/Al. PBD or 2-(4-biphenylyl)-5-phenyl-1,3,4-oxadiazole is an electron transport material with a lower HOMO than that of **II-12**, which should facilitate the charge recombination in **II-12.**[10] The combination of a thin LiF layer and Al has been shown to form an efficient cathode.[11] A simple flatband energy diagram is shown in Figure III.4 to justify the choice of PBD and ITO as electron transport layer and anode, respectively. The ITO surface was treated in a UV-ozone oven for 10 minutes, and the structure was thermally evaporated

without exposure to air with a base vacuum better than 10^{-6} Torr. A quartz substrate was placed beside the OLED substrate to collect the deposited **II-12**, for comparison of thin film PL with its EL spectrum.[12]

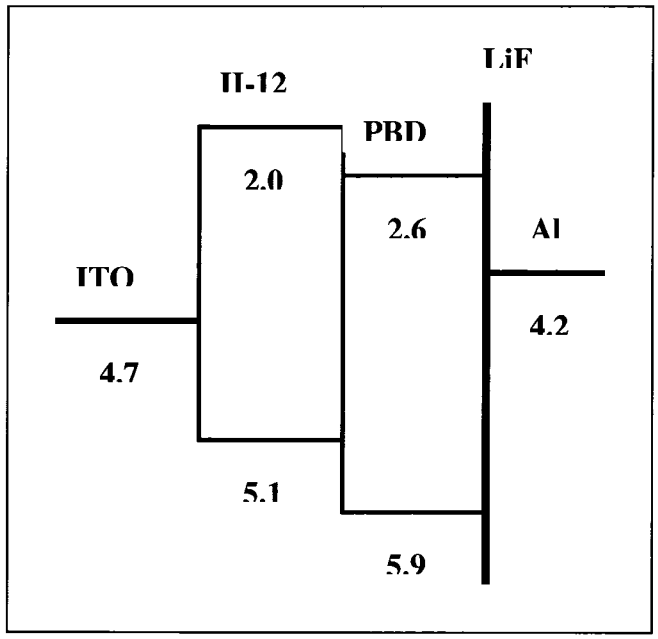

Figure III.4. The flatband energy diagram of ITO/**II-12**/PBD/LiF/Al device

The device performance was tested and the result is displayed in Figure III.5. A typical current density-voltage and luminance-voltage characteristics of the OLED was observed. The OLED reaches a high luminance of 1400 Cd/m^2 below 10 V for a current density around 1600 A/m^2. The quantum luminous efficiency of 1 Cd/ A was obtained at 9 V but it decreased at higher voltages. The inset of Figure III.5 shows the EL spectrum taken at 9 V, which is independent of the voltage and is in agreement with the PL taken on the quartz witness sample excited at 350 nm. Due to the polycrystalline nature of the deposited film of **II-12**, the observed absorption was broader, has multiple bands and shifted to the longer wavelengths in comparison with the spectrum of **II-12** in solution.

As a result, the PL spectrum of thin film was also broader and the device emitted the whitish yellow color.

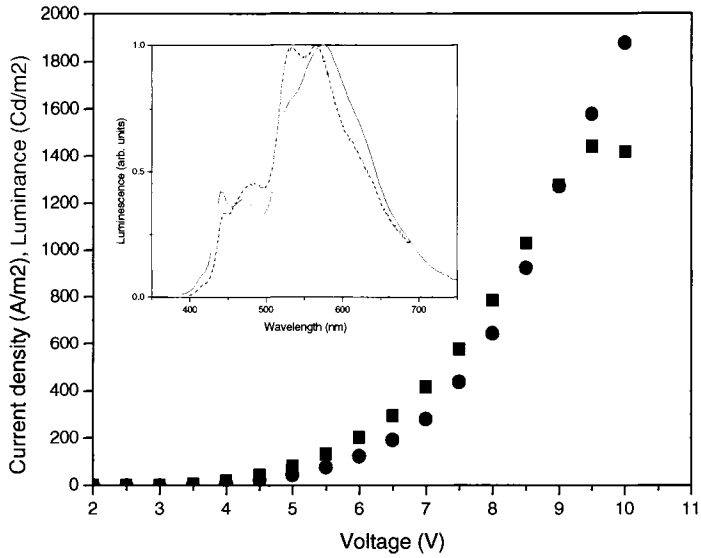

Figure III.5. Voltage – current – brightness (current density in circles and luminance in squares) characteristics of an ITO/**II-12**/PBD/LiF/Al OLED. Inset: EL (solid line) of OLED and PL of **II-12** (dashed line)

III.2.2.2. Hybrid Transistor Device

The metal-base transistor is often referred to as the semiconductor-metal-semiconductor (SMS) transistor. A general structure of SMS transistor includes a thin metal film which is vacuum deposited onto a semiconductor surface. Another piece of semiconductor is shaped to a fine point and is pressed gently onto the metal film. The metal-base transistor has no commercial value but it has been used as a tool to study fundamental properties of hot electrons in metals. The metal-base transistor offers certain potential advantages such as low base resistance.[13]

A hybrid semiconductor/metal/semiconductor (SMS) transistor was made based on compound **II-11** with the structure of: Ga-In/p-Si/Sn/**II-11**/PEDOT:PSS/Al. The

$I_C(V_{CB})$ was measured at different values of constant I_E, for $0 \leq I_E \leq 1$ mA at steps of 200 μA, in which I_E means hole injection from emitter to base, I_C means hole injection from the base to the collector, and V_{CB} means the base/collector junction, while Sn is the base (Figure III.6). The results indicate that at positive V_{CB} the collector is able to collect all positive charge carriers emitted by the emitter. At negative V_{CB}, the base/collector junction is forwarded biased and the base drains both currents, I_E and I_C. It can be seen that for the reverse-biased base/collector junction, the value of I_C saturates at $I_C \cong I_E$, without evidence of a significant leakage current. The absence of leakage current is more evident in the curve measured at I_E=0, which essentially corresponds to the Sn/p-Si junction characteristic curve.[14] Some other characteristics of the transistor are also measured and the results are published in reference 15. As an example, the replacement of Al with Au in device structure demonstrates that current densities of 0.5 mA/mm^2 can be achieved in device at V_{EC} = 5V, while such current densities could be arrived at V_{EC} ≈50V for the device bearing Al in structure. This result clearly indicates that due to the differences between the energy levels of Al and Au, Au effectively favors hole injection into compound **II-11.** This result is in agreement with the one mentioned in section III.2.2.1 regarding to the p-type characteristic of compound **II-11**. 2,6-Diphenylindenofluorene has been shown to be a weak n-type semiconductor material useful for a number of potential applications such as in OLED and SMS transistors, while it could be used as an appropriate p-type material in OLED.

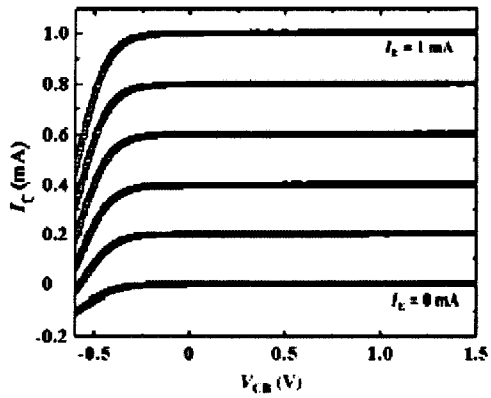

Figure III.6. $I_C(V_{CB})$ characteristics of the transistor for different I_E values ($0 \leq I_E \leq 1$ mA at steps of 200 μA)

As a conclusion, SMS transistors using the compound **II-11** as an emitter behave like permeable-base transistors with low operating voltages in both common-base and common-emitter modes and a feature of current amplification.

III. 3. Optical Properties

III.3.1. UV-Vis Absorption

The UV-Vis absorption properties of the conjugated compounds based on indenofluorene are presented in Table III.2. Figure III.7 shows the normalized UV-Vis absorption of the compounds in solution (DMF) in two separated graphs to prevent the overlapping of the peaks since all the compounds have absorption in the same area.

Two absorption peaks were observed for compounds **II-(11-15)** and **II-18**, whereas **II-16**, **II-17** and **II-19** had only one broad peak. The peaks at the higher wavelength (345-381 nm) are assigned to the π-π* transition of the conjugated aromatic rings, and those at a shorter wavelength (311-365 nm) are attributed to the electronic transition of each aromatic unit.[16] The absorption peak of the compound **II-12** is red

shifted due to the non-bonding electrons of the sulfur in π-system. This elevated electron density reduced the optical band gap of this compound (**II-12**, 3.1 eV) compared to the compound **II-11** (3.3 eV). Among all, compound **II-16** bearing methoxy group has the lowest band gap due to the higher λ_{onset}.

Table III.2. Optical properties of compounds **II-(11-19)**

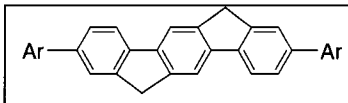	**Aryl group**	λ_{abs} **(nm)**[a]	λ_{PL} **(nm)**	E_g **(eV)**[b]
II-11		345, 358	377, 395, 420	3.3 (379)
II-12		365, 381	396, 416, 443	3.1 (399)
II-13		350, 365	378, 398, 421	3.2 (383)
II-14	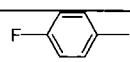	346, 356	376, 394, 417	3.3 (375)
II-15	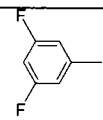	350, 360	383-401, 430	3.2 (385)
II-16	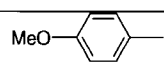	353	385, 403, 432	3.0 (413)
II-17	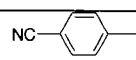	358	428	3.1 (400)
II-18		311, 345	393	3.3 (378)
II-19	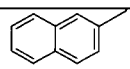	355	394, 403, 432	3.2 (387)

[a] In DMF

[b] Calculated from the empirical formula, E_g (optical, eV) = $1240/\lambda_{onset}$ (values in parentheses)

Compared to the UV-Vis absorption of indenofluorene (333 nm), the absorptions of all the 2,6-disubstituted indenofluorenes are red shifted. This result clearly indicates that by the incorporation of two aryl groups in indenofluorene structure, the conjugation lengths of the resulting compounds are increased leading to the absorption of longer wavelength. The effect of extended conjugation lengths is also observed in optical band gap of compounds **II-(11-19)** compared to the one of indenofluorene (3.7 eV). As it was expected, the increased conjugation lengths decrease the band gaps of all compounds significantly.

The UV absorption of 2,6-diphenylindenofluorene (**II-11**) in thin film showed two peaks at 330 and 370 nm. The edge of the absorption peak was at 420 nm which is in longer wavelength compared to the solution (379 nm). This indicates that an efficient charge transfer occurs between the molecules in a well-packed film. The optical band gaps are calculated using the on-set of UV absorption and are presented in Table III.2.

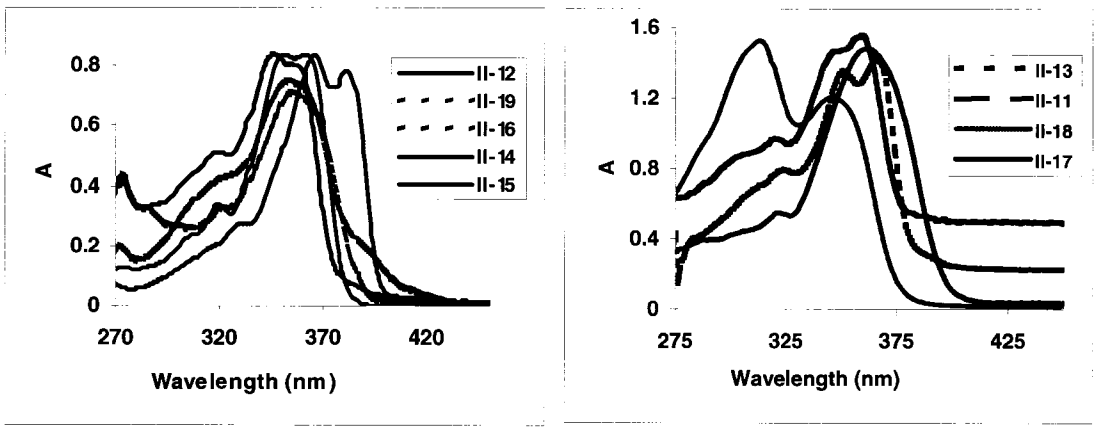

Figure III.7. UV-Vis absorption spectra of the compounds **II-(11-19)** in DMF

III.3.2. Photoluminescence Properties

The photoluminescence properties of the compounds **II-(11-19)** are compared and the relevant data are reported in Table III.2. From the results it appears that as thienyl ring is presented in molecule, the PL emission is red shifted with the same reason of UV absorption (Figure III.8). Among all, two compounds **II-(17-18)** displayed one peak while the other seven compounds showed two emission peaks with a shoulder of higher wavelength. The PL emission of compound **II-15** is 13 nm red shifted compared to the emission peak of the compound **II-14**. This indicates that the electron withdrawing effect of four fluorine units in molecular structure increased the electron delocalization more efficiently.

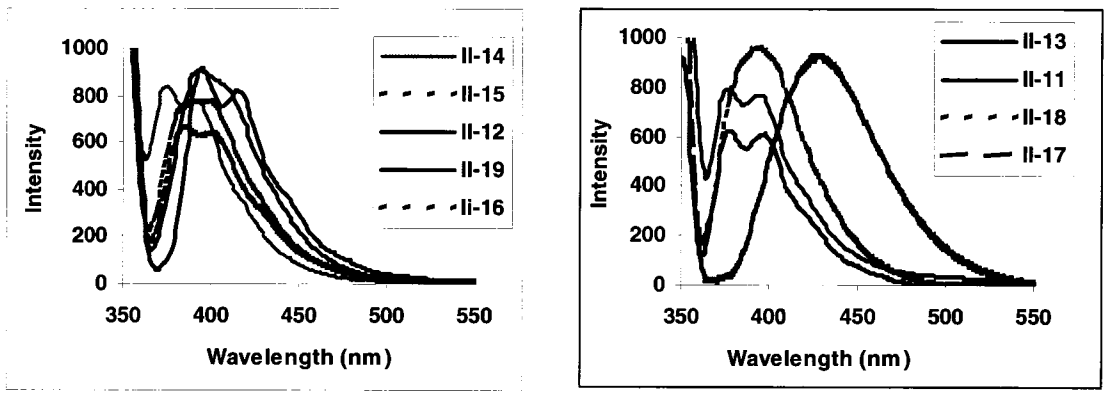

Figure III.8. PL emission spectra of the compounds **II-(11-19)** in DMF

Among all nine compounds, the electroluminescent properties of **II-11** and **II-12** were tested in the device structure, while the photoluminescent characteristics of two compounds were measured in film. In both cases the PL results were in agreements with the EL taken on devices. Due to the polycrystalline nature of deposited films of both **II-11** and **II-12**, the observed PL were shifted to the longer wavelengths in comparison with the spectrum of the compounds in solution.

In order to determine the effect of morphology on PL emission, the PL emission of four films prepared from **II-11** in different conditions are also measured. Thin film of 2,6-diphenylindenofluorene was vacuum deposited onto clean glass under dynamic vacuum of 10^{-3} Pa. The source temperature was 300 ± 2 °C and film was deposited in 30 min. Four films **A**, **B**, **C** and **D** were prepared, which refer to the one deposited on the substrate held at 30, 75, 120 and 165 °C, respectively. The results indicate a significant red shift to 460, 500 and 530 nm for film **A** (Figure III.9) compared to the solution.

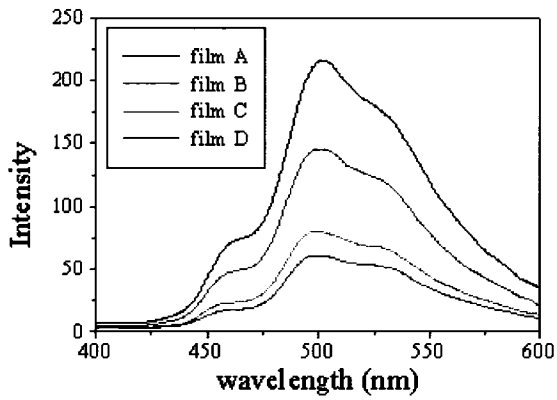

Figure III.9. PL emission spectra of the **II-11** in film

The PL spectra of the other three films **B**, **C** and **D** are similar to that of film **A**. It should be mentioned that the morphology of films did not effect on PL emission, since the four films have different morphology, but the same emission.

The quantum yield of compounds **II-(11-19)** was calculated by equation of:

$$\Phi_s = \Phi_r \frac{\Im_s}{\Im_r} \cdot \frac{A_r}{A_s}$$

Letters *s* and *r* refer to the sample and reference, respectively. $\Im$ is the integrated area of emission peak and A is the absorbance. The data are summarised in Table III.3.

Table III.3. Physical constant and quantum yields of the compounds **II-(11-19)**

Compound	$\Im$	A	Φ_s (%)[a]
II-11	8257	0.031854	39
II-12	10552	0.035619	44
II-13	9096	0.039611	34
II-14	10130	0.031622	48
II-15	20310	0.069856	43
II-16	10870	0.027437	59
II-17	22339	0.042919	78
II-18	7942	0.064551	18
II-19	11610	0.031296	55

[a] Quantum yield (%) in reference to quinine sulfate (1μM in 1N H_2SO_4)

Quinine sulfate (1 μM in 1 N H_2SO_4)[17] was used as reference to determine the fluorescence quantum yield of compounds. Fluorescence emission spectra of compounds (**II-11**: 2.5 μM, **II-(12-13)** and **II-(16-19)**: 0.5 μM, **II-14**: 1 μM and **II-15**: 0.25 μM) were collected at 90° to the angle of excitation.

III.3.3. Electroluminesence properties

The electroluminescence properties of compound **II-11** were investigated using a single layer light-emitting diode (LED) device fabricated in the configuration of ITO/**II-11**/Al. The energy diagram of the device is displayed in Figure III.10. Compound **II-11** was first vacuum deposited on ITO at 30 °C, then aluminum electrode was vacuum

evaporated onto the 2,6-diphenylindenofluorene layer. This device emits green light with peaks at 465, 500 and 530 nm (Figure III.11).

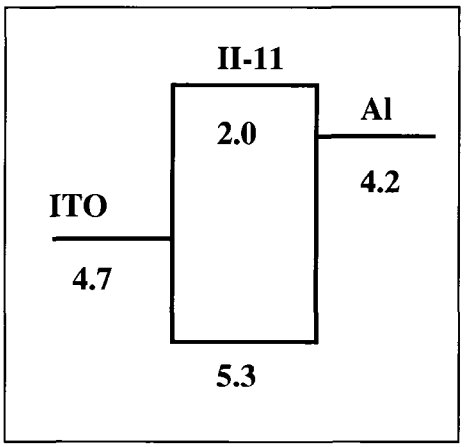

Figure III.10. Schematic energy diagram of ITO/**II-11**/Al device

The device performance was also studied which shows an onset voltage of about 20 V. Under 35 V, the device has a maximum brightness of over 150 Cd/m^2 (Figure III.11).

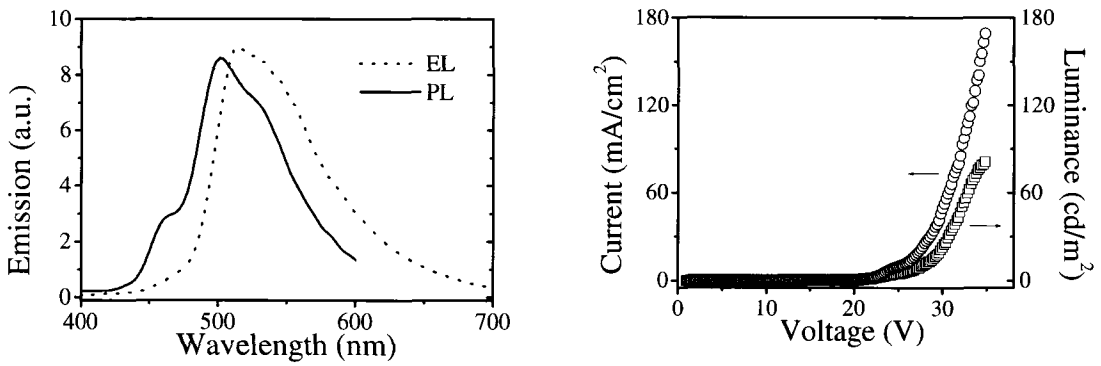

Figure III.11. Voltage – current – brightness characteristic (right) and electroluminescence spectra (left) of the LED device of ITO/**II-11**/Al

The effect of morphology on OLED was tested on two devices prepared in different conditions. The devices had the same configurations (ITO/**II-11**/Al) but the

substrate temperatures were 30 and 120 °C, respectively. The former device displayed higher luminance at lower voltage (Figure III.12) due to the morphological differences.

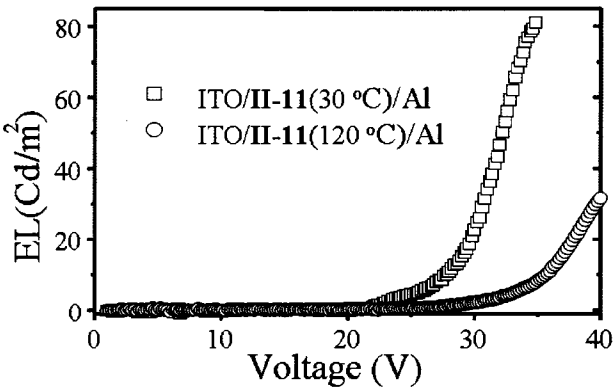

Figure III.12. Effect of morphology on EL of the device ITO/**II-11**/Al

Among all nine indenofluorene derivatives were mentioned in Chapter II, 2,6-diphenylindenofluorene (**II-11**) formed single crystals during the sublimation. Therefore, it was expected that the same crystals would form during the devices fabrications. To confirm this, thin film of 2,6-diphenylindenofluorene was prepared in different conditions and the morphology of films was studied.

Four films were prepared as explained in section III.3.2. AFM (Figure III.13) and X-ray diffraction (Figure III.14) were used to characterize the structure and morphology. The AFM results reveal that film **A** consists of needle-like grains while film **B** consists of both needle-like grains and hill-like grains. Films **C** and **D** have hill-like grains with the average size of 1.0×0.4 μm and square-like grains with the average size of 0.5×0.5 μm. For films **B**, **C** and **D** the size of hill-like grains increased with the substrate temperature.[15]

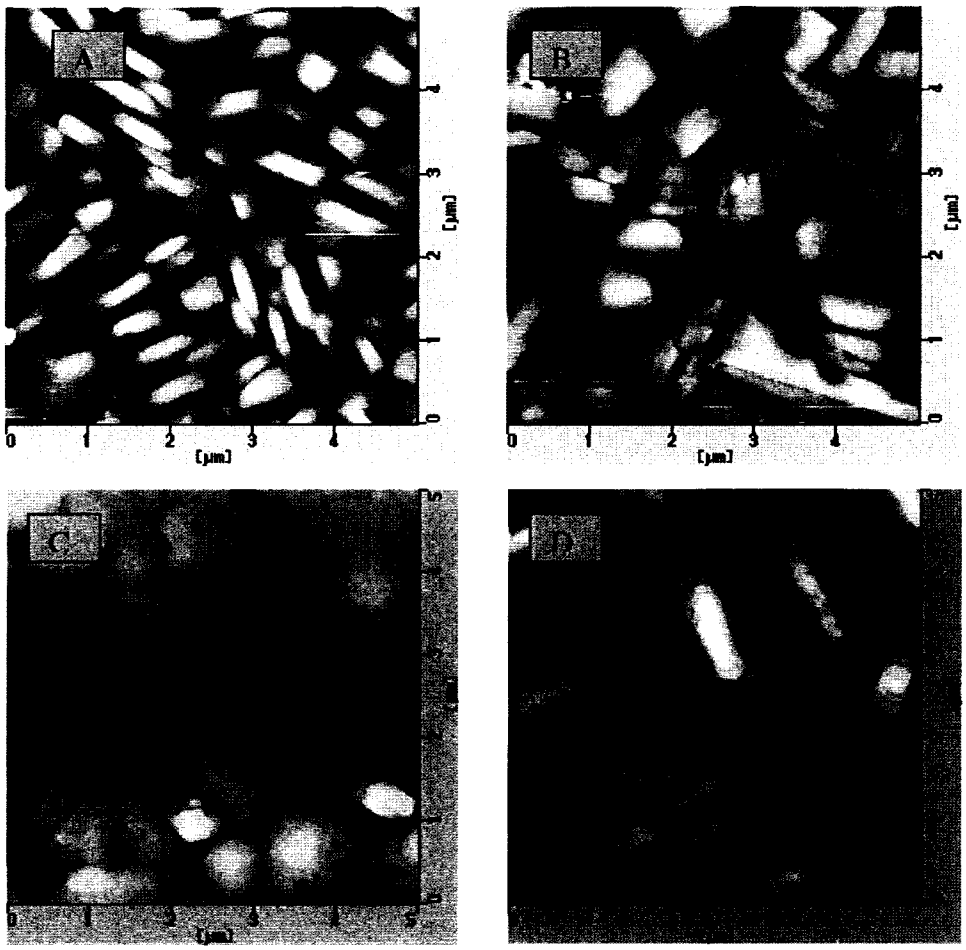

Figure III.13 AFM images of 2,6-diphenylindenofluorene

The X-ray diffraction patterns of four films are shown in Figure III.14. Molecular size of 2,6-diphenylindenofluorene is about 22 × 8 Å. There are at least two phases related to the observed two types of grains. One (α) forms the needle-like grains while the other (β) forms the hill-like grains. The former has the peaks at 2θ = 4.0, 8.3, 16.7° and the later is related to the peaks at 2θ = 5.1, 10.3, 20.9°. For phase α, the observed values are (001) = 21.5 Å, (010) = 2.9 Å, (100) = 2.1 Å; for phase β, the values are (001)

= 17.5 Å, (010) = 4.6 Å, (100) = 2.1 Å. Thus, films A and B consist of grains of both phases. Films C and D consists of mainly β-phase grains.

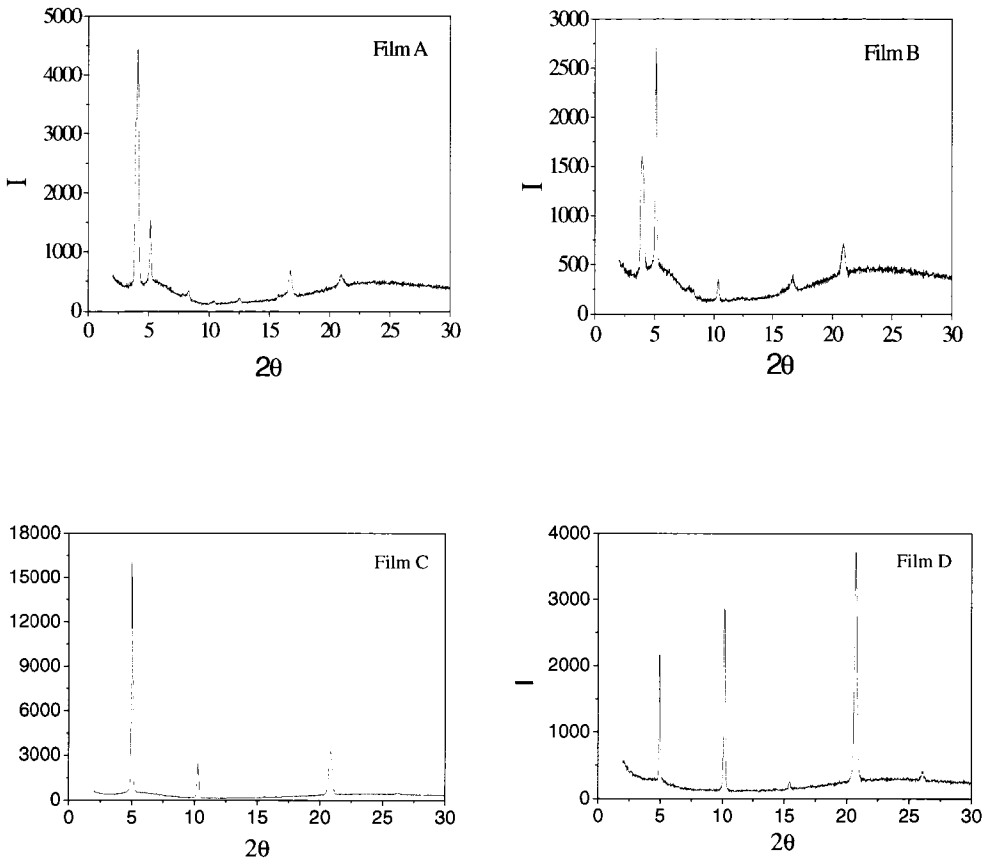

Figure III.14. X-ray diffraction patterns of 2,6-diphenylindenofluorene

In summary, the morphological studies confirmed that 2,6-diphenylindenofluorene could form crystals during the device fabrications under the given conditions. The crystals have different shapes and sizes with the same emission wavelength (Figure III.9), which implies that the PL and EL properties of the devices made from compound **II-11** would not be affected much by the crystalline morphologies under a broad range of fabrication conditions.

III.4. Conclusion

A series of indenofluorene derivatives were fully characterized by spectroscopic means. The morphology of thin films of 2,6-diphenylindenofluorene was examined by atomic force microscopy and X-ray diffraction analysis. Two different crystalline phases were found to exist depending on the deposition conditions.

All nine compounds emit blue light in the range of 393-443 nm. The 2,6-diphenylindenofluorene thin film emits around 500-530 nm, while the OLED based on this compound emits green light. 2,6-Dithienylindenofluorene was characterized as an organic semiconductor compound in field-effect transistor and light-emitting diode devices.

As it was mentioned in Chapter 1, it was hypothesized that by incorporation of aromatic rings in 2,6-positions of indenofluorene, the conjugation length of the resulting compounds would increase, leading to the decreased band gap, and emit light at longer wavelengths. The electrochemical studies clearly confirmed that due to the extended conjugation lengths, the band gaps of compounds **II-(11-13)** decreased significantly compared to the indenofluorene (optical band gap, 3.71 eV). The results of UV absorption and photoluminescence are also in agreements with the hypothesis confirming once again the extended conjugation length of all nine compounds compared to indenofluorene.

III.5. Experimental Section

Measurments

The UV absorption of the compounds were recorded using a UV-Vis Lambda 900 spectrophotometer while the photoluminescence of products were measured by Shimadzu RF-1501 spectrofluorophotometer. The CV of thin film of 2,6-diphenylindenofluorene was determined using a BAS100w electrochemistry workstation with a three-electrode system, ITO/**II-11** thin film as working electrode, Pt wire electrode as counter electrode and Ag wire electrode as reference electrode. The OLED was tested using a programmable Keithley 2400 SourceMeter unit and a Minulta LS-110 Luminance meter. The layer thickness measurements of the transistors were performed using a Dektab 3 surface profiler.

Device Fabrication

Transistor

The transistors were prepared by evaporating a 25-nm-thick layer of Sn on a p-type Si(100) substrate; this layer acted as the collector. Prior to Sn deposition, the Si substrate was etched in a 5% solution of HF to remove surface oxide and then GaIn eutectic alloy contact was applied to the unpolished side to act as an ohmic contact. The p-Si/Sn surface was partially covered with a thick poly(methyl mathacrylate), PMMA, layer by deep coating, using a highly concentrated PMMA:acetone solution. The emitter consisted of a film of **II-11**, 67-nm thick, deposited onto Si/Sn by thermal sublimation at a pressure of 2×10^{-6} torr. A PEDOT:PSS layer was deposited on top of the **II-11** layer by spin-coating in sequence; this layer was dried for 4 h in vacuum at 60 ^{o}C. Aluminum

contact strips were evaporated on top of the PEDOT:PSS layer to complete the device structure with an active area of ≈ $1mm^2$.

OLED

The OLEDs were fabricated on glass with the following layer structure: ITO(1500 Å) /**II-12** (500 Å)/PBD (500 Å)/LiF (15 Å)/Al(800 Å). ITO is tin-doped indium oxide as the transparent anode. The ITO surface was treated by UV ozone for 10 min prior to loading the substrate into the multisource vacuum chamber. The substrate was kept at room temperature and not exposed to air until it was removed from the chamber.

References

1. Sakamoto, Y.; Suzuki, T.; Kobayashi, M.; Gao, Y.; Fukai, Y.; Inoue, Y.; Sato, F.; Tokito, S. *J. Am. Chem. Soc.* **2004**, *126*, 8138.
2. Facchetti, A.; Yoon, M. H.; Stern, C. L.; Katz, H. E.; Marks, T. J. *Angew. Chem. Int. Ed.* **2003**, *42*, 3900.
3. Leung, L. M.; Lo, W. Y.; So, S. K.; Lee, K. M.; Choi, W. K. *J. Am. Chem. Soc.* **2002**, *122*, 5640.
4. Wong, K. T.; Chien, Y. Y.; Chen, R. T.; Wang, C. F.; Lin, Y. T.; Chiang, H. H.; Hsieh, P. Y.; Wu, C. C.; Chou, C. H.; Su, Y. O.; Lee, G. H.; Peng, S. M. *J. Am. Chem. Soc.* **2002**, *124*, 11576.
5. Meng, H.; Bao, Z.; Lovinger, A. J.; Wang, B. C.; Mujsce, A. M. *J. Am. Chem. Soc.* **2001**, *123*, 9214.
6. Lim, E.; Jung, B. J.; Shim, H. K. *Macromolecules* **2003**, *36*, 4288.
7. Bao, Z. *U. S. Pat.* 6, 452, 207 B1 **2002**.

8. Loy, E. D.; Koene, E. B.; Thompson, M. E. *Adv. Funct. Mater.* **2002**, *12*, 245.

9. Wang, L.; Ng, M.; Yu, L. *Phys. Rev.* **2000**, *62*, 4973.

10. Adachi, C.; Tsutsui, T.; Saito, S. *Appl. Phys. Lett.* **1989**, *55*, 1489.

11. Hung, L.; Tang, C.; Mason, M. *Appl. Phys. Lett.* **1997**, *70*, 152.

12. Py, C.; Gorjanc, T. C.; Hadizad, T.; Zhang, J.; Wang, Z. Y. J. *Vac. Sci. Technol. A.* **2006**, *24*, 654.

13. Ng, K. K. *Complete Guide to Semiconductor Devices*, Second edition **2002**, 289.

14. Serbena, J. P. M.; Hummelgen, I. A.; Hadizad, T.; Wang, Z. Y. *Small* **2006**, *2*, 372.

15. Hadizad, T.; Zhang, J.; Yan, D.; Wang, Z. Y.; Serbena, J. P. M.; Meruvia, M. S.; Hummelgen, I. A. *J. Mater. Sci: Mater. Electron.* Accepted: 25 October **2006**.

16. Hadizad, T.; Zhang, J.; Wang, Z. Y.; Gorjanc, T. C.; Py, C. *Org. Lett.* **2005**, *7*, 795.

17. Hercules, D. M. *Fluorescence and phosphorescence analysis: principles and applications* **1966**, 59.

Chapter IV

Synthesis and Characterization of Indenofluorenone Derivatives

IV.1. Donor-Acceptor system in small molecules and polymers

Fluorophores with the attractive emission properties such as a range of colors, high quantum yield and high hole/electron mobility are desirable for application in organic light emitting diods (OLEDs).[1] There are two major ways to control the emission wavelength. One is to alter the conjugation length. It should be mentioned that, in the case of conjugated polymers, the maximal absorption and emission occur for a certain conjugation length that is called "effective conjugation length".[2] Therefore, it is important to reach to this effective conjugation length without twisting along the polymer chain. The second way is the introduction of the electron-donating and electron-accepting moieties. This strategy can tolerate the twist between consecutive repeating units. A strong interaction between the electron rich unit (donor) and the electron poor unit (acceptor) may even enhance the double bond character between the repeating units via delocalization of electrons throughout the polymer chain.[3] Therefore, the mixing of monomers with high HOMO and low LUMO will reduce the band gap due to the intrachain charge transfer, resulting in the red shift of emission.

In order to get full-color displays, efficient red, green and blue emitting materials are required. Although green and orange emitters are available for commercial uses, there is still a need for suitable red[4] and blue emitters.

Common electron-withdrawing groups are cyano, nitro and carbonyl.[5] The most widely used electron donating groups are thiophene and pyrrole because of being electron rich.[6] It has been reported that compounds bearing carbonyl groups such as polyfluorenone, show low reduction potentials (low LUMO) due to the electron withdrawing effect of the ketone group. This redox process is also reversible,[7] while in

the case of compounds with the cyano group the redox process is irreversible.[8] Thus, indenofluorenone can be considered to be an acceptor due to the presence of the two strong electron-withdrawing groups.

IV.2. Design and requirement for a D – A system

Based on availability of starting materials, a few synthetic routes were designed for the synthesis of a donor-acceptor system in which indenofluorenone is chosen as an acceptor (Figures IV.1-IV.4). The key starting compound in the first approach (Figure IV.1) is 2,5-bis(4-bromophenyl)-1,4-xylene, which will lead to final products in two different pathways using the Suzuki coupling reaction. The success of this proposed approach is owing to solubility of all intermediates. 2,6-Bis[4-(diphenylamino)phenyl]indenofluorenone was successfully synthesized using this approach as an alternative strategy.

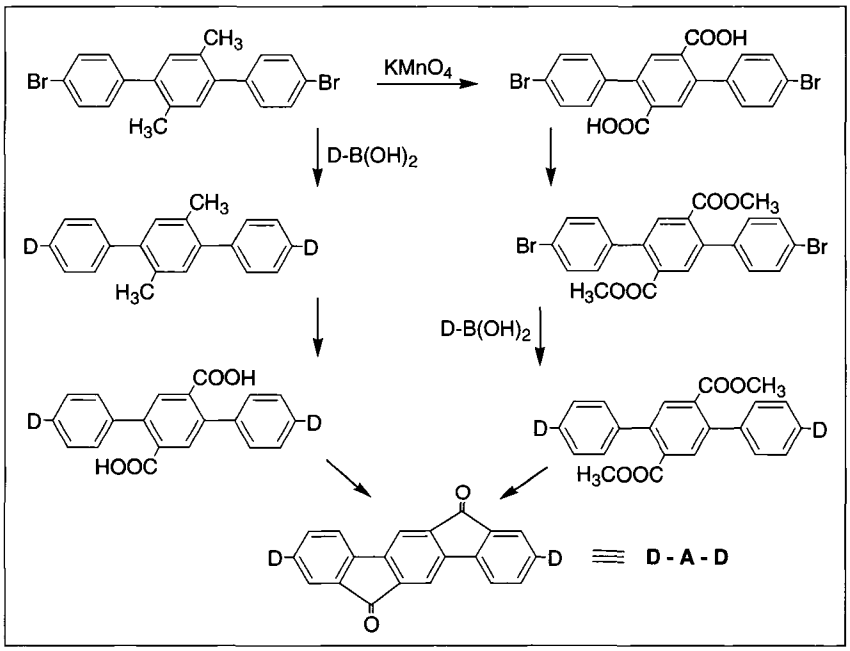

Figure IV.1. Proposed synthetic routes to indenofluorenone-containing D-A system

Another possible route involves the protection of two carbonyl groups of 2,6-dibromoindenofluorenone as ketal or imine groups, followed by attachment of the donor units and deprotection (Figure IV.2). This synthetic route also takes an advantage of a good solubility of starting ketal and imine compounds. Two keto groups of 2,6-dibromoindenofluorenone were successfully converted to imine to provide diimino-containing indenofluorene (compound **IV-12**) with enhanced solubility. However, due to the other feasible synthetic approaches, this method was not continued.

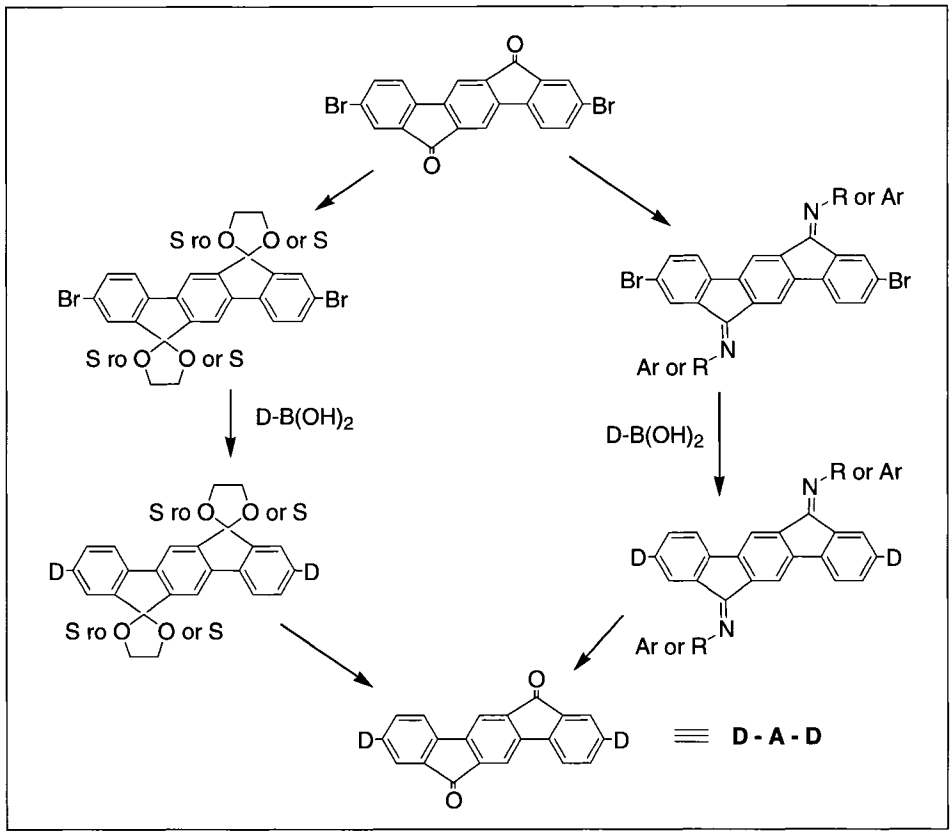

Figure IV.2. Proposed synthetic routes to indenofluorenone-containing D-A system via protection of ketone groups

A third approach involves the attachment of the donor groups to 2,6-dibromoindenofluorene, followed by oxidation of the methyl groups to the keto group (Figure IV.3). It is not suitable if any donor molecules are prone to oxidation. This

method was found to be a preferred synthetic route to synthesize 2,6-dithienylindenofluorenone since the thienyl groups were stable during the oxidation step.

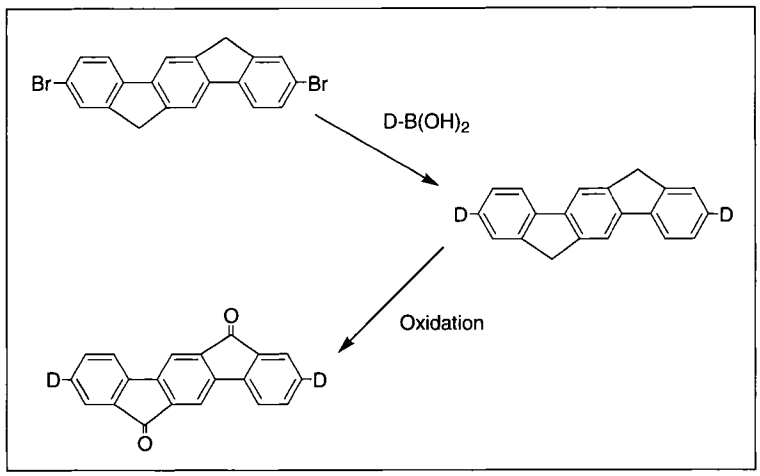

Figure IV.3. Proposed synthetic route to indenofluorenone-containing D-A system starting with dibromoindenofluorene

The last approach involves a direct coupling of 2,6-dibromoindenofluorenone with a donor molecule (Figure IV.4). This method was found to be a suitable synthetic route for the donor molecules stable in basic conditions at high temperatures (>100 °C) since 2,6-dibromoindenofluorenone is not soluble in common solvents at low temperatures. 2,6-Bis[4-(diphenylamino)phenyl]indenofluorenone and EDOT-indenofluorenone were synthesized using this approach. Thus, 2,6-dibromoindenofluorenone is a key compound for two of the above synthetic routes (Figures IV.2 and IV.4). However, the solubility of 2,6-dibromoindenofluorenone might be an issue.

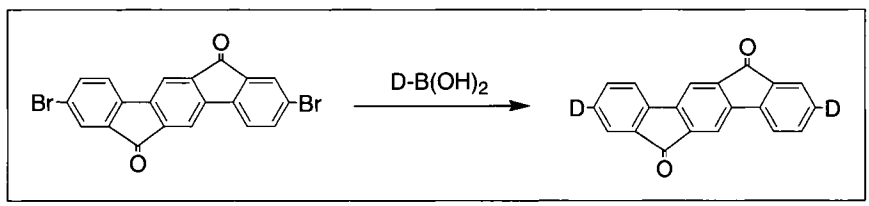

Figure IV.4. Proposed synthetic routes to indenofluorenone-containing D-A system starting with dibromoindenofluorenone

IV.3. Synthesis of 2,6-dibromoindenofluorenone

Since 2,6-dibromoindenofluorenone is a key compound for a series of 2,6-disubstituted indenofluorenone (D-A system), three methods have been attempted to prepare this compound. Electrophilic substitution on aromatic rings by bromine is not a favorable procedure for this purpose[9] due to the presence of two strong electron-withdrawing carbonyl groups. The carbonyl groups withdraw the electron density from the π-system, making the benzene rings less reactive towards an electrophile. The deactivated compounds may react with bromine only if an appropriate catalyst is present.

IV.3.1. Bromination of indenofluorenone using HgO

A mixture of mercuric oxide and bromine has been used as a brominating reagent for saturated hydrocarbons; however, no advantage over conventional methods for aromatics has been reported.

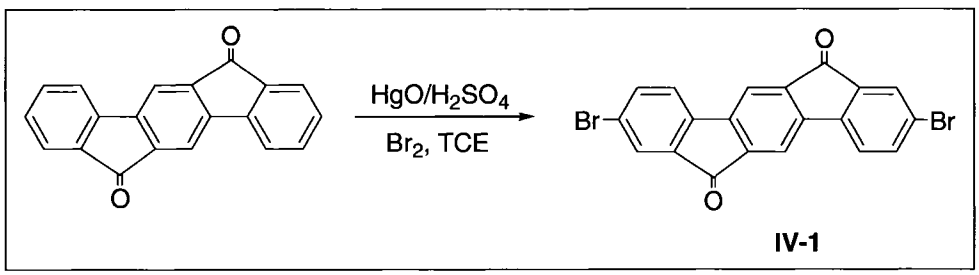

Scheme IV.1. Bromination of indenofluorenone using mercuric oxide

Two different free radical mechanisms have been proposed for this reaction. In the first mechanism, standard free radical bromination takes place and mercuric oxide serves simply to trap the evolved hydrogen bromide.[10] In second mechanism, the role of mercury oxide is different, and it interacts with bromine to form bromine monoxide (Br_2O) followed by bromination of the hydrocarbon.[10] Bromination of indenofluorenone

with this method is unfavorable since indenofluorenone has no tendency to form free radical. Bromination of indenofluorenone using HgO resulted in low yield.

It has been reported that the addition of concentrated sulfuric acid as a catalyst to the mixture of mercuric oxide and bromine can be effective for the bromination of deactivated aromatic rings.[11] The bromination of indenofluorenone with mercuric oxide in the presence of concentrated sulfuric acid was successful and compound **IV-1** was obtained in a moderate yield (30%) after purification by vacuum sublimation (Scheme IV.1).

IV.3.2. Bromination of indenofluorenone using $CuBr_2/Al_2O_3$

Copper (II) halides have been used for halogenation of aromatic hydrocarbons in nonpolar solvents. For aromatic compounds bearing alkyl chains, the halogenation reaction can lead to the formation of a mixture of both aromatic rings and alkyl chains being halogenated.[12]

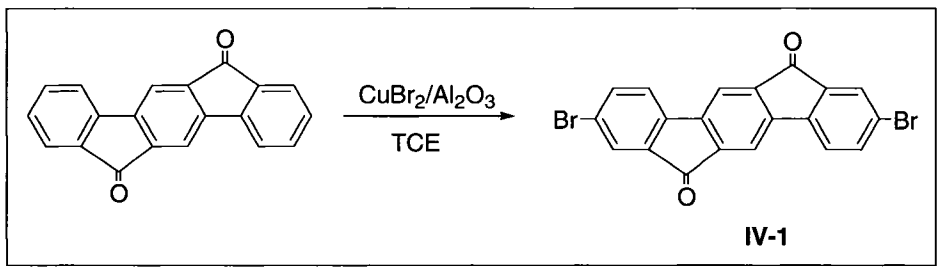

Scheme IV.2. Bromination of indenofluorenone using copper(II) bromide

It has been reported that halogenation of most aromatic compounds under mild conditions can be achieved with copper(II) halides supported on alumina. Alumina-supported copper(II) bromide selectively brominates the aromatic ring with no side-chain bromination in the case of alkylated aromatics.

The proposed mechanism for this reaction indicates that an aromatic radical cation forms through one electron transfer from the aromatic ring to copper(II) halide. Since activated alumina is electron-accepting, it can absorb the radical cation of the aromatic compound to facilitate the generation of the radical cation.[13] Copper(II) bromide is more reactive in comparison with copper(II) chloride towards the aromatic compounds (Scheme IV.2). This method is not sensitive to the activation of aromatic compounds.

Copper(II) bromide supported on alumina was then used to brominate the indenofluorenone. 2,6-Dibromoindenofluorenone (**IV-1**) was obtained in a moderate yield (29%). Due to the presence of alumina, purification using a Soxhelet extraction (1,2-dichlorobenzene) was needed.

IV.3.3. Synthesis of 2,6-dibromoindenofluorenone without direct bromination

In this route, one of the starting materials bears the bromo groups and the bromination step can be omitted (Figure IV.1). Thus, 2,6-dibromoindenofluorenone was synthesized in four steps starting from 1,4-xylene. Since 4-bromophenylboronic acid was chosen as the unit bearing the bromo group, the iodination of 1,4-xylene was needed in order to prevent any competitive reaction in the Suzuki coupling (Scheme IV.3).

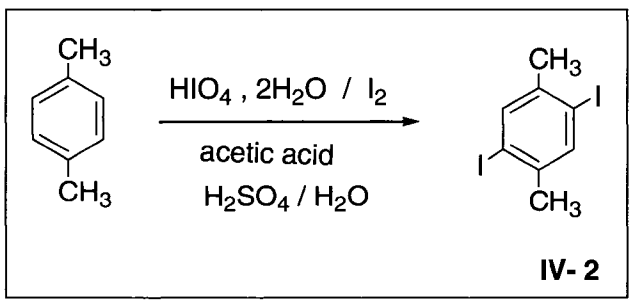

Scheme IV.3. Synthesis of 2,5-diiodo-1,4-xylene

Among all the aryl halides, the extensive use of iodoaromatic compounds has attracted broad interest.[14] The most convenient procedure for direct iodination of an aromatic compound involves the use of the positive iodine (I^+) as a reactive species. A mixture of periodic acid and iodine is a common iodinating reagent (Scheme IV.3) and proceeds more efficiently under acidic conditions.[15] The iodination reaction of 1,4-xylene was attempted in the presence of iodine, periodic acid, concentrated sulfuric acid and acetic acid. The exothermic reaction was controlled to keep the temperature at 70 °C constantly. Washing with sodium bisulfite solution and methanol, followed by crystallization from heptane, afforded compound **IV-2** in 66% yield (mp: 104 °C).[16]

A Suzuki coupling of compound **IV-2** and 4-bromophenylboronic acid was then carried out (Scheme IV.4). Because the iodide is more reactive than the bromide in the oxidative addition to the palladium(0) catalyst, the palladium atom is selectively inserted into the C-I bond.[17, 18] Thus, compound **IV-3** was obtained as beige solid in a moderate yield (56%) after purification by extraction three times with dichloromethane. Mass spectroscopy was used to confirm the presence of the bromo groups in compound **IV-3**.

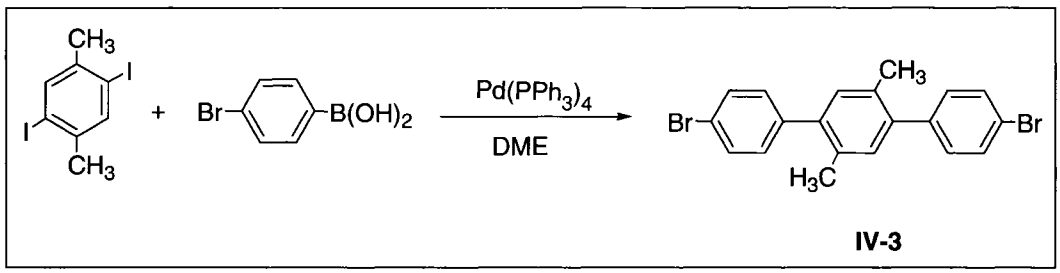

Scheme IV.4. Synthesis of 2,5- bis(4-bromophenyl)-1,4-xylene

It should be mentioned that neither electrophilic substitution reaction on 2,5-diphenyl-1,4-xylene nor bromination method using $CuBr_2/Al_2O_3$ or HgO were appropriate

for the synthesis of compound **IV-3**. In both cases, the reaction produced a mixture of products that were difficult to separate and identify.

Two methyl groups in compound **IV-3** can be oxidized to carboxylic acid using $KMnO_4$ in the presence of pyridine,[19] followed by acid-catalyzed cyclization to afford the target intermediate **IV-1** (Scheme IV.5). A solution of compound **IV-3** in pyridine and water was heated to reflux with stirring, and then potassium permangenate was added portionwise. Excess of potassium permanganate was required to achieve the completion of oxidation of both methyl groups. After several hours the color of potassium permangenate faded and more permangenate was added until the color was persistent. The reaction mixture was filtered and the filtrate was acidified to give compound **IV-4** in high yield (95%).

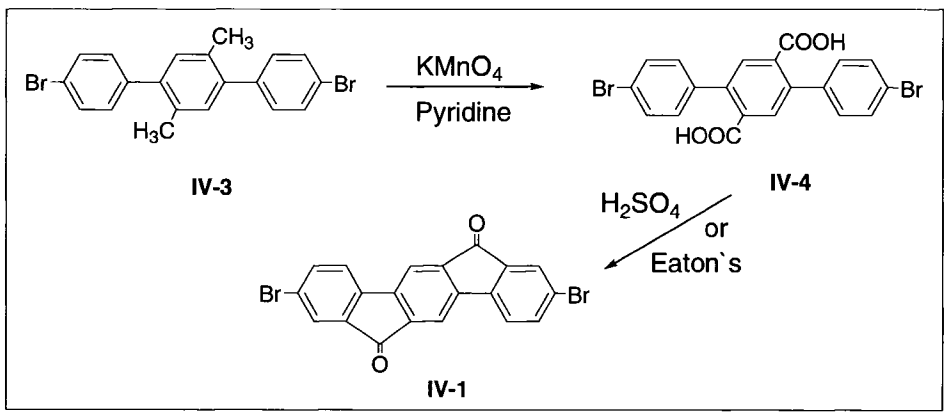

Scheme IV.5. Conversion of compound **IV-3** to 2,6-dibromoindenofluorenone

Using either concentrated sulfuric acid or Eaton's solution, two carboxylic acid groups are converted to the ketones to yield compound **IV-1**. The reaction mechanism is explained in details in Chapter II (II.2.2). 2,6-Dibromoindenofluorenone (**IV-1**) was successfully obtained by reacting compound **IV-4** with concentrated sulfuric acid, as red-purple solid in a moderate yield (49%). There was no difference between the two acids

(concentrated sulfuric acid and Eaton's solution) regarding the purity of final product and yield (Scheme IV.5).

IV.3.4. Characterization of 2,6-dibromoindenofluorenone

Due to the poor solubility of 2,6-dibromoindenofluorenone in common organic solvents, mass spectroscopy is the only conventional tool to confirm the molecular structure of this compound. Like indenofluorene derivatives, this molecule shows a stable molecular ion by electron ionization (EI). Since bromine has two isotopes with almost equal natural abundance (^{81}Br is 98.0% of ^{79}Br), the *M+2* peak with an intensity twice as that of the molecular ion becomes very significant. The *M+4* peak appears with the same intensity as the molecular ion. The mass spectrum of 2,6-dibromoindenofluorenone is presented in figure IV.5.

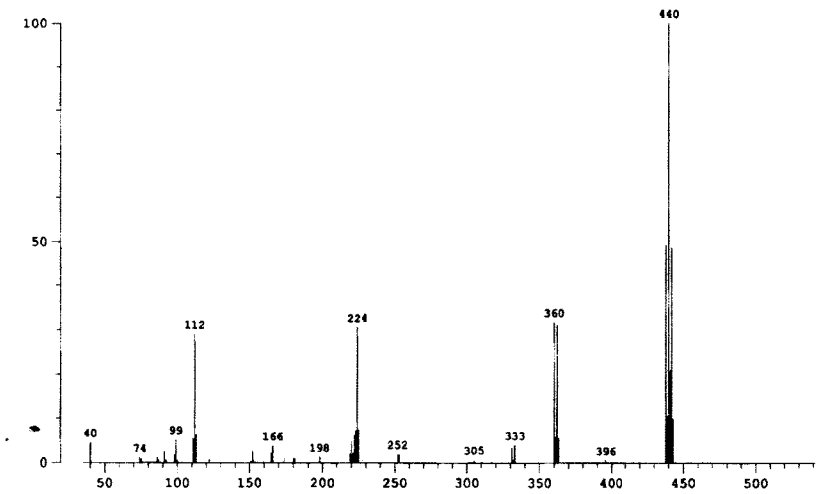

Figure IV.5. Mass spectrum of 2,6-dibromoindenofluorenone

IV.4. Thiophene-Containing Indenofluorenone Chromophore

Of the known thiophene-based semiconductors, many exhibit hole-transporting (p-type) activity due to their high-energy HOMO level. They can, therefore, be easily oxidized and as a result, can be used as an electron-donor unit in a D-A system.[20] Two thiophene derivatives (EDOT and thienyl) are selected as donor groups to compare the effect of structural differences on electron donating properties of the molecules. It is expected that EDOT with two oxygen units in structure will behave as a stronger electron donor than thienyl group.

As a unique derivative of thiophene, 3,4-(ethylenedioxythiophene) (EDOT), has been extensively investigated during the past decade. This compound has recently become the focus of considerable attention because the corresponding polymer exhibits exceptional environmental stability in the oxidized state as well as a low oxidation potential and moderate band gap.[21, 22] The low oxidation potential allows EDOT to be used as a strong electron donor in a π-conjugated system.[23]

Compound **IV-5** (2-EDOTboronic ester) was prepared by the known procedure[24] in a moderate yield, involving the lithiation of EDOT and the reaction with 2-isopropoxy-4,4′,5,5′-tetramethyl-1,3,2-dioxaborolane. Compound **IV-5** was then coupled with 2,6-dibromoindenoflurenone (using Suzuki coupling reaction) yielding the first donor-acceptor system of the series.

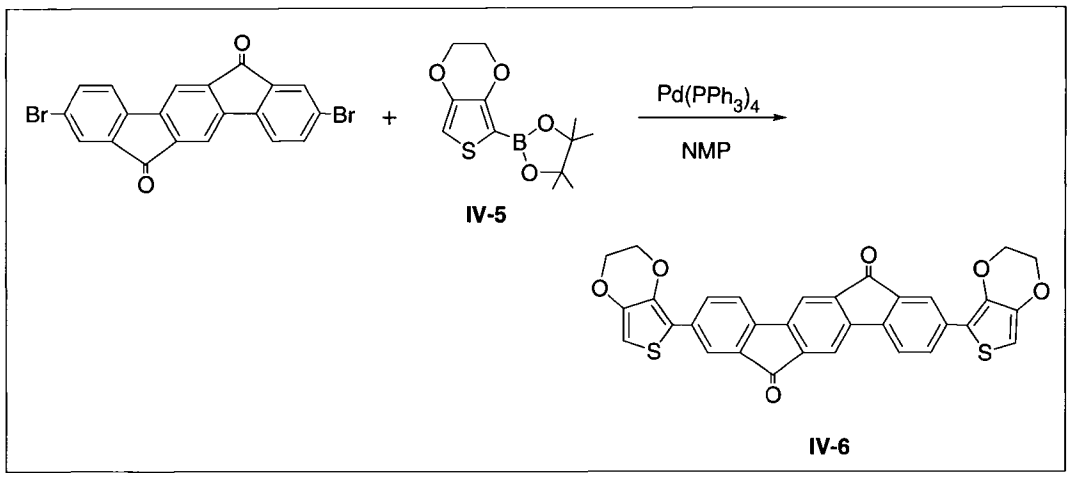

Scheme IV.6. Synthesis of EDOT-indenofluorenone

Due to the poor solubility of 2,6-dibromoindenoflurenone in common organic solvents at moderate temperatures, a high boiling point solvent such as N-methylpyrolidinone (NMP) was used for the reaction. Purification by vacuum sublimation afforded compound **IV-6** (green in color) with a melting point over 400 °C. It should be mentioned that two EDOT groups could tolerate such high temperature (Scheme IV.6). Due to the low solubility of the final product in common solvents, mass spectroscopy was used to confirm its molecular weight (EI, *m/z*: 562) which indicates the completion of the reaction.

Thienyl groups were the second thiophene derivatives chosen as donor units. Three reaction conditions were applied for the synthesis of 2,6-dithienylindenofluorenone:

Condition one: A Suzuki coupling reaction starting from 2-thiopheneboronic acid and 2,6-dibromoindenofluorenone at low temperature (100 °C). Due to the poor solubility of 2,6-dibromoindenofluorenone the reaction failed, even though it was expected that aryl bromide activated by two strong electron-withdrawing groups should facilitate the reaction.[25] The unreacted 2,6- dibromoindenofluorenone was recovered.

Condition two: The reaction of 2-thiopheneboronic acid and 2,6-dibromoindenofluorenone must be conducted at high temperature in order to dissolve the starting materials. Thus, a Suzuki coupling reaction was performed using 2-thiopheneboronic acid and 2,6-dibromoindenofluorenone at relatively high temperature (160 °C). However, the reaction was not successful and once again the un-reacted 2,6-dibromoindenofluorenone was recovered. It was reported that 2-thiopheneboronic acid is unstable under the basic conditions,[26] while 2,6-dithienylindenofluorene **(II-12)** was successfully obtained from the reaction of 2,6-dibromoindenofluorene **(II-10)** and 2-thiopheneboronic acid under the basic conditions at 100 °C (Chapter II). It seemed that 2-thiopheneboronic acid is not stable at high temperature (>100 °C) under the basic conditions.

Condition three: Given the disadvantages mentioned above, oxidation of two methylene moieties of 2,6-dithienylindenofluorene **(II-12)** was most favorable for synthesizing a D-A system containing thiophene as a donor unit (Scheme IV.7).

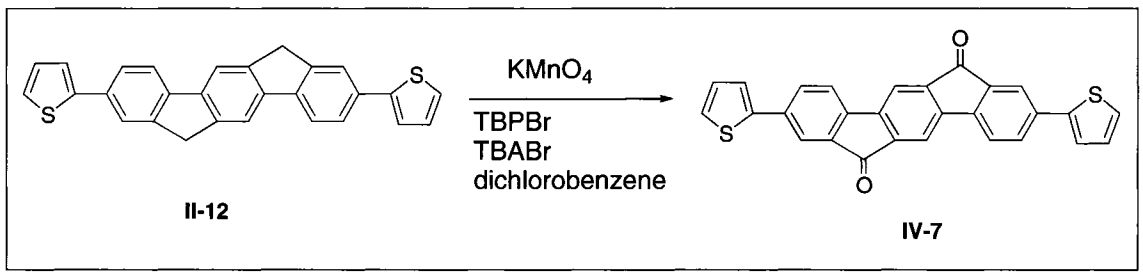

Scheme IV.7. Synthesis of 2,6-dithienylindenofluorenone

The most efficient oxidizing agent for oxidation of the methylene group was found to be potassium permangenate. 2,6-Dithienylindenofluorene **(II-12)** is soluble in some organic solvents at high temperatures (170-180 °C) while potassium permangenate

is insoluble in the organic layer but dissolves readily in water. In order for the oxidation reaction to proceed, well-mixing of the two phases is required.

A phase transfer catalysts such as a quaternary ammonium ion can facilitate the reaction to take place in the organic layer.[27] Due to poor solubility of final product **(IV-7)** in common organic solvents and the presence of ketone unit in molecular structure, infrared spectroscopy was the most useful method to confirm the structure of product. Mass spectroscopy was used for further confirmation of the molecular structure. The infrared spectrum of 2,6-dithienylindenofluorenone displays the characteristic C=O peak at 1709 cm^{-1} (Figure IV.6). A broad peak was observed at 3400 cm^{-1} which belongs to the water. This compound shows a melting point of 401 °C and a crystallization temperature of 391 °C (measured by DSC).

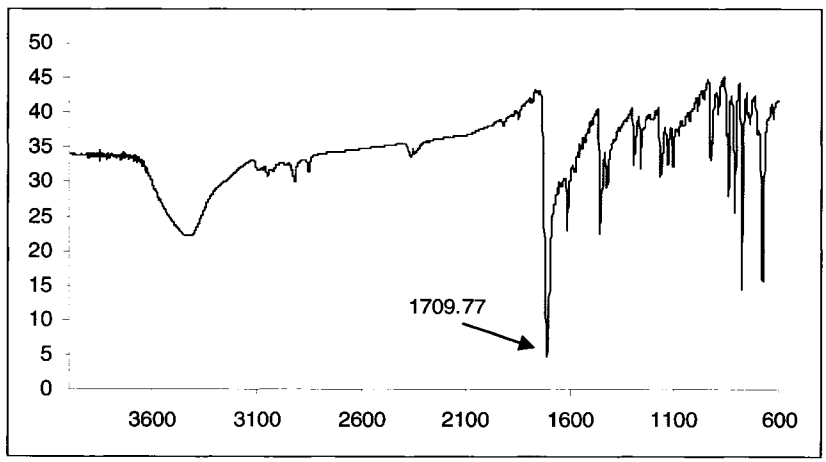

Figure IV.6. Infrared spectrum of 2,6-dithienylindenofluorenone

IV.5. 2,6-Bis[4-(diphenylamino)phenyl]indenofluorenone Chromophore

Two basic properties have led to triarylamines being known as a hole-transport material in organic electroluminescent devices:[28] the readily oxidizable nitrogen center and its ability to transport positive charge via its radical cations species.[29] Radical cation

formation should be possible both electrically and photochemically. Thus, triarylamines can be used as a donor in D-A systems. Compared to the thiophene derivatives (EDOT and thienyl) were chosen as donor groups, it is expected that triphenylamine will be a weaker electron donor than EDOT. The electron-donating ability of triphenylamine groups is predicted to be similar to that of thienyl units.

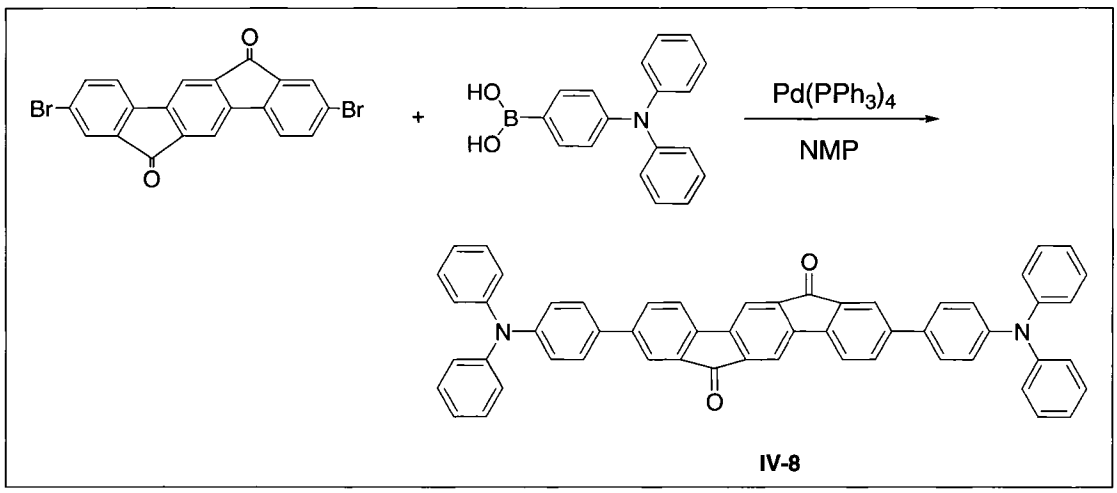

Scheme IV.8. Synthesis of 2,6-bis[4-(diphenylamino)phenyl]indenofluorenone

Once again the Suzuki coupling was used to synthesize compound **IV-8** (Scheme IV.8). Due to the inability of the mass spectrometer to measure molecular weights above 700 amu (atomic mass unit) and poor solubility of the compound in common organic solvents used for electrospray ionization method, confirmation of the reaction was impossible by this method. NMR could not be used to confirm the structure of the product due to the overlapping of aromatic protons, while infrared spectroscopy was inappropreate for this purpose because there was no significant difference between the structures of the starting material and the product in terms of the keto groups. Therefore, an indirect method was chosen to confirm the reaction: comparison between the

absorption and emission spectra of the starting material and the final product. Even though, this method also can not confirm the molecular structure of final product.

To overcome to this problem, an alternative strategy was applied to synthesize compound **IV-8** (Scheme IV.9).

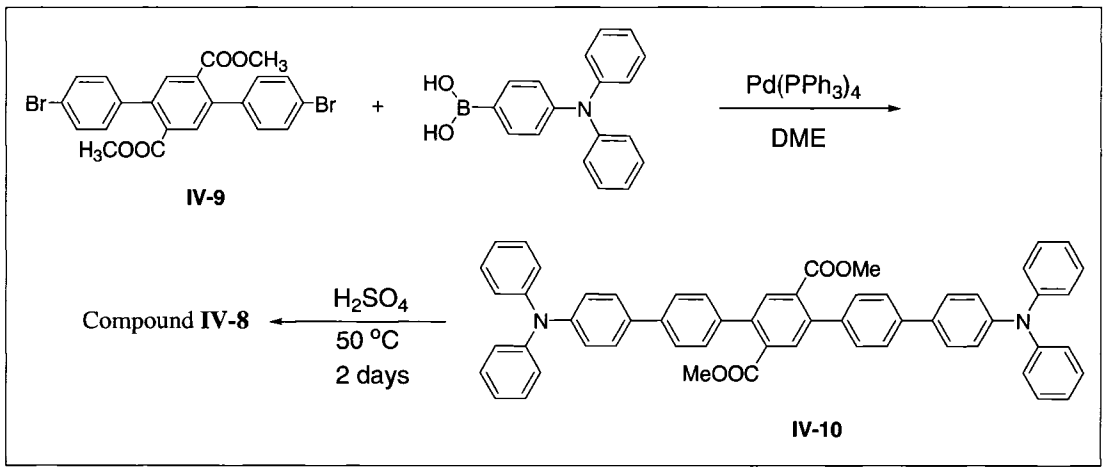

Scheme IV.9. Synthesis of 2,6-bis[4-(diphenylamino)phenyl]indenofluorenone starting with compound **IV-9**

(Diphenylamino)phenylboronic acid was first reacted with dimethyl-2,5-bis(4-bromophenyl)terephthalate to form compound **IV-10** which is soluble in common organic solvents and can be characterized by mass and infrared spectra. Mass spectroscopy confirmed the molecular weight of **IV-10** (ESI, *m/z*: 832) while the IR spectrum of the compound presented two characteristic peaks at 1724 cm^{-1} for C=O of the ester group and at 1278 cm^{-1} for C-N of aromatics. This compound was then treated with concentrated sulfuric acid for 16 – 17 h at room temperature followed by 16 – 17 h at 50 °C[30] to convert the ester groups to the corresponding ketone. The resulting product could only be identified by infrared spectrum that indicated a characteristic peak for C=O bond significantly shifted to the lower frequency (1711 cm^{-1}).

IV.6. Thermal stability

Similar to the indenofluorene derivatives explained in Chapter II, indenofluorenone derivatives are also synthesized for use in OLEDs and therefore it is important that their thermal stabilities be measured. Differential scanning calorimetry (DSC) was chosen as an accurate thermal analysis technique. The results are summarized in Table IV.1.

Table IV.1. Thermal stability of indenofluorenone derivatives

Compound	T_m °C[a]	T_c °C[a]
2,6-Diphenylindenofluorenone (II-4)	399	393
2,6-Dithienylindenofluorenone (IV-7)	401	390

[a] DSC analysis under N_2 at a heating rate of 10 °C/min.
T_m = Melting point, T_c = Crystallization temperature.

It is expected that changes to the chemical structure and the nature of substituents will vary the thermal properties of compounds. Among all four compounds, (2,6-diphenylindenofluorenone, **IV-6**, **IV-7** and **IV-8**), 2,6-diphenylindenofluorenone **(II-4)** and 2,6-dithienylindenofluorenone **(IV-7)** are most likely to be crystalline. A melting point of 399 °C was obtained for compound **II-4** while this compound was crystallized at 393 °C upon cooling. Similar phenomena were observed for compound **IV-7.** This compound showed a melting point of 401 °C and a crystallization temperature of 391 °C (Figure IV).

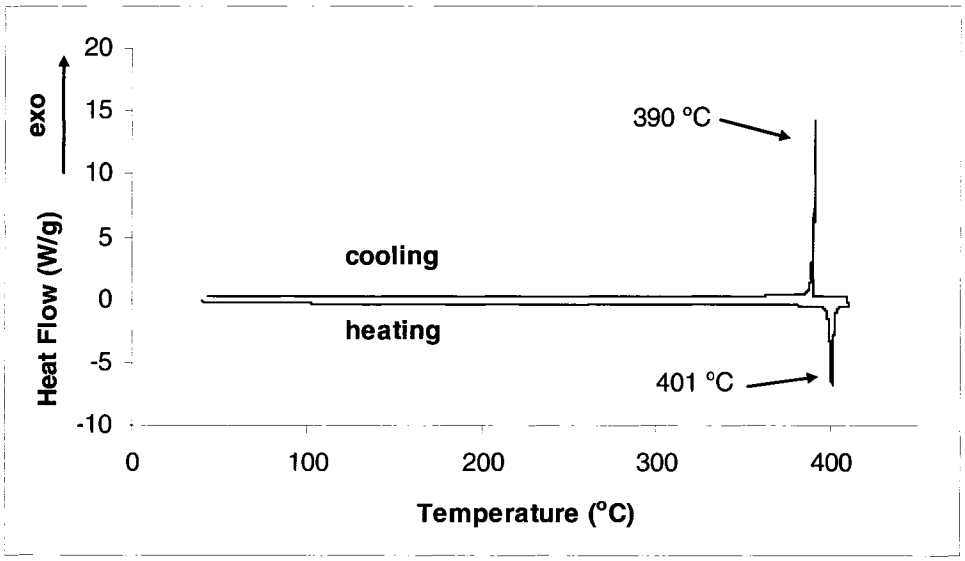

Figure IV.7. DSC trace of 2,6-dithienylindenofluorenone at a heating rate of 10 °C/min

It seems that the presence of both phenyl and thienyl groups at 2,6-positions of indenofluorenone have the same effect on thermal stability of the products. The other two compounds (**IV-6** and **IV-8**) decomposed before melting (decomposition temperature was at 317 °C for **IV-6** while **IV-8** decomposed at 271 °C).

IV.7. Optical properties

The UV-Vis absorption and photoluminescence properties of compounds based on indenofluorenone as a strong acceptor are presented in Table IV.2. UV and PL data of 2,6-dibromoindenofluorenone are included for comparison. As expected, once the electron donor units are incorporated into the system, the UV absorption of the molecule is shifted towards the higher wavelength due to the extended conjugation as well as delocalized electrons resulting from the D-A system.

The comparison between UV absorption of 2,6-diphenylindenofluorenone (526 nm) and its reduced analogue (2,6-diphenylindenofluorene, 345 nm) indicates that the

band gap decreases significantly when two ketone units are presented. The band gap of 2,6-diphenylindenofluorene **(II-11)** was 3.30 eV while the one of 2,6-diphenylindenofluorenone **(II-4)** was found to be 2.1 eV. This result proves that the conjugation length increased due to the formation of a D-A system. The same trend is observed for 2,6-dithienylindenofluorenone (550 nm with the band gap of 2.0 eV) and 2,6-dithienylindenofluorene (365 nm with the band gap of 3.1 eV). The UV absorption is also highly affected by the nature of donor moieties. Of all the donor units used in this work, EDOT was found to have the biggest electron-donating power based on a significant red shift of the UV absorption and the small band gap of compound **IV-6** (567 nm and 1.8 eV respectively). This result also confirms that the conjugation length of compound **IV-6** is extended more than the one of 2,6-diphenylindenofluorenone **(II-4)** and 2,6-dithienylindenofluorenone **(IV-7).**

The thiophene and triphenylamine moieties, both of which are electron rich, were found to have similar electron-donating power based on the UV absorptions and band gaps of the corresponding final products. 2,6-Dithienylindenofluorenone (**IV-7**) showed a UV absorption of 550 nm with a band gap of 2.0 eV while the UV absorption and band gap of 2,6-bis[4-(diphenylamino)phenyl]indenofluorenone **(IV-8)** were 552 nm and 1.9 eV, respectively. The result of UV absorption and band gap demonstrates that both thiophene and triphenylamine contribute in a similar way to the D-A system. The optical band gaps of compounds were calculated using the on-set of UV absorption and are listed in Table IV.2.

Table IV.2. UV-Vis absorption, photoluminescence and band gap of indenofluorenone derivatives

Compound	λ_{abs} (nm)	λ_{pl} (nm)	$\lambda_{on\text{-}set}$ (nm)	E_g (eV)[a]
2,6-Dibromoindenofluorenone (IV-1)	498	580	565	2.2
2,6-Diphenylindenofluorenone (II-4)	526	600	594	2.1
EDOT-indenofluorenone (IV-6)	567	715	683	1.8
2,6-Dithienylindenofluorenone (IV-7)	550	597	620	2.0
2,6-Bis[4-(diphenylamino)phenyl] indenofluorenone (IV-8)	552	597	647	1.9

[a] Calculated from the empirical formula, E_g (optical, eV) = $1240/\lambda_{onset}$ (at the right side of the absorption peak)

As it was mentioned in section IV.5, compound **IV-8** was synthesized using two different synthetic routes: a direct coupling reaction of 2,6-Dibromoindenofluorenone and (diphenylamino)phenylboronic acid (Scheme IV.8) and an indirect method as outlined in Scheme IV.9. The differences between the UV-Vis absorption and PL emission of starting material and final product could confirm the success of direct coupling reaction. The maximum UV-Vis absorption of 2,6-dibromoindenofluorenone is of 498 nm and its emission peak is at 580 nm, while the UV absorption and PL emission of compound **IV-8** are of 552 nm and 597 nm, respectively. The longer absorption and emission wavelengths are the result of the longer conjugation length due to the more delocalized electrons. The presence of a monosubstituted or disubstituted product cannot, however, be proven by this method since both compounds are expected to have a smaller band gap than that of 2,6-dibromoindenofluorenone.

The UV absorption and PL emission of the compound **IV-8** made from the indirect method (Scheme IV.9) are a complete match with those of compound **IV-8** obtained from direct coupling reaction (λ_{abs} = 550 nm and λ_{PL} = 597 nm). This confirms the two facts: the Suzuki coupling was successful for the synthesis of compound **IV-8** (Scheme IV.8); the conversion of the diester to the ketone with concentrated sulfuric acid was complete (Scheme IV.9). The normalized UV-Vis absorption of compounds **II-4** and **IV-(6-8)** in solution (DMF) are displayed in Figure IV.8.

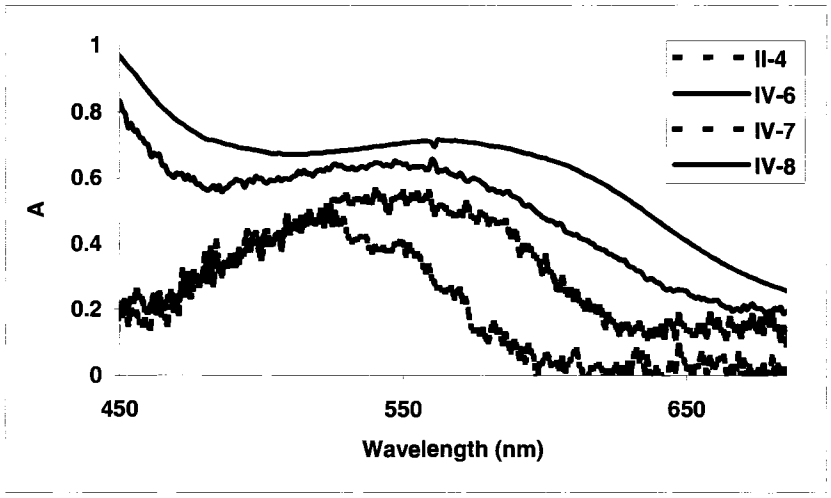

Figure IV.8. UV-Vis absorption spectra of the compounds **II-4** and **IV-(6-8)** in DMF

The photoluminescence properties of five compounds are compared and the results are summarized in Table IV.2. Similar to the in UV absorptions, no significant difference was observed in the emission wavelengths of compounds **IV-7** and **IV-8**. The PL spectra of compounds **II-4** and **IV-(6-8)** are compared in Figure IV.9. As expected, the PL emission of compound **IV-6** is exclusively red shifted with the incorporation of EDOT in system due to enhancement of the donor effect of the two ethylenedioxy groups. Therefore, the replacement of thiophene by EDOT units produces a large number

of red shift of absorption and emission bands indicating a decrease in the HOMO-LUMO gap.

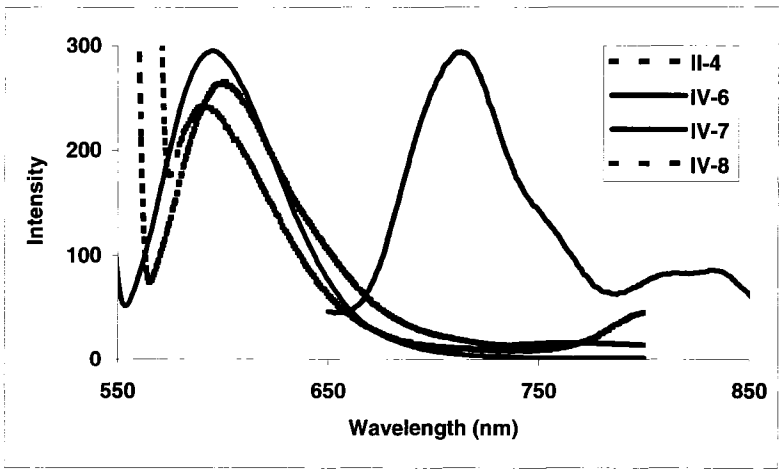

Figure IV. 9. PL emission spectra of compounds **II-4** and **IV-(6-8)** in DMF

IV.8. Conclusion

A series of new compounds was designed and synthesized based on a donor-acceptor system in which indenofluorenone was used as an acceptor. 2,6-Dibromoindenofluorenone was successfully synthesized by three alternative methods. EDOT-indenofluorenone chromophore was synthesized in one step and with a moderate yield. The Suzuki coupling with thiopheneboronic acid failed due to poor stability of thiopheneboronic acid under basic conditions and elevated temperatures. An indirect method was successfully applied to the synthesis of 2,6-dithienylindenofluorenone via the oxidation of the intermediate of 2,6-dithienylindenofluorene.

The UV absorption and photoluminescence of the compounds **II-4** and **IV-(6-8)** showed a significant red shift (180 nm roughly) in comparison with those compounds having a indenofluorene core due to the extended conjugation length of D-A system. The

PL emission of EDOT-indenofluorenone chromophore exhibits an larger red shift (118 nm) compared with 2,6-dithienylindenofluorenone due to enhancement of the electron-donating ability of the two alkoxy groups on EDOT. The UV absorption and PL emission of 2,6-bis[4-(diphenylamino)phenyl]indenofluorenone were similar to that of 2,6-dithienylindenofluorenone indicating that the electron-donating ability of thiophene and triphenylamine are similar.

IV.9. Experimental Section

Materials and Measurements

All starting materials [eg; 1,4-xylene, 4-bromophenylboronic acid and (diphenylamino)phenylboronic acid] were purchased from Aldrich Canada Inc. unless otherwise stated. All reagents were used as received without further purification. Indenofluorenone and 2,6-dithienylindenofluorene were prepared by the procedures explained in chapter 2. Infrared spectra were recorded on a Varian 1000 FT-IR Scimitar series. ^{1}H NMR and ^{13}C NMR spectra were measured by a Bruker AMX-400 spectrophotometer, respectively. Melting points of all final products were measured by Differential Scanning Calorimetry (DSC) on DSC Q100 Instrument at 10 ^{o}C/min heating rate under nitrogen. The University of Ottawa Mass Spectroscopy Center performed mass spectral analysis. The UV absorption of the compounds were recorded using a UV-Vis Lambda 900 spectrophotometer while the photoluminescence of products were measured by Shimadzu RF-1501 Spectrofluorophotometer.

Synthesis of 2,6-dibromoindenofluorenone (IV-1)

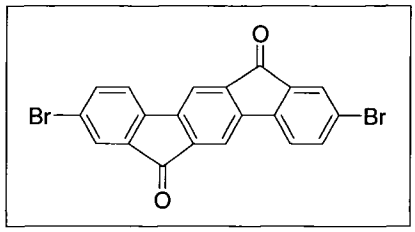

Three different methods were used for the synthesis of this compound. The procedures are as follows:

Method 1: Bromination of indenofluorenone using HgO

Indenofluorenone (2.000 g, 7.1 mmol) was dissolved in tetrachloroethane (TCE, 300 mL) at 150 °C under vigorous stirring. To this solution was added (in small portions) mercuric oxide (7.580 g, 35.0 mmol, red crystal) and sulfuric acid (10 mL). Bromine (3.400 g, 21.3 mmol) was the last reagent that was added dropwise using dropping funnel. The mixture was refluxed for 24 h, and then was filtered hot and washed with boiled TCE. The filtrate and washings were combined and all the solvents were removed by rotary evaporation to give 9.900 g of crude compound. After vacuum sublimation (300 °C, 10^{-5} torr, 3 h) the final product was obtained: 0.950 g (30.5%); MS (EI, *m/z*): 440 (M^+, 100%); Mp: >410 °C (DSC).

Method 2: Bromination of indenofluorenone using $CuBr_2/Al_2O_3$

For this reaction alumina-supported copper(II) bromide need to be prepared freshly.

To a solution of copper(II) bromide (20.0 g) in distilled water (200 mL) was added 40.0 g of neutral alumina (~150 mesh) and stirred for a while. The water was

removed using rotary evaporator at 80 °C under reduced pressure to give a brown powder. The resulting reagent was then dried under vacuum for 10 h.

To a solution of indenofluorenone (3.000 g, 10.6 mmol) in TCE (250 mL) was added 60.0 g of freshly prepared copper(II) bromide on alumina. The reaction mixture was stirred at reflux under argon atmosphere for two days. The solution was filtered hot and washed with boiling TCE three times. The solvent of filtrate was removed under reduced pressure to give 0.620 g of red product. No further purification was needed for this product.

The solid left after filtration that was pink in color, was poured in hydrochloric acid (2 N, ~ 300 mL) and stirred for a while. The result was a dark green solution of $CuBr_2$ and a pink solid that was a mixture of product and Al_2O_3. It was then filtered and further purification was applied on solid by dichlorobenzene using soxhelet to yield 0.730 g of red product. Acetone was used to wash out the trace of $CuBr_2$. The product was 1.350 g (29%); MS (EI, *m/z*): 440 (M^+, 100%); Mp: >400 °C (DSC).

It should be mentioned that the presence of Al_2O_3 is essential in this reaction, as the reaction dose not proceed with $CuBr_2$ not adsorbed on alumina.

Method 3: Synthesis of dibromoindenofluorenone

In this method one of the starting materials already bore bromo unit, therefore, the method was totally different from the other two mentioned above. The four steps used in this synthetic route, are as follows:

Step 1: Synthesis of 2,5-diiodo-1,4-xylene (IV-2)

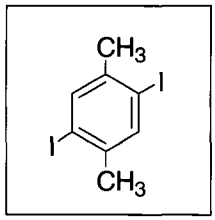

In a three-necked flask, a mixture of 1,4-xylene (10.0 g, 94.3 mmol), periodic acid dihydrate (8.600 g, 37.6 mmol), iodine (19.2 g, 75.7 mmol), acetic acid (45.2 mL), water (9 mL) and concentrated sulfuric acid (1.5 mL) were stirred at 70 °C. An exothermic reaction occurred and the temperature raised up to 90 °C, but it was controlled and allowed to cool down to 70 °C and continued stirring at this temperature for 4 h. The reaction mixture was then poured into a solution of sodium bisulfite (14.2 g in 283 mL of water), stirred for a while, filtered and the solid was washed with some water. The resulting solid was suspended in methanol and the white solid was filtered and washed with more methanol. The product was recrystalized from heptane to give 23.3 g (66%) of pure product; Mp: 104 °C; MS (EI, *m/z*): 358 (M^+, 100%); ^{1}H NMR (DMSO-d_6, 400 MHz) δ_H 7.64 (s, 2H), 2.33 (s, 6H).

Step 2: Synthesis of 2,5-bis(4-bromophenyl)-1,4-xylene (IV-3)

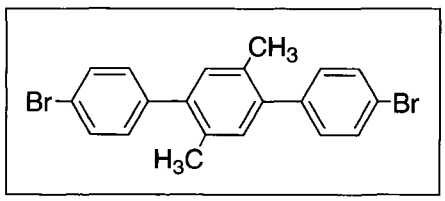

A Suzuki coupling was performed for this synthesis. A three-necked flask equipped with magnetic stirring bar, reflux condenser and argon inlet was charged (under argon atmosphere) with 2,5-diiodo-1,4-xylene (6.000 g, 16.7 mmol) and $Pd(PPh_3)_4$ (0.936

g, 0.8 mmol). To this mixture dimethoxyethane (DME, 240 mL) was added and it was stirred under argon at room temperature for few minutes. 4-Bromophenylboronic acid (6.800 g, 33.8 mmol) and Na_2CO_3 solution (2 M, 186 mL) were added and the reaction mixture was refluxed under argon for 18 h. After cooling to room temperature, the reaction mixture was extracted with dichloromethane three times and the organic layer was washed with water three times. It was then dried over $MgSO_4$ and filtered over a mixture of silica gel and celite. All the solvents were removed by rotary evaporator and the resulting beige solid was washed with minimum volume of acetone to give 3.900 g (56%) of product; Mp: 193 – 195 °C; MS (EI, *m/z*): 416 (M^+, 100%).

Step 3: Synthesis of 2,5-bis(4-bromophenyl)terephthalic acid (IV-4)

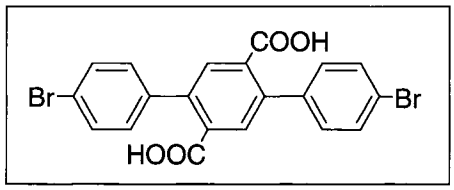

A one-liter three-necked flask equipped with a mechanical stirrer and reflux condenser was charged with 2,5-bis(4-bromophenyl)1,4-xylene (7.300 g, 17.5 mmol), pyridine (350 mL), potassium permangenate (22.0 g) and water (70 mL). The reaction mixture was heated to reflux until the purple color of reagent turned to brown. At this point more $KMnO_4$ and water were added and this was continued until the purple color did not changed. The total KMnO4 was about 100.0 g. After 24 h it was stopped heating and filtered the reaction mixture hot and washed with some boiled water. The pyridine and some water were evaporated by rotary evaporator and to the resulted solution was added concentrated hydrochloric acid and the PH was adjusted to 2. The beaker was kept

on ice for about one hour. The white product was filtered by suction and dried in the vacuum oven at 80 °C to give 7.900 g of pure product (94.6%); IR (KBr cm^{-1}): 1697 (C=O, carbonyl); Mp: 340 °C (DSC); ^{1}H NMR (DMSO-d_6, 400 MHz): δ_H 13.26 (s, broad, 2H), 7.72 (s, 2H), 7.64 (d, 4H, J=6.0 Hz), 7.36 (d, 4H, J=9.0 Hz). ^{13}C NMR (DMSO-d_6, 100 MHz): 168.8, 139.4, 139.2, 134.4, 132.0, 131.6, 130.9, 121.6.

Step 4-a: Conversion of diacid (IV-4) to diketone (IV-1) using concentrated H_2SO_4

Concentrated sulfuric acid (80 mL) was added to 2,5-bis(4-bromophenyl)terephthalic acid (1.000 g, 2.1 mmol) and stirred for 24 h. The yellowish color of reaction mixture turned to green slowly and the progress of reaction was followed by the addition of small amount of reaction mixture to some water and judged by the color of precipitate. After 24 h, it was poured in ice cautiously and the red-purple solid was filtered, washed with some water and dried in the vacuum oven at 50 °C to give 0.452 g of product (48.9%); MS (EI, *m/z*): 440 (M^+, 100%); Mp: >410 °C (DSC).

Step 4-b: Conversion of diacid (IV-4) to diketone (IV-1) using Eaton's reagent

The same synthetic procedure as in the case of 2,6-diphenylindenofluorenone (**II-4**) was employed with a slight change of reaction temperature that was 60 – 65 °C and the reaction time which was 24 h. Starting from 1.000 g of 2,5-bis(4-bromophenyl)terephthalic acid, 0.288 g of product was obtained (31.2%); MS (EI, *m/z*): 440 (M^+, 100%); Mp: >410 °C (DSC).

Synthesis of 2(3,4-ethylenedioxythiophene)boronic ester (IV-5)

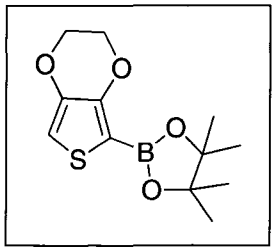

A solution of 3,4-ethylenedioxythiophene (EDOT, 2.000g, 14.1 mmol) in dry THF (30 mL) was placed in a three-neck completely dry flask and cooled to –78 °C under argon atmosphere. To this solution, n-BuLi (6.2 ml, 2.5 M) was added dropwise using a glass syringe. The temperature was slowly raised to 0 °C and the yellow mixture was stirred at the same temperature for 30 min. The reaction mixture was then re-cooled to -78 °C and a mixture of 2-isopropoxy-4,4`,5,5`-tetramethyl-1,3,2-dioxaborolane (5.8 mL, 28.0 mmol) in dry THF (10 mL) was added through a pre-dried dropping funnel and the reaction mixture was stirred for 6 h. After raising the temperature to the rt, the reaction mixture was poured in a mixture of crushed ice and NH_4Cl and crude product was extracted into diethyl ether three times. The combined organic layers were dried over $MgSO_4$ and all the solvents were removed by rotary evaporator. To the light brown sticky compound some methanol was added and pure product was crystallized as a yellow crystals (2.360 g, 62.6%); Mp: 86-88 °C; MS (EI, *m/z*): 268 (M^+, 100%); ^1H NMR (DMSO-d_6, 400 MHz): δ_H 6.60 (s, 1H), 4.27 (t, 2H, J=15.0 Hz), 4.18 (t, 2H, J=15.0 Hz), 1.30 (s, 12H); ^{13}C NMR (DMSO-d_6, 100 MHz): 150.5, 142.7, 128.5, 128.4, 127.9, 107.8, 83.2, 64.5, 64.0.

Synthesis of EDOT-indenofluorenone (IV-6)

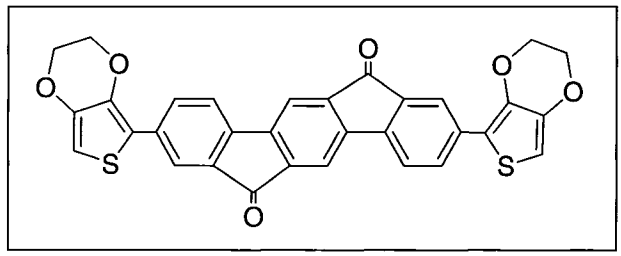

Compound **IV-5** (0.230 g, 0.9 mmol), 2,6-dibromoindenofluorenone (0.150 g, 3.4 $\times$ 10^{-1} mmol), and tetrakis(triphenylphosphine)palladium(0) (0.058 g, 4.9 $\times$ 10^{-2} mmol) were placed in a three-neck flask and stirred under argon for few minutes. To this mixture, N-methylpyrolidinone (NMP, 30 mL) was added and the reaction mixture was heated up to 160 °C to dissolve all the starting materials. An aqueous solution of Na_2CO_3 (0.772 g) was added and heating was continued at the same temperature for overnight all the times under argon atmosphere. After cooling down to room temperature, the mixture was poured in water, filtered, washed with more water and dried. The green solid product was then purified by vacuum sublimation (0.045 g, 23.6%); Mp: >400 °C (DSC); MS: (EI, *m/z*): 562 (M^+, 6.9%).

Synthesis of 2,6-dithienylindenofluorenone (IV-7)

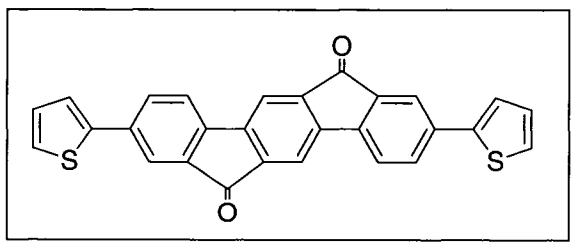

Potassium permangenate (0.074 g, 0.5 mmol), 2,6-dithienylindenofluorene (**II-12**, 0.050 g, 0.1 mmol), and tetrabutylphosphonium bromide (TBPBr, 0.016 g, 4.7 $\times$ 10^{-2} mmol) were put into the round-bottomed flask and dichlorobenzene (20 mL) was added.

The reaction mixture was stirred and refluxed. After reacting for 6 h, the temperature was reduced to 100 °C and then the next portion of $KMnO_4$ (0.040 g, 0.2 mmol) and TBPBr (0.016 g, 4.7×10^{-2} mmol) were added to the solution and continued to reflux. After 8 h, the temperature was reduced again and the third portion of $KMnO_4$ (0.037 g, 0.2 mmol) and tetrabutylammonium bromide (TBABr, 0.005 g, 1.6×10^{-2} mmol) were added to the reaction mixture. After another 8 h reflux the last portion of $KMnO_4$ (0.074 g, 0.5 mmol) and TBABr (0.022 g, 6.8×10^{-2} mmol) were added and continued to reflux for 12 more h. It was then poured in a solution of sodium bisulfite, and the organic phase was evaporated using rotary evaporator. The final product was purified by sublimation (340 °C, 10^{-5} torr, 3 h) as a dark green solid (0.015 g, 28.3%); MS (EI, *m/z*): 446 (M^+, 100%); IR (KBr, cm^{-1}): 1709 (C=O, carbonyl); Mp: 401 °C (DSC). This compound crystallized upon cooling at 391 °C.

Synthesis of 2,6-bis[4-(diphenylamino)phenyl]indenofluorenone (IV-8)

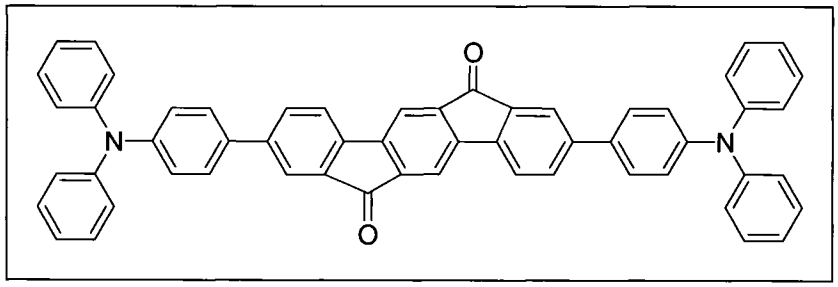

The same procedure of Suzuki coupling was applied for this synthesis. 2,6-dibromoindenofluorenone (0.150 g, 3.4×10^{-1} mmol), (diphenylamino)phenylboronic acid (0.246 g, 8.5×10^{-1} mmol) and $Pd(PPh_3)_4$ (0.058 mg, 4.9×10^{-2} mmol) were dissolved in NMP (30 mL) at about 160 °C while it was stirring under argon atmosphere

to remove oxygen. A solution of sodium carbonate (0.772 g) was added and stirred at the same temperature for 24 h. After cooling down to room temperature, it was poured in water, filtered and dried. The reaction yield was too low after vacuum sublimation. Mp: >400 °C (DSC). UV absorption: 552 nm; PL emission: 597 nm.

Synthesis of 2,5-bis(4-bromophenyl)terephthalate (IV-9)

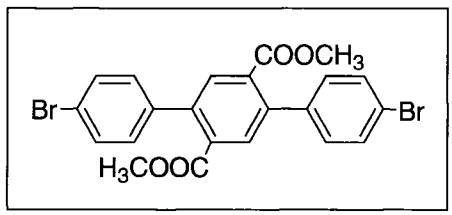

Compound **IV-4** (2,5-bis(4-bromophenyl)terephthalic acid, 5.000 g, 10.5 mmol) and methanol (120 mL) were placed in a one-necked round-bottomed flask and connected to condenser. To this mixture a catalytic amount of concentrated sulfuric acid (2 mL) was added. The starting compound was not soluble in cold methanol, therefore to complete the reaction heating was required. The reaction mixture was heated up to 90 °C for 24 h and the progress of reaction was monitored by thin layer chromatography (silica, hexane/ethyl acetate = 8:2, v/v). All the solvents were removed by rotary evaporator and crude product was dissolved in dichloromethane.

To remove the unreacted starting materials and mono-converted compounds, NaOH (5%) was added. The organic phase was separated, washed with water for few times and dried over $MgSO_4$ and evaporated all the solvents to give 4.300 g (81.3%) of pure product. The purity of this product was confirmed by ^1H NMR and ^{13}C NMR, and since it was going to be used as a monomer for polymerization, therefore two different methods were applied for further purification on this compound: column chromatography

(silica, hexane/ethyl acetate = 9:1 v/v) and crystallization (dichloromethane/methanol). IR (KBr, cm^{-1}): 1732 (C=O, carbonyl); Mp: 206.7 °C. ^1H NMR ($CDCl_3$, 400 MHz): δ_H 7.82 (s, 2H), 7.57 (d, 4H, J=9.0 Hz), 7.25 (d, 4H, J=9.0 Hz), 3.71 (s, 6H). ^{13}C NMR ($CDCl_3$, 100 MHz): 167.5, 139.7, 138.5, 133.4, 132.3, 131.8, 130.7, 121.9, 52.9.

Synthesis of 2,5-bis[4-(4-diphenylamino)phenyl)phenyl]terephthalate (IV-10)

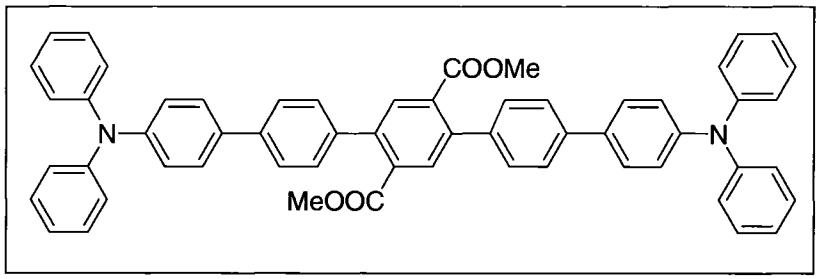

Due to the difficulties for confirmation of compound **IV-8**, another alternative route was chosen. In this route at first triphenylamine was connected to 2,5-diphenyl terephthalic ester that was soluble in normal solvents and could be confirmed by mass spectroscopy and IR. In next step ring was closed to convert two ester groups to ketons that can easily be confirmed by IR.

Compound **IV-9** [2,5-bis(4-bromophenyl)terephthalate, 0.100 g, 19.8 × 10^{-2} mmol], (diphenylamino)phenylboronic acid (0.145 g, 0.5 mmol) and 0.060 g of $Pd(PPh_3)_4$ were introduced in a three-necked flask equipped with magnetic stirrer and reflux condenser. The same Suzuki coupling was followed after the addition of solvent (DME, 30 mL) and Na_2CO_3 solution (0.800g). The reaction mixture was refluxed for 4 h and the progress of reaction was followed by TLC (solvent, hexane: ethyl acetate=8:2 v/v). The yellow solution was poured in water that turned milky. To separate the very fine solids, it was centrifuged for 20 min at the highest possible speed and product was

collected as a pale solid, dried in vacuum at 60 °C. MS (ESI, *m/z*): 832; IR (KBr, cm^{-1}): 1724 (C=O, carbonyl), 1278 (C-N), 1588 (C=C, aromatic), 1118 (C-O, ester).

Synthesis of 2,6-bis[4-(diphenylamino)phenyl]indenofluorenone via closing of compound IV-10

To about 0.030 g of 2,5-bis[4-(4-diphenylamino)phenyl)phenyl]terephthalate **(IV-10)** in a test tube was added about 3 mL of concentrated sulfuric acid and the mixture was stirred at room temperature for 24 h. The color of mixture turned to very dark green right after the addition of acid. After 24 hours of stirring the reaction mixture was poured in water, filtered and washed with more water and dried at 80 °C. The IR spectrum of compound was compared with the one of starting material that showed a peak for C=O group shifted to the lower wavenumber (1724-1716 cm^{-1}) confirming that the conversion of ester to ketone was successful. Since this peak was not very sharp, therefore the closing step was continued for another 24 h in concentrated sulfuric acid at 50 °C. It was then poured in water, filtered, washed with more water and dried. IR (KBr, cm^{-1}): 1711 (C=O, carbonyl), 1274 (C-N), 1590 (C=C, aromatic); Mp: >400 °C (DSC).

Synthesis of methyl 4-aminobenzoate (IV-11)

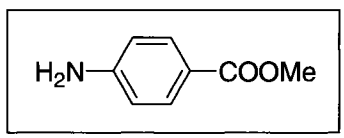

A solution of 4-aminobenzoic acid (6.600 g, 48.2 mmol) and sulfuric acid (5.6 mL) in methanol (400 mL) was heated under reflux for 17 h. The yellow solution was then poured in saturated $NaHCO_3$ solution. After stirring for a while, the solvent was

removed in vacuum. The residue was taken up in a solution of $NaCl/Na_2CO_3$ and extracted three times with ethyl acetate. The combined organic layers were dried over sodium sulfate and the solvent was evaporated to dryness. The pale solid was 6.880 g (94.6%); Mp: 115 – 117 °C (Lit: 110-113 °C); ^1H NMR ($CDCl_3$, 400 MHz): δ_H 7.85 (d, 2H), 6.63 (d, 2H), 4.09 (s, 2H), 3.84 (s, 3H).

Synthesis of diimine IV-12

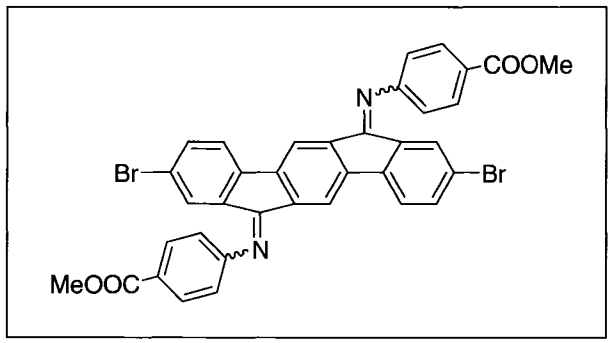

Dibromoindenofluorenone (0.100 g, 2.3×10^{-1} mmol), methyl 4-aminobenzoate (0.544 g, 3.6 mmol) and DABCO (1,4-diazabicyclo[2.2.2]octane, 0.162 g, 14.4×10^{-1} mmol) were placed in a three-neck round-bottom flask and dissolved in dichlorobenzene (50 mL) at 150 °C under argon atmosphere. After addition of titanium tetrachloride (0.425 g, 2.2 mmol), the reaction was kept at reflux for 48 h. The reaction mixture was filtered hot and the solid was washed with boiled solvent. All the filtrates were combined and the solvent was evaporated completely. The product was purified using ethyl acetate to give 0.139 g (87%) of redish-orange product; Mp: 304 °C (DSC, decomposed); MS (EI, *m/z*): 706 (M^+, 100%); IR (KBr, cm^{-1}): 1713 (C=O, carbonyl), 1650 (C=N, imine), 1596 (C=C, aromatic), 1099 (C-O, ester); ^1H NMR ($CDCl_3$, 400 MHz): δ_H 6.6-8.1 (m, 16H), 4.0 (s, 3H), 3.9 (s, 3H).

References

1. Gross, M.; Muller, D. C.; Nothofer, H. G.; Scherf, U.; Neher, D.; Brauchle, C.; Meerholz, K. *Nature* **2000**, *405*, 661.
2. Ayyappanpillai, A. *Chem. Soc. Rev.* **2003**, *32*, 181.
3. Tsuie, B.; Reddinger, J. L.; Sotzing, G. A.; Soloducho, J.; Katritzky, A. R.; Reynolds, J. R. *J. Mater. Chem.* **1999**, *9*, 2189.
4. Setayesh, S.; Marsitzky, D.; Mullen, K. *Macromolecules* **2000**, *33*, 2016.
5. Casalbore-Miceli, G.; Gallazzi, M. C.; Zwcchin, S.; Camaioni, N.; Geri, A.; Bertarelli, C. *Adv. Funct. Mater.* **2003**, *13*, 307.
6. Velusamy, M.; Thomas, K. R. J.; Lin, J. T.; Hsu, Y. C.; Ho, K. C. *Org. Lett.* **2005**, *7*, 1899.
7. Porizo, W.; Destri, S.; Giovanella, U.; Pasini, M.; Motta, T.; Natali, D.; Sampietro, M.; Campione, M. *Thin Solid Films* **2005,** *492*, 212.
8. Uckert, F.; Tak, Y. H.; Mullen, K.; Bassler, H. *Adv. Mater.* **2000**, *12*, 905.
9. Ding, J. Day, M.; Robertson, G.; Roovers, J. *Macromolecules* **2002,** *35*, 3474.
10. Bunce, N. J. *Can. J. Chem.* **1972**, *50*, 3109.
11. Afzal Khan, S.; Munawar, M. A.; Siddiq, M. *J. Org. Chem.* **1988,** *53*, 1790.
12. Kovacic, P.; Davis, K. E. *J. Am. Chem. Soc.* **1964,** *86*, 427.
13. Kodomari, M.; Satoh, H.; Yoshitomi, S. *J. Org. Chem.* **1988,** *53*, 2093.
14. Zhou, Q.; Swager, T. M. *J. Am. Chem. Soc.* **1995,** *117*, 12593.
15. Stojan, S.; Petra, K.; Marko, Z. *Synlett.* **2002,** *4*, 598.
16. Perry, R. J.; Wilson, B. D.; turner, S. R.; Blevins, R. W. *Macromolecules* **1995,** *28*, 3509.

17. Hassan, J.; Gozzi, C.; Schulz, E.; Lemaire, M. *J. Organomet. Chem.* **2003,** *687*, 280.

18. Dingemans, T. J.; Sanjeeva Murthy, N.; Samulski, E. T. *J. Phys. Chem. B.* **2001,** *105*, 8845.

19. Watson, W. H. *US. Pat.* 3,365, 425, (**1968**).

20. Meng, H.,; Zheng, J.; Lovinger, A. J.; Wang, B. C.; Patten, P. G. V.; Bao, Z. *Chem. Mater.* **2003**, *15*, 1778.

21. Groenendaal, L. B.; Jonas, F.; Freitag, D.; Pielartzik, H.; Reynolds, J. R. *Adv. Mater.* **2000**, *12*, 481.

22. Roncali, J. *Chem. Rev.* **1997**, *97*, 173.

23. Turbiez, M.; Frere, P.; Roncali, J. *Tetrahedron* **2005**, *61*, 3045.

24. Mohanakrishnan, A. K.; Hucke, A.; Lyon, M. A.; Lakshmikantham, M. V.; Cava, M. P. *Tetrahedron* **1999**, *55*, 11745.

25. Kim, Y. M.; Yu, S. *J. Am. Chem. Soc.* **2003**,*125*, 1696.

26. Forster, M.; Annan, K. O.; Scherf, U. *Macromulecules* **1999**, *32*, 3159.

27. Takanashi, K.; Chiba, H.; Higuchi, M.; Yamamoto, K. *Org. Lett.* **2004**, *6*, 1709.

28. Yamamoto, T.; Nishiyama, M.; Koie, Y. *Tetrahedron Lett.* **1998**, *39*, 2367.

29. Wu, J.; Baumgarten, M.; Debije, M. G.; Warman, J. M.; Mullen, K. *Angew. Chem. Int. Ed.* **2004**, *43*, 5331.

30. Jacob, J.; sax, S.; Piok, T.; List, E. J, W.; Grimsdale, A, C.; Mullen, K. *J. Am. Chem. Soc.* **2004**, *126*, 6987.

Chapter V

Indenofluorenone-Containing Polymers: Synthesis, Characterization and Properties

V.1. Introduction

Fluorenones are an important class of compounds because of their applications in polymeric and organic light-emitting diodes (PLEDs/OLEDs). Polyfluorenes are conjugated polymers known as efficient blue emitters. However, a low-energy green photoluminescence band appears in the emission from polyfluorenes over time and degrades the blue emission.[1] Different mechanisms were proposed for this green emission.[2,3] Among all, the mechanism of the green emission band originating from fluorenone defects, attracts more attention.[4] Thus, the study of fluorenone becomes an important subject as it is an electron-deficient compound and exhibits electron-transporting property.[5] Therefore, addition of an extra carbonyl group in fluorenone structure along with an additional phenyl ring (indenofluorenone) should lead to an efficient electron acceptor.

As noted in Chapter IV, indenofluorenone plays an important role as an electron-acceptor in a donor-acceptor system due to the electron-withdrawing ability of the carbonyl moieties. The comparison between UV absorptions of 2,6-diphenylindenofluorenone (525 nm) and its reduced analogue (2,6-diphenylindenofluorene, 345 nm) indicates the significant low band gap when two ketone units are presented. Therefore, it is expected that incorporation of indenofluorenone group into the polymer backbone as an electron acceptor can further decrease the band gap.

As outlined in Figure V.I, three synthetic routes were proposed for the indenofluorenone-containing polymers. A direct coupling of electron-donating units with indenofluorenone using either a Suzuki or Grignard reaction was the first choice of

synthetic routes, since 2,6-dibromoindenofluorenone was available in high yield and in high purity, as described in Chapter IV. However, this monomer was found only to be soluble in high boiling solvents with low concentration, which makes one-step polymerization starting with 2,6-dibromoindenofluorenone quite difficult.

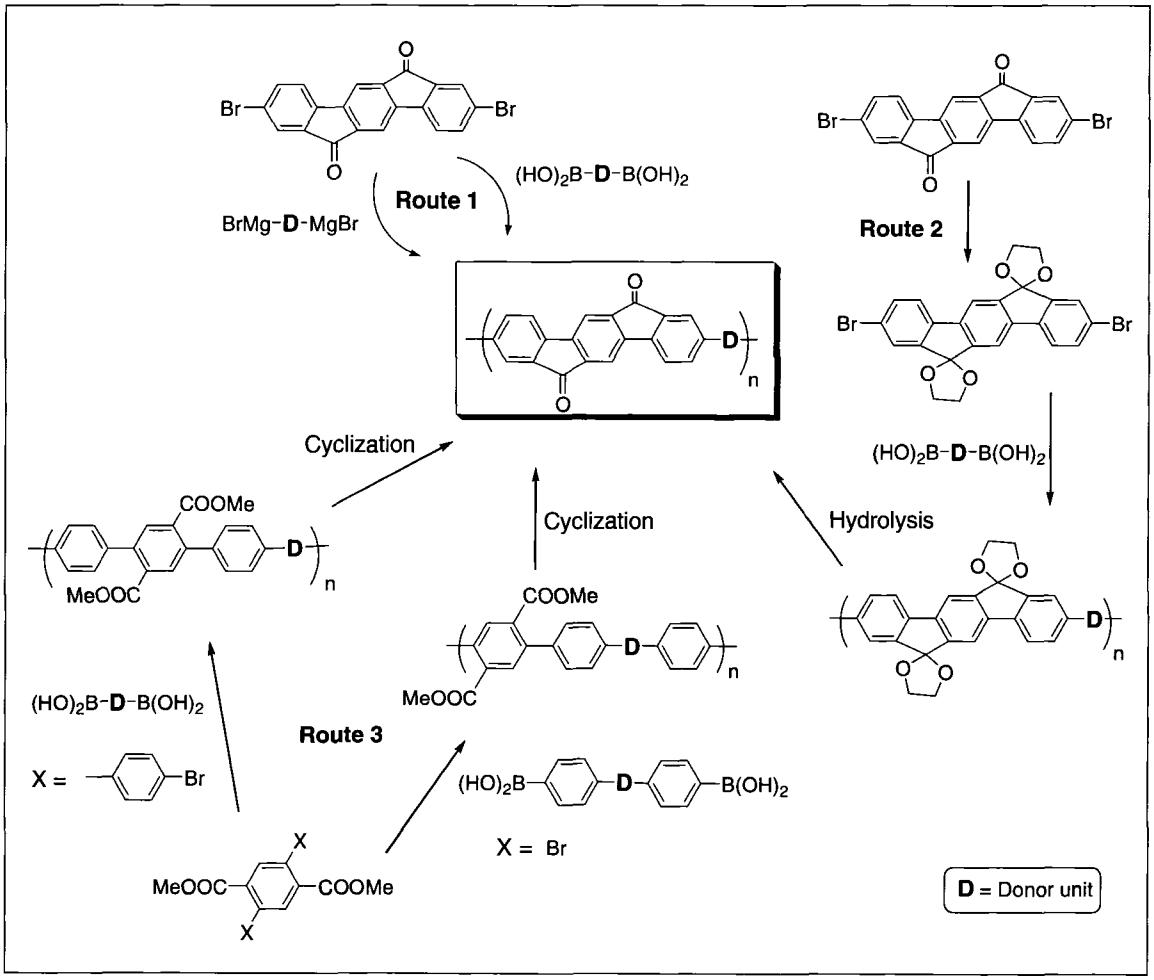

Figure V.I. Proposed synthetic routes to indenofluorenone-containing polymers

The second route utilizes a ketal derivative of 2,6-dibromoindenofluorenone[5,6] hoping to increase the monomer solubility in polymerization. After polymerization by a Suzuki reaction, the ketal groups can be hydrolyzed to the original ketone units. Once again, because of poor solubility of 2,6-dibromoindenofluorenone in common solvents, the conversion of ketone groups to the ketal did not proceed.

The last choice was to use dimethyl 2,5-bis(4-bromophenyl)terephthalate (**IV-9**) and dimethyl 2,5-dibromoterephthalate (**II-1**). Since these compounds are soluble in most common organic solvents, by the Suzuki coupling they can be polymerized with monomers bearing two boronic acid units. A cyclization step using either concentrated sulfuric acid or Eaton's reagent should then convert the ester groups of polymer to the ketones. Indeed, this synthetic route was established in this thesis work.

V.2. Monomer Synthesis and Characterization

In order to make a new series of D-A type polymers, four monomers were chosen, hoping that by the cross coupling of the monomers, four polymers would be obtained. Dimethyl 2,5-bis(4-bromophenyl)terephthalate (**IV-9**) and dimethyl 2,5-dibromoterephthalate (**II-1**) were selected as the monomers bearing bromo units while 9,9-dioctylfluorene-2,7-bis(trimethyleneborate) and 4,4′-bis(4,4,5,5-tetramethyl-1,3,2-dioxaborolane-2-yl)-N-hexyldiphenylamine were chosen as the monomers having boronic ester groups.

V.2.1. Synthesis of Arylboronic ester Monomer

Since dimethyl 2,5-bis(4-bromophenyl)terephthalate (**IV-9**) and dimethyl 2,5-dibromoterephthalate (**II-1**) are available for use in Suzuki coupling reaction, an arylboronic ester monomer is needed. Besides commercially available monomers, such as 9,9-dioctylfluorene-2,7-bis(trimethyleneborate) (Scheme V.3), a new donor-type monomer (**V-1**) is designed.

Considering the solubility of the monomer and subsequent polymers, as well as the electron-donating ability of the monomer as a donor, introduction of the alkyl chain into the monomer structure was desirable (**V-1**, Scheme V.1).[7]

The selection of alkyl chain is important. It has been reported that, the introduction of sterically demanding solubilizing alkyl chains leads to a considerable torsion about phenylene-phenylene bonds in poly-*p*-phenylene, which seriously inhibits the conjugative interaction along the polymer chain.[8] The result of this hampers π-conjugation, which leads to an increased optical band gap of corresponding polymer. On the other hand, the presence of alkyl groups on nitrogen makes a better electron donor in comparison with aryls. However, the small side chain will not increase the solubility and electron-donating ability of the monomer effectively. Among all the alkyl chains, hexyl and octyl groups are the most common alkyls used for this purpose.

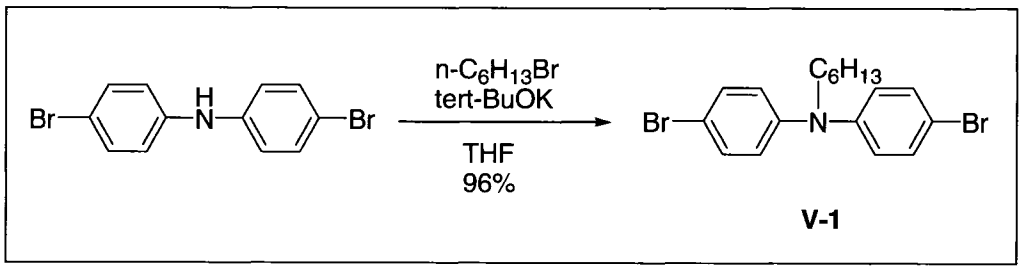

Scheme V.1. Alkylation of 4,4′-dibromodiphenylamine

Compound **V-1** was synthesized from commercially available 4,4′-dibromodiphenylamine in 96% yield (Scheme V.1).[7] The known procedure was slightly modified to accommodate the monomer synthesis in larger scale (20 g of starting material). The modification was applied to the ratio of starting materials as well as the time of the reaction.

Since the Suzuki coupling was to be used in polymerization, the conversion of two bromo units to boronic esters was needed. Slight modification was applied to a known reaction procedure to achieve pure monomer suitable for the next step. The modification was done on the ratio of the reactants, as the excess amount of n-butyllithium and 2-isopropoxy-4,4′,5,5′-tetramethyl-1,3,2-dioxaborolane were used for the reaction. Some unreacted starting materials were observed when the procedure reported in the literature, was used.

The lithiation step on N-hexyl-4,4′-dibromodiphenylamine was attempted first. To the resulting strong nucleophile (lithium salt of N-hexyl-4,4′-dibromodiphenylamine), was introduced 2-isopropoxy-4,4′,5,5′-tetramethyl-1,3,2-dioxaborolane to complete the exchange of bromo to boronic ester (Scheme V.2.). Monomer **V-2** was achieved as yellowish-white crystals with a moderate yield (45.6%). It should be mentioned that the conversion of bromo units to the boronic acid moieties was also another alternative, but boronic ester was favored due to the higher reactivity comparing with boronic acid.

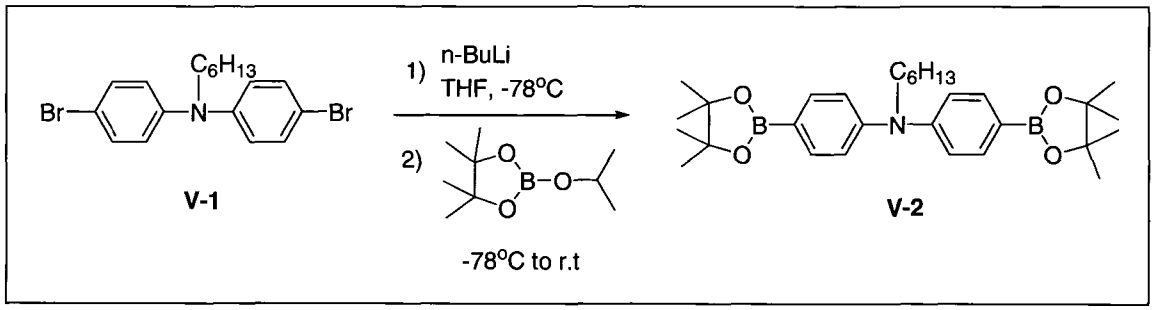

Scheme V.2. Synthesis of monomer **V-2**

V.2.2. Characterization of Monomer (V-2)

Both compound **V-1** and monomer **V-2** were characterized by ^{1}H and ^{13}C NMR spectroscopy. In ^{1}H NMR spectrum of compound **V-1** no signal was observed

corresponding to proton of N-H group. This result indicates that the alkylation reaction was completed. A set of doublets could be seen for the aromatic protons at ~ 6.80 ppm and 7.33 ppm. For the CH_2 group adjusent to nitrogen, a triplet was observed at 3.60 ppm while the rest of the protons in alkyl chain appeared at the upfield (~ 0.85 ppm to 1.60 ppm).

The ^1H NMR spectrum of monomer **V-2** is displayed in Figure V.2. It reveals the same doublets as compound **V-1** for the aromatic protons but downfielded (7.03 ppm for Hb and 7.72 ppm for Ha) due to the presence of boronic ester groups.

In the case of compound **V-2**, the CH_2 group adjacent to the nitrogen appeared at 3.75 ppm, similar to the CH_2 group in compound **V-1**. In this case, a singlet was observed at 1.32 ppm integrated for 24 protons of the eight methyl groups.

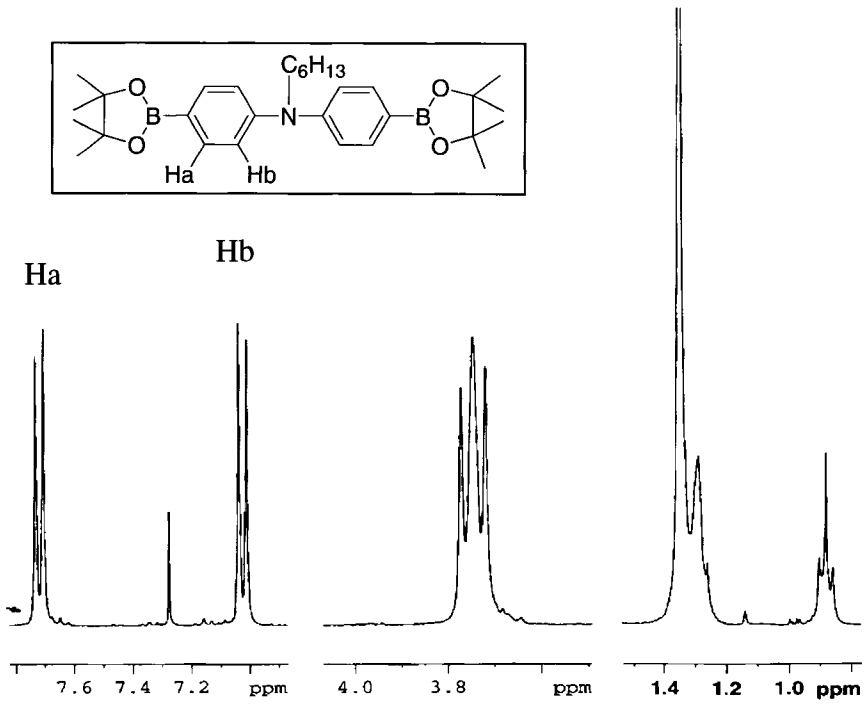

Figure V.2. The ^1H NMR spectrum (400 MHz) of monomer **V-2** in $CDCl_3$

V.3. Polymer Synthesis

Polymers **V-(3-6)** were obtained by the polymerization reaction of monomers **IV-9** and **II-1** with two arylboronic ester monomers. Dimethyl 2,5-bis(4-bromophenyl)terephthalate **(IV-9)** was used to make the polymers **V-(3-4)**, while dimethyl 2,5-dibromoterephthalate **(II-1)** was selected for the polymers **V-(5-6)**.

V.3.1. Polymerization Using Dimethyl 2,5-Bis(4-bromophenyl)terephthalate as Monomer

The monomer, dimethyl 2,5-bis(4-bromophenyl)terephthalate (**IV-9**), was chosen for the first set of indenofluorenone-containing polymers. Polymers **V-(3-4)** were obtained by polymerizations of monomer **IV-9** with two different monomers bearing boronic ester groups, i.e. 9,9-dioctylfluorene-2,7-bis(trimethyleneborate) and 4,4′-bis(4,4,5,5-tetramethyl-1,3,2-dioxaborolane-2-yl)- N-hexyldiphenylamine **(V-2)** (Scheme V.3).

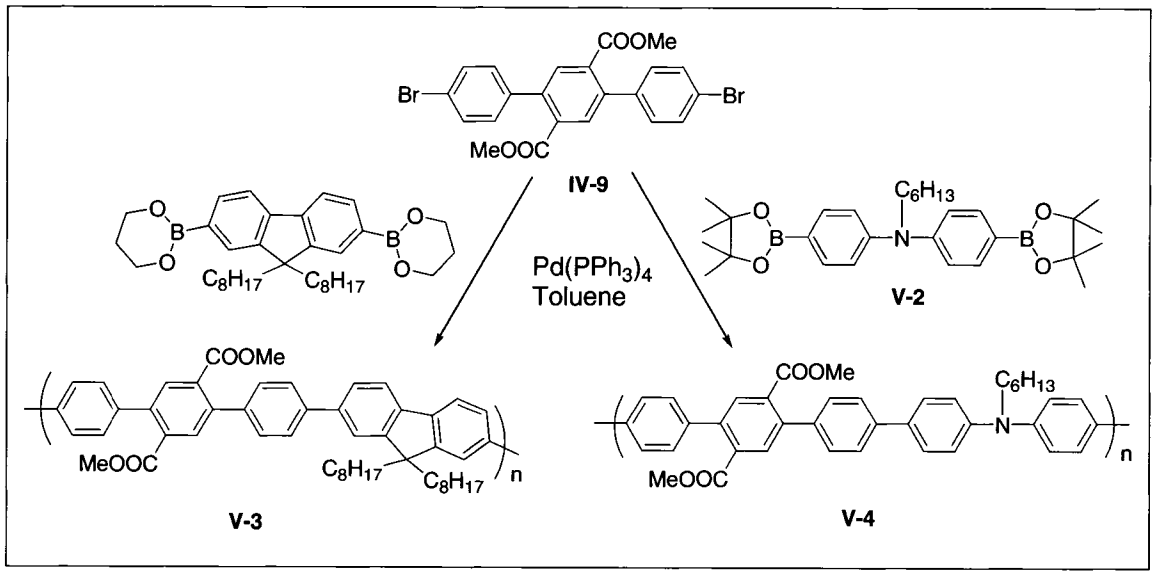

Scheme V.3. Synthesis of polymers **V-(3-4)**

Polymerizations were done using the Suzuki coupling reaction in degassed toluene (20% concentration of two monomers) at 90 °C in the presence of terakis(triphenylphosphine)palladium(0) (0.5 mol%) as catalyst. The molar ratio of monomers was 1:1 and a solution of sodium carbonate (7 molar equivalent) was used as base. Aliquat 336 (2-3 drops) was used as a phase transfer catalyst. The reaction proceeded for 24 hours. Since it was reported that the residual of both bromine and boronic acid as end groups of polymer back bones could quench the emission and lead to the stability problem in LED applications,[9] polymerization reactions were terminated using an end-capping reagent. The first end capping reagent was phenylboronic acid (10 mol %) to react with bromo end of polymer chain and the second end capping compound was bromobenzene (10 mol %) to react with boronic acid units. The resulting polymers were coagulated in methanol.

It should be mentioned that the amount of catalyst was critical for the polymerization reaction. The large amount of catalyst will cause the low molecular weight while the reaction may not proceed well with a very small amount of catalyst since the reactivity of Pd catalyst will be affected by air. The polymerization reaction failed to produce high molecular weight polymer **V-3** when using 0.5 mol % of catalyst. The high molecular weight was achieved for this polymer with the use of 0.4 mol % of catalyst. The reaction is also sensitive to the amount of base while the presence of a phase transfer catalyst is essential. Concentration of the reaction mixture is another factor that needs to be considered, since the low concentration tends to lead the products with very low molecular weights.

V.3.2. Polymerization Using Dimethyl 2,5-dibromoterephthalate as Monomer

The monomer, dimethyl 2,5-dibromoterephthalate (**II-1**), was chosen for the second set of indenofluorenone-containing polymers, because the two ester groups can be converted to ketone to form indenofluorenone. Polymers **V-(5-6)** were prepared under the same polymerization condition as for polymers **V-(3-4).**

Monomer **II-1** was used to polymerize with two different monomers having boronic ester groups, i.e. 9,9-dioctylfluorene-2,7-bis(trimethyleneborate) and **V-2** (Scheme V.4). A Suzuki coupling was applied to prepare these two polymers in toluene in the presence of terakis(triphenylphosphine)palladium(0). Sodium carbonate solution was chosen as a base and aliqute 336 as a phase transfer catalyst. The polymers were end-capped using phenylboronic acid and bromobenzene.

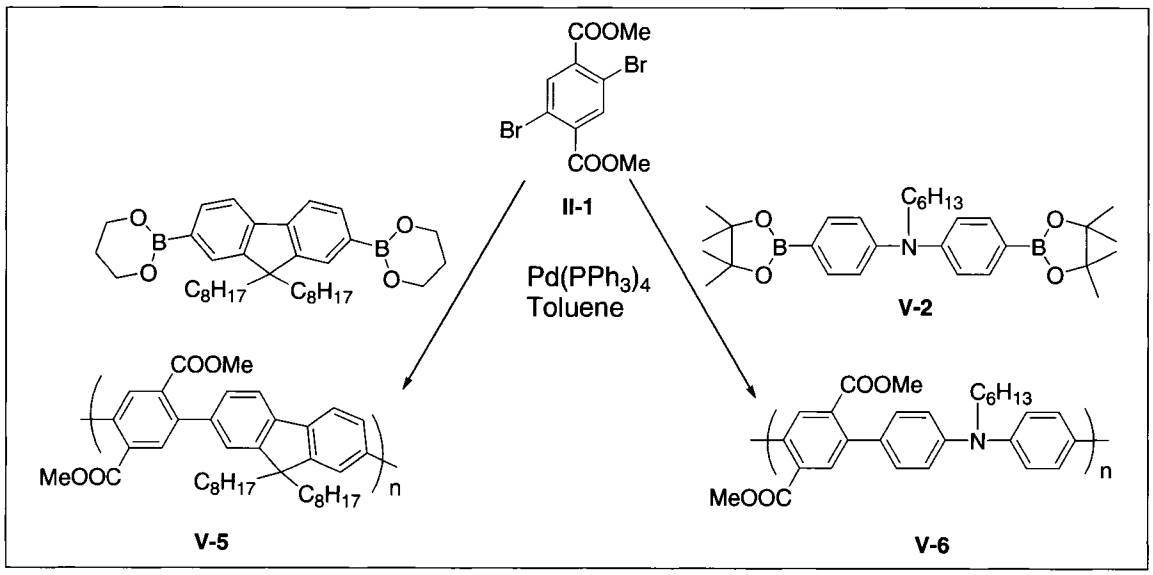

Scheme V.4. Synthesis of polymers **V-(5-6)**

V.3.3. Cyclization (Conversion of Ester groups to Ketones)

Cyclization of polymer **V-5** was tried on polymer powder and film. Three strong acids (concentrated sulfuric acid, Eaton's reagent and oleum) were used to convert the ester groups of **V-5** powder to the ketones. While only concentrated sulfuric acid was used for the conversion of **V-5** film to **V-9**. Cyclization of polymers **V-(3-4)** and **V-6** were only tried on polymers powder (Scheme V.5).

In order to cyclize polymer **V-5** powder, three different acids mentioned above were tried. The acid was added to the polymer in a test tube and the amount of acid used for this conversion was high (4-5 mL of acid for 20 mg of polymer). The cyclization failed using Eaton's solution based on the results from IR spectroscopy which reveals that, there was no significant change in wavenumber of carbonyl groups from ester to ketone. This result confirms that Eaton's reagent is not strong enough for the conversion, while the oleum was very strong for this reaction, as a hard and black solid was obtained from the reaction. The best acid for this reaction was found to be concentrated sulfuric acid which gave the same results in two different conditions (stirring at room temperature for 5-6 hours or at 50 °C for 1-2 hours). Partially cyclized structures were the results of these two conditions while changing the reaction condition to the stirring at 50 °C for overnight resulted more conversion (based on the position of carbonyl peak in IR spectra).

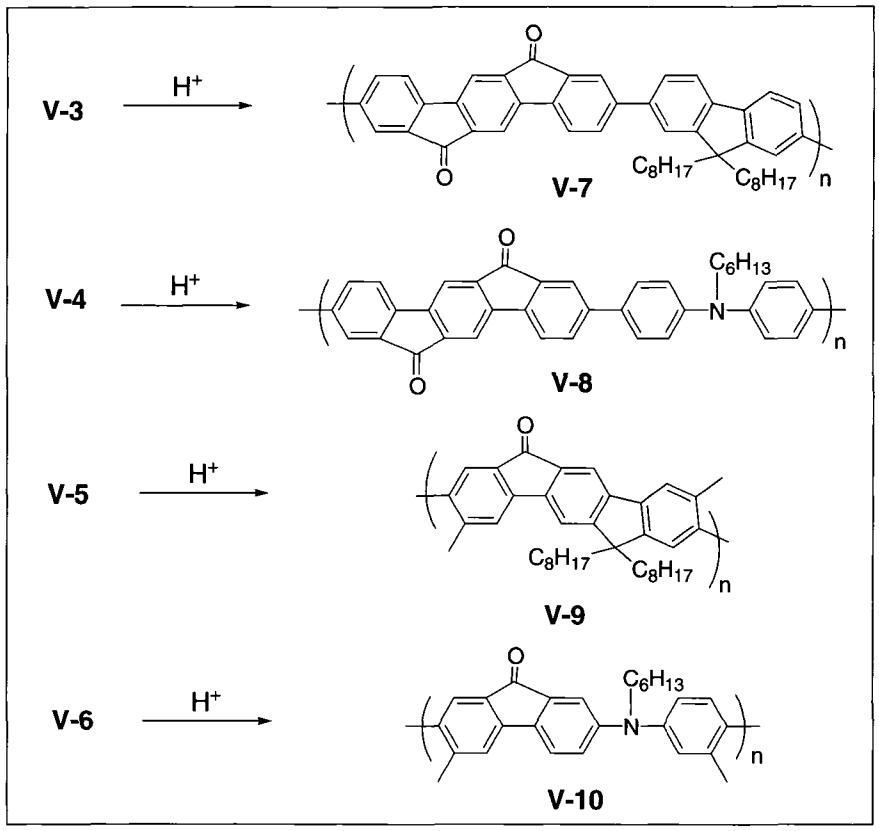

Scheme V.5. Conversion of the polymers **V-(3-6)** under acidic condition

As for the cyclization of polymers **V-(3-4)**, oleum and the Eaton's reagents failed with the same reasons as for polymer **V-5**. The ester groups of these polymers were successfully converted to the ketones by concentrated sulfuric acid. Partially cyclized polymer [**(V-7)**, Scheme V.5] was obtained at room temperature in one day. Increasing the reaction temperature to 50 °C for overnight did not change the results, while increasing the reaction time to three days at room temperature led to the higher degree of cyclization (due to the position of the carbonyl peaks in IR spectra). The reaction temperature of 50 °C for overnight was also afforded the high degree of cyclization for polymer **V-4** to **V-8**, while room temperature was not appropriate for this conversion.

Conversion of ester groups in polymer **V-6** to ketones (**V-10**) was not successful in concentrated sulfuric acid at room temperature as well as oleum and the Eaton's

reagent. While the most favorite condition for this polymer was sulfuric acid at 50 °C overnight (Scheme V.5). The results are summarized in table V.1.

Table V.1. Cyclization of polymers **V-(3-6)** powder in different conditions

Compounds	Concentrated H_2SO_4, R.T	Concentrated H_2SO_4, 50 °C	Eaton's reagent	Oleum
V-3 → V-7	+ [a]	+ [b]	–	–
V-4 → V-8	–	+	–	–
V-5 → V-9	+	+	–	–
V-6 → V-10	–	+	–	–

[a] One day, partial cyclization
[b] Overnight, partial cyclization

Cyclization of polymer **V-5** film was tried in two different conditions in concentrated sulfuric acid. *In-situ* cyclization was the first condition tried to convert polymer **V-5** film to polymer **V-9**. Since the final applications of the cyclized polymers are to be used in devices, the ability of the polymers to form film need to be studied. Polymer **V-9** produced from the cyclization of polymer powder was not soluble in common organic solvents. Therefore, the film made from polymer **V-5** was treated using concentrated sulfuric acid. The film was prepared from the solution of polymer in THF, and it was then covered by acid. After about one hour, the brownish red film was washed with water. The infrared spectroscopy reveals that the cyclization was successful, even though the peak corresponding to the ketone groups was not very sharp. This can be due to the partially conversion of esters to ketones. It should be mentioned that, since the polymer chains become shorter after cyclization, free-standing film was obtained when sulfuric acid was washed with water.

The second condition for cyclization of polymer **V-5** film was the conversion of esters to ketones using catalytic amount of acid. The difference between this condition and cyclization of polymer powder was the amount of acid used for cyclization. As it was mentioned, the result of cyclization under the first condition was a free-standing film, while for the device application it is necessary to keep film on the substrate. The goal of this condition was to make film from the solution which contains the acid for cyclization. In this case the cyclization and film formation would have been done simultaneously to prevent the formation of free-standing film. To do so, polymer **V-5** was dissolved in THF and the catalytic amount of acid was then added. This condition failed for polymer **V-5** because the polymer precipitated out of the solution immediately after the addition of acid, making it impossible to form film.

In summary, only the cyclization of polymer powders is found to be an appropriate way to convert polymers **V-(3-6)** to polymers **V-(7-10)**. The films of cyclized polymers can then be made by vacuum deposition.

V.3.4. Hydrolysis of Ester groups in Polymer V-3

In order to confirm the ketone formation from direct cyclization of polymers **V-(3-6)** and to control the cyclization, the hydrolysis of ester groups in polymer **V-3** to the acid **V-11** was carried out. The study of structure-property relationship of the polymers (**V-3**, its corresponding cyclized polymer **V-7** and intermediate **V-11**) would prove the direct conversion. On the other hand, the conversion of ester groups to the acid will facilitate the functionalization of the polymer, thus the addition of a variety of alkyl groups and aryl moieties are designed.

The reaction was performed based on the methods reported in literature for small molecules. Polymer **V-3** was treated with NaOH (10%) at 90 °C in dimethoxyethane (DME). The reaction progress was monitored by IR spectroscopy. Once all the esters were hydrolyzed, hydrochloric acid (20%) was used to convert the salt to the acid (Scheme V.6).

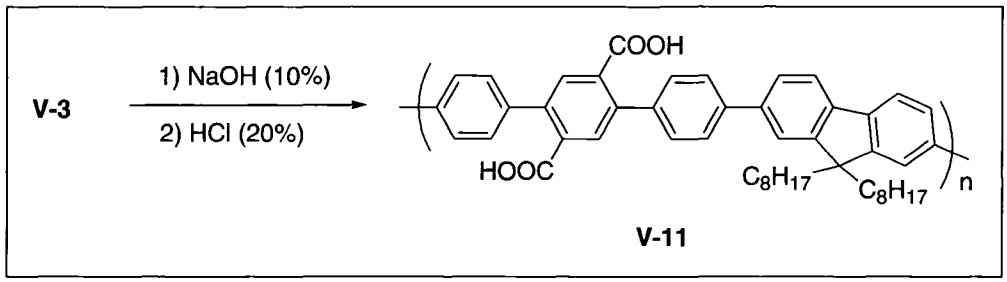

Scheme V.6. Conversion of ester groups of polymer **V-3** to the acid

It should be mentioned that, the prolonged reaction time from two days to one week and the use of an excess amount of base did not make any differences in conversion of **V-3** to **V-11**.

V.4. Characterization of Polymers

V.4.1. Infrared Spectroscopy

Infrared spectroscopy was used to distinguish between the polymers bearing ester groups **[V-(3-6)]** and their corresponding cyclized polymers **[V-(7-10)]**. The carbonyl of ester groups appears at 1750-1730 cm^{-1} while the carbonyl of ketones has a strong peak at 1725-1705 cm^{-1}. This difference can be clearly seen in the IR spectra of two series of polymers. As an example, the IR spectra of polymers **V-6** and **V-10** are displayed in Figure V.3.

In the case of polymers **V-(3-6)**, a slight difference is observed in the frequency of carbonyl peaks. This difference is due to the strength of electron donating properties of donor monomer in polymer chain. Both diphenylamine and fluorene monomers are electron donor in polymer structure but this effect is stronger for diphenylamine due to the unpaired electrons on nitrogen atoms. As a result the electron density on the phenyl ring bearing two ester groups will be increased.[10] Therefore, the peak related to the carbonyl group is shifted to the lower frequency when diphenylamine is presented as electron donor monomer [**V-4** and **V-6**].

In the case of cyclized polymers, the peaks correspond to the carbonyl groups are shifted to the lower frequencies due to the conversion of esters to the ketones. The carbonyl group of polymer **V-7** shows a broad peak at 1719 cm^{-1}, revealing that the closing step was not complete and a mixture of ester and ketone are presented in the polymer backbone. This polymer was prepared by the direct cyclization of the powder of polymer **V-3** (section V.3.3), in concentrated sulfuric acid at room temperature for one day. When the reaction time was increased to three days, the conversion completed, as evident by the shifting of the C=O peak to 1707 cm^{-1} (typical peak position for ketone, Table V.2).

As for polymer **V-8**, two different types of cyclized polymers (based on the position of C=O peaks in IR spectrum) could be obtained under different reaction conditions. When the cyclization was performed at room temperature, a partially cyclized polymer (orange in color) was the result, showing the C=O peak at 1723 cm^{-1} which reveals the mixture of two different types of carbonyl groups (ester and ketone).

Table V.2. Characteristic IR peaks for polymers

Compound	Cyclization condition[a]	Characteristic IR peaks (cm^{-1})	Comments
V-3	_____	1732 (C=O, ester)	_____
V-4	_____	1728 (C=O, ester)	_____
V-5	_____	1735 (C=O, ester)	_____
V-6	_____	1729 (C=O, ester)	_____
V-7	r.t, H_2SO_4, three day	1707 (C=O, ketone)	Completely cyclized
V-7	r.t, H_2SO_4, One day	1719 (C=O, ketone + ester)	Partially cyclized
V-8	50 °C, H_2SO_4, One day	1710 (C=O, ketone)	Completely cyclized
V-8	r.t, H_2SO_4, One day	1723 (C=O, ketone + ester)	Partially cyclized
V-9	50 °C, H_2SO_4, One day	1707 (C=O, ketone)	Completely cyclized
V-9	r.t, H_2SO_4, 5-6 h 50 °C, H_2SO_4, 1-2 h	1716 (C=O, ketone + ester)	Partially cyclized
V-10	50 °C, H_2SO_4, One day	1707 (C=O, ketone)	Completely cyclized
V-11	_____	1702 (C=O, acid)	_____

[a] Cyclization were applied on the powder of polymers **V-(3-6)**

Heating the reaction mixture at 50 °C changed the results to the higher degree of conversion of esters to the ketones (green in color) with the C=O peak of 1710 cm^{-1} (the same reason as for the **V-7**, Table V.2).

Polymer **V-9** was obtained with a partial conversion of the esters to the ketones under two different reaction conditions. The broad peak appeared at 1716 cm^{-1} when the reaction was performed at 50 °C for one hour revealing that the cyclization was not complete. While changing the reaction condition to the room temperature for 5-6 hours did not make any differences. Stirring at 50 °C overnight changed the result to the more conversion (Table V.2). The carbonyl peak was shifted towards the shorter wavenumber (1707 cm-1) but still not very sharp. It was found that the complete conversion of polymer **V-5** to **V-9** is not easy due to the rigidity of resulting polymer.

The appearance of the characteristic carbonyl stretch of the ketone moiety at 1707 cm^{-1}, indicates clearly the successful transformation of the ester to ketone functionality in polymer **V-10** (Table V.2). As an example, the IR spectra of polymers **V-6** and **V-10** are shown in Figure V.3.

It should be mentioned that the conversion of ester to ketone are estimated based on the carbonyl position in IR spectra, since this method gives the results qualitavely. The polymers bearing ester groups [**V-(3-6)**], showed the carbonyl peak near 1730 cm^{-1}, while the carbonyl peak was observed at 1710 cm^{-1} for the model compounds having the ketone groups (Chapter IV). The mixture of two different types of compounds (one having ester and the other bearing ketone) exhibited the carbonyl peak at 1721 cm^{-1}. As a conclusion, the polymers with the carbonyl peaks of below 1710 cm^{-1} are expected to bear ketone groups only. These polymers are called "cyclized polymers". Those polymers with the carbonyl peaks between 1710-1720 cm^{-1} are called "partially cyclized polymers" due to the presence of both ketone and ester in the molecular structure.

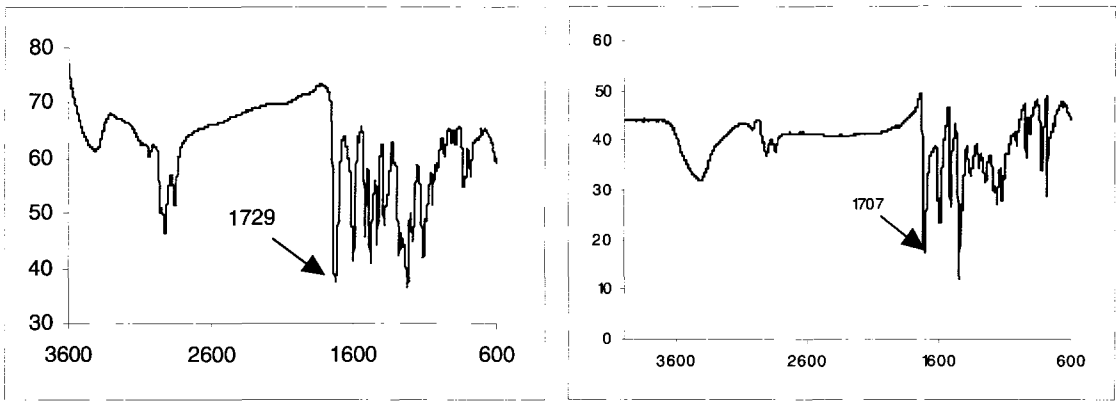

Figure V.3. IR spectra of polymers **V-6** (left) and **V-10** (right)

The structure of polymer **V-11** was confirmed by IR spectroscopy (Figure V.4). After two days reaction, the peak corresponding to the carbonyl group was completely shifted from 1729 cm^{-1} (ester) to 1702 cm^{-1}. There was some overlapping in the carbonyl peak when two polymers (**V-3** and **V-11**) were mixed together. To confirm that, if the conversion of esters to the acids are complete and the overlaps in ketone peak is not because of the unreacted esters, the reaction time was increased from two days to one week using the excess amount of base. The IR spectroscopy of salt showed the carbonyl peak shifted towards the shorter wavenumber (1659 cm^{-1}) with no overlapping with the ester peak, revealing the complete conversion of esters to the salts. When the polymer salt was acidified, the peak corresponding to the carbonyl group was shifted back to the 1702 cm^{-1}. Since it is impossible for the salt to be converted to ester after acidification, the peak at 1702 cm^{-1} must be related to the acid polymer.

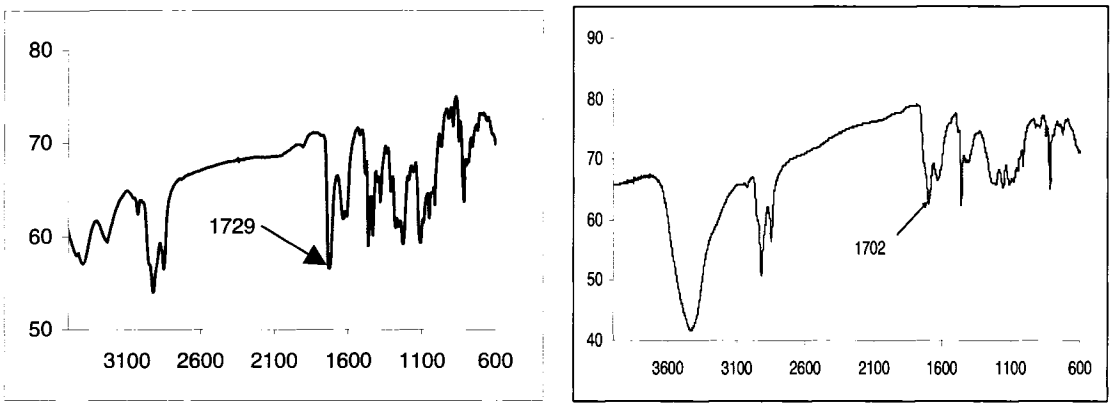

Figure V.4. The IR spectra of polymer **V-3** (left) and its corresponding acid (**V-11**) (right)

V.4.2. Nuclear Magnetic Resonance Spectroscopy

The data from all the ^{1}H NMR and ^{13}C NMR spectra of polymers **V-(3-6)** are reported in the experimental section. The ^{1}H NMR spectrum of the **V-4** is shown in Figure V.5. A singlet can be seen at 7.92 ppm for Ha. This proton is downfielded due to the presence of electron withdrawing group (C=O) on phenyl ring. Doublet at 7.69 ppm corresponds to Hb while Hc appeared at 7.63 ppm as another doublet. These two protons are also shifted to the downfield since they are close to ring bearing electron withdrawing groups. As for the Hd and He, two more doublets are observed at 7.47 ppm (Hd) and 7.17 ppm (He) respectively. The protons of methyl on ester group can be seen at 3.74 ppm while the other aliphatic protons have peaks in the range of 0.93 – 1.78 ppm.

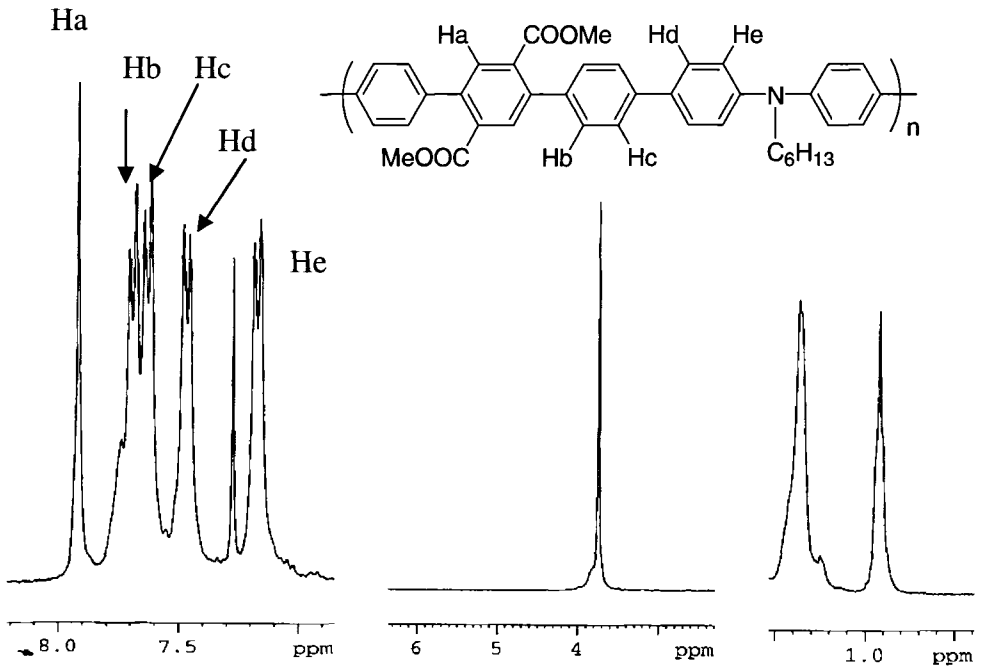

Figure V.5. The ^{1}H NMR spectrum of polymer **V-4** in $CDCl_3$

^{1}H NMR spectrum of polymer **V-5** confirms the structure of compound. A downfielded singlet peak at 7.94 ppm belongs to proton on phenyl ring bearing two ester groups. While two doublets at 7.83 ppm and 7.43 ppm as well as a singlet at 7.35 ppm related to the protons on fluorene group. Like compound **V-4**, the protons of methyl on ester groups appeared at 3.68 ppm as a singlet and the rest of aliphatic protons related to two alkyl chains can be observed at 0.81 – 1.27 ppm.

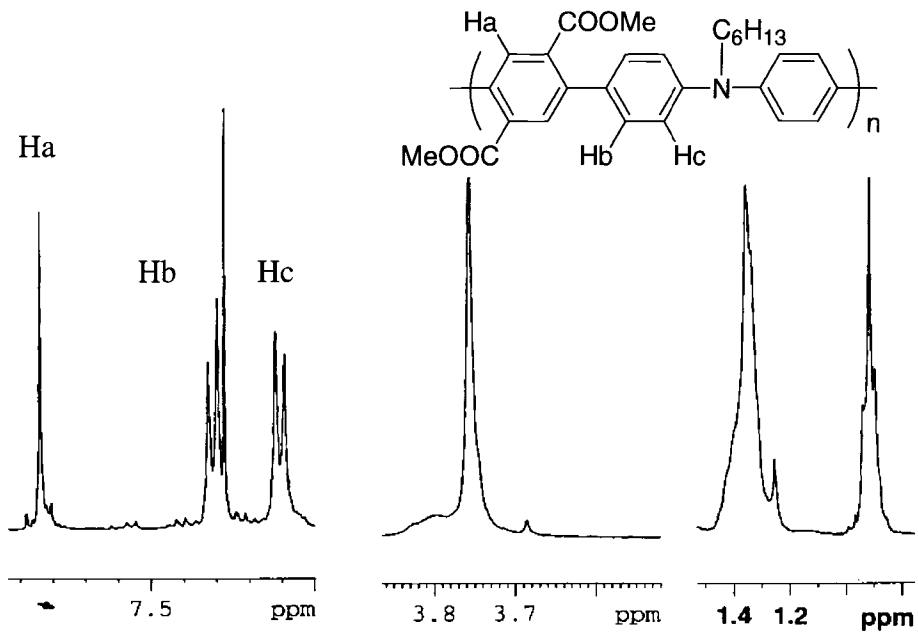

Figure V.6. The ^{1}H NMR spectrum of polymer **V-6** in $CDCl_3$

The ^{1}H NMR spectrum of polymer **V-6** is shown in Figure V.6. The same singlet at 7.84 ppm is observed for the proton connected to the phenyl ring with two ester groups (Ha). Compared to polymer **V-4**, there are only two doublets at 7.31 ppm and 7.10 ppm which belong to the Hb and Hc respectively and no changes were seen in aliphatic region.

V.4.3. Viscosity Measurment

Inherent viscosity was applied to estimate the molecular weight of polymers. This factor was measured using a solution of each polymer (0.5%) in THF at 30 °C. The results are reported in Table V.3.

Among the several factors that effect on viscosity of the polymers, the amount of catalyst and base are utmost importance. Both polymers **V-3** and **V-5** failed to have high molecular weight when 10 mol% of catalyst was used. In the case of polymer **V-3**, high

molecular weight polymer was not achieved with 0.5 mol% of catalyst, while high molecular weight was obtained for polymer **V-5** with this amount of catalyst.

Table V.3. Inherent viscosity and thermal characteristics of polymers **V-(3-10)**

Polymer	η_{inh} (dL/g)[a]	Tg (°C)[b]	T_d (°C)[c]
V-3	0.99	125	420
V-4	1.44	NA	408
V-5	0.68	99	418
V-6	0.35	120	390
V-7	NA	NA	291
V-8	NA	NA	283
V-10	NA	NA	317
V-11	NA	NA	396

[a] Inherent viscosity in THF at 30 °C (0.5 g/dL).
[b] DSC analysis under N_2 at a heating rate of 10 °C/min, fourth scan.
[c] Temperature for 5% weight loss, as assessed by TGA under N_2 at a heating rate of 20 °C/min.

The role of a base should also be addressed. It was found that the excess of base was essential to attain high molecular weight polymers. The reactivity of monomers is another important factor. The lower molecular weight of polymers **V-5** and **V-6** compared to polymers **V-3** and **V-4** is due to the steric hindrance between two ester groups of one monomer and alkyl chains of the second monomer.

The inherent viscosity could not be measured for polymers **V-(7-10)** because of their poor solubility. On the other hand, since these polymers are made from direct conversion of the corresponding ester-containing polymers, their viscosity is assumed to be the same as their parent polymers.

V.4.4. Thermal Analysis

Glass transition temperatures (T_g) of polymers **V-(3-6)** taken using differential scanning calorimetry (DSC) were in the range of 99 °C to 125 °C. The results are summarized in Table V.3. Polymers **V-3** and **V-5** are fluorene-based polymers with one (**V-5**) and three (**V-3**) extra phenyl rings in polymer segments. It was expected that due to the decreased mobility in polymer chains, the T_g of polyfluorene (75 °C) would increase by the addition of phenyl rings in polymer units. This phenomenon is clearly observed in T_g of two polymers **V-3** and **V-5**. Polymer **V-5** with one extra phenyl ring in polymer backbone (compared to polyfluorene) showed a glass transition temperature at 99 °C, while polymer **V-3** having three extra phenyl rings in polymer backbone (compared to polyfluorene) exhibited a T_g at 125 °C. Similar value of T_g was observed for polymer **V-6** (120 °C) revealing that the mobility of polymer chains in all three polymers (**V-3** and **V-(5-6)**) are similar. Polymer **V-4** did not exhibit the glass transition temperature. The DSC trace of polymer **V-6** is displayed if Figure V.7. Polymer **V-11** did not exhibit T_g, but a crystallization temperature (T_c) at 312 °C and a melting point (T_m) at 329 °C (Figure V.8). This clearly indicates that the presence of the ester units in polymers **V-(3-6)** effectively suppresses the crystallizability of the polymer chains.

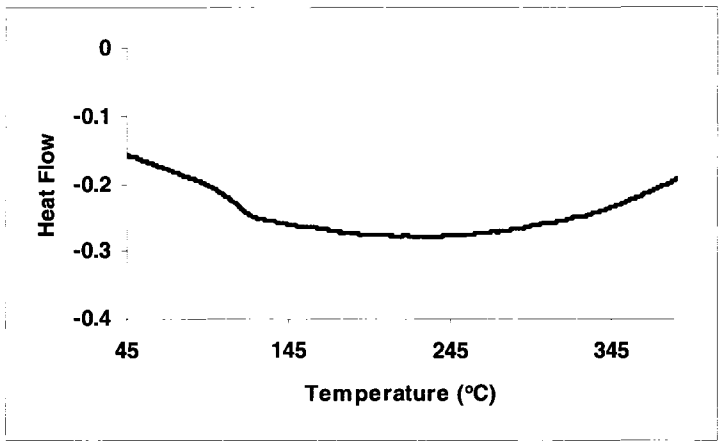

Figure V.7. DSC trace of polymer **V-6**. Third heating scan at a heating rate of 10 °C/min under nitrogen

The decomposition temperature of the polymers **V-(3-6)** as assessed by the onset temperature (T_d) of 5% weight loss by TG, occurred in the range of 390-420 °C in nitrogen (Table V.3). The polymers **V-4** and **V-6** displayed the lower T_d compared to their corresponding fluorene analogues due to the presence of nitrogen which seems to impart low tolerance to heat. The decomposition temperature was dramatically decreased for the polymers **V-(7-8)** and **V-10** revealing the thermal instability of the polymers. This indicates that the carbonyl groups have lower thermal stability in comparison with the esters. On the other hand, the conversion of ester groups in polymer **V-3** to the acid (polymer **V-11**) decreased the thermal stability of the polymer to 396 °C. The differences in thermal properties of polymers **V-3**, its corresponding cyclized polymer (**V-7**) and hydrolyzed polymer (**V-11**) confirm that the product of direct cyclization of **V-3** is not an acid.

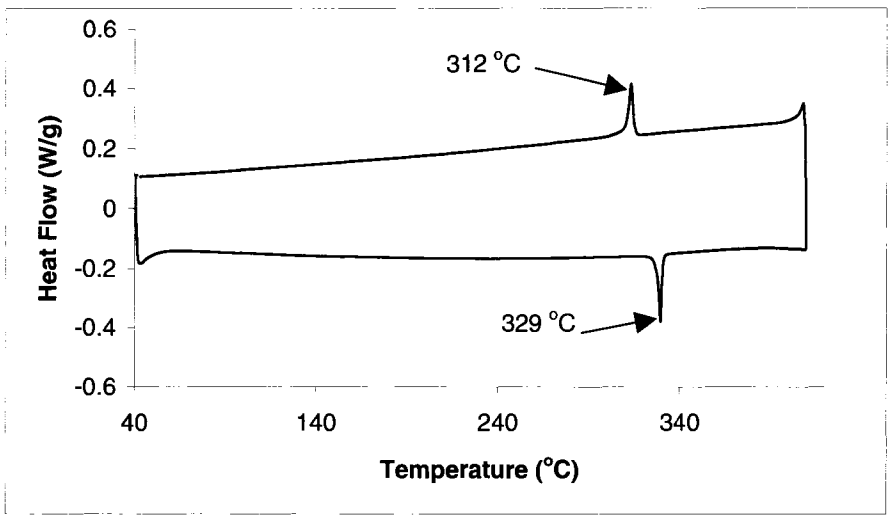

Figure V.8. DSC trace of polymer **V-11** at a heating rate of 10 °C/min

V.5. Optical and Electrochemical Properties

V.5.1. UV-Vis Absorption

The spectroscopic data of the polymers are summarized in Table V.4. In solution, the polymers **V-(3-6)** gave only one absorption peak in a range of 355-376 nm. This peak is associated with the π-π* transition mainly occurred in the monomeric units. As for the polymers **V-4** and **V-6** this peak is about 15-20 nm red shifted due to the non-bonding electrons of the nitrogen in π-system. This elevated electron density reduced the optical band gap of polymers from 3.1 eV (for polymers **V-3** and **V-5**) to 2.9 eV (for polymers **V-4** and **V-6**), confirming that the band gaps are dependent on the electron-donating properties of the donor segment. The n-π* transition in around 300 nm was also expected, although it might be hidden under the strong π-π* transition band.[11]

Table V.4. Optical properties of polymers **V-(3-10)**

Compound	λ_{abs} (nm)[a]	λ_{PL} (nm)[a]	λ_{onset}(nm)	E_g (eV)[b]
V-3	356	471	400	3.1
V-4	370	546	420	2.9
V-5	355	462	400	3.1
V-6	376	541	425	2.9
V-7	516 (355)	606	600	2.1
V-8	470 (370)	546	535	2.3
V-9	461 (353)	557 (film, 590)	510	2.4
V-10	539 (372)	537	606	2.0
V-11	358	430	395	3.1

[a] In DMF for **V-3** and **V-9**, in THF for **V-(4-8)** and **V-10**

[b] Calculated from the empirical formula, E_g (optical, eV) = $1240/\lambda_{onset}$

Polymers **V-(7-10)** showed two distinct absorption peaks (λ_{max}): one around 350-370 nm and another in a range of 460-540 nm. The former peaks are assigned to the π-π^* transition of monomer units in polymers, whereas the lower-energy peaks are mainly associated with electronic transition occurred in the main chain. The appearance of the later peaks at the longer wavelength reveals that these polymers have the expanded conjugation system. The UV-absorption of polymer **V-3** and its corresponding cyclized polymer (**V-7**) are compared in Figure V.9. Due to the increased conjugation length in polymers **V-(7-10)** compared to the polymers **V-(3-6)**, the band gap of former polymers are significantly decreased. It should be mentioned that the optical band gap of polymers are deducted from the onset of the absorption peaks.

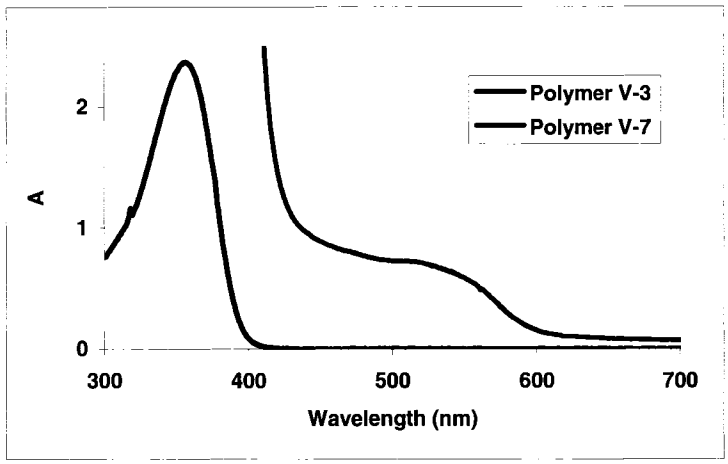

Figure V.9. UV-Vis spectra of polymers **V-3** and **V-7** in DMF solution

The UV-Vis absorption of polymer **V-11** showed the same peak (358 nm) as the corresponding ester polymer (**V-3**), revealing that the conversion of ester to carboxylic acid does not make any differences in UV-absorption.

V.5.2. Photoluminescence Properties

The photoluminescent data of the polymers are presented in table V.4. Among all, two polymers, **V-3** and **V-5,** emit light at lower wavelength, whereas the emission of polymers **V-4** and **V-6** are red shifted. This indicates that, the diphenylamine groups in polymer backbone are stronger electron donor comparing to the fluorene groups. Due to the steric hindrance in polymer **V-5** compared to the polymer **V-3** that leads to the twisting of polymer chain, a slight difference (about 10 nm of blue-shifting) is observed in PL emission.

The cyclized polymer of **V-7** shows a red shift in PL emission with the peak at 606 nm (excited at 550 nm), revealing that the conjugation length of polymer is significantly increased compared to the parent polymer **V-3** (Figure V.10). The same phenomenon is observed in polymer **V-9** which shows a yellow fluorescence with the

λ_{max} of 557 nm (when excited at 430 nm), compared to polymer **V-5**. The significant difference between the PL emission of polymers **V-7** (606 nm) and **V-9** (557 nm) is because of the twisting of polymer chain due to the rigidity as well as steric hindrance in later polymer. The PL emission of polymer **V-9** in the thin solid film is dramatically red-shifted (590 nm) compared to the solution. This indicates that, an intermolecular charge transfer mechanism takes place in well-packed film.[12]

The PL emission of polymers **V-8** and **V-10** did not change compared to the corresponding ester polymers when irradiated at 370 and 372 nm, respectively. The PL emission of these two polymers was completely quenched when excited at the longer wavelength (470 and 540 nm, respectively). This indicates that the longer alkyl chains and the orientation of them in fluorene monomer in polymers **V-7** and **V-9** prevent the quenching of PL emission at longer wavelength.

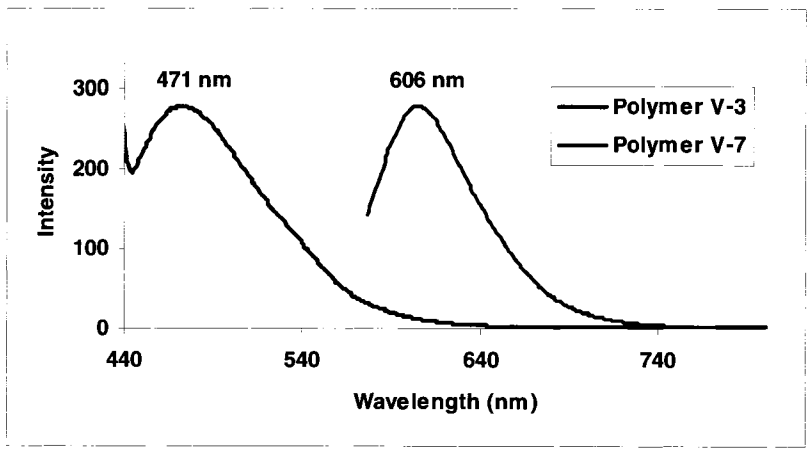

Figure V.10. Photoluminescence spectra of polymers **V-3** and **V-7**

V.5.3. Electrochemical Characteristics

The electrochemical behavior of the polymers was investigated by cyclic voltammetry (CV). The THF solution consisting 0.1 molar tetrabutylammonium

hexafluorophosphate was used as electrolyte. For polymers **V-3** and **V-5** no p-doping (oxidation) and n-doping (reduction) peaks were observed, while the onset potential of oxidation process appeared at 0.77 V vs Ag^+/Ag for **V-4** and 0.93 V for **V-6** (Table V.5). This p-doping is considered to occur mainly at the donor unit[13]. In reductive potential region, no n-doping peak was observed for the polymers, revealing that, the reduction states of the polymers are not stable (Figure V.11). The onset potential of reduction was calculated using the optical band gap minus the onset of oxidation potential, assuming that the interface barrier for charge injection in the electrochemical process is minimized.

Table V.5. Electrochemical properties of polymers **V-4** and **V-6**

Compound	E_{ox} (V)[a]	E_{red} (V)[b]	HOMO (eV)[c]	LUMO (eV)[c]	E_g (eV)[d]
V-4	0.77	-2.13	5.17	2.27	2.9
V-6	0.93	-1.97	5.33	2.43	2.9

[a] E_{ox} is the onset potential of oxidation
[b] E_{red} is calculated from $E_{g\,(opt)} - E_{ox}$
[c] Calculated from empirical formula, $E_{(HOMO)} = -(E_{ox} + 4.40)$ (eV), $E_{(LUMO)} = -(E_{red} + 4.40)$ (eV)
[d] Optical band gap

The highest occupied molecular orbital (HOMO) and lowest unoccupied molecular orbital (LUMO) levels of the polymers were estimated by the empirical formula [$(E_{(HOMO)} = -(E_{ox} + 4.40)$, $E_{(LUMO)} = -(E_{red} + 4.40)$].[14] The high LUMO levels and low HOMO values indicate that the polymers are not highly conjugated.

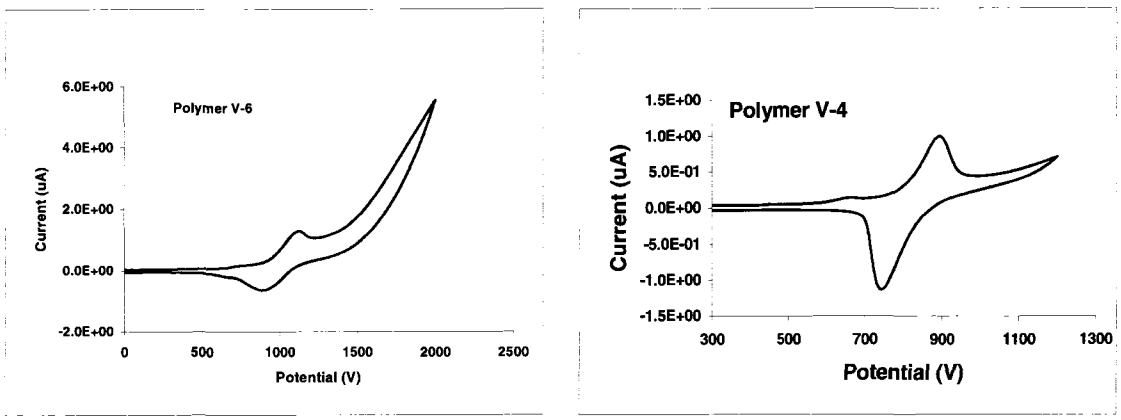

Figure V.11. Cyclic voltammogram of polymers **V-4** and **V-6**

V.6. Conclusion

The design and synthesis of a new series of D-A type polymers, **V-(3-6),** was successfully performed through the Suzuki coupling reaction. Cyclization of these polymers in concentrated sulfuric acid created the second series of polymers, **V-(7-10),** while the hydrolysis of polymer **V-3** afforded polymer **V-11.**

The thermal stability of the polymers was measured by TGA and DSC. The glass transition temperature of polymer **V-3** was higher than the one of polymer **V-5** revealing the higher flexibility in polymer chain of **V-5.** Decomposition temperature of polymers **V-(3-6)** reveals the high thermal stability while polymers **V-(7-8)** and **V-10** showed the relatively lower stability against heat. The differences in thermal properties of polymers **V-3, V-7** and **V-11** confirmed the success of direct cyclization of polymer **V-3.**

Absorption and photoluminescence of polymers **V-(7-10)** were red shifted due to the enhanced conjugation length. As well, these polymers showed lower band gaps compared to the corresponding esters-containing polymers **[V-(3-6)].**

V.7. Experimental Section

Materials and Measurments

All starting materials [such as 4,4′-dibromodiphenylamine and monomer 9,9-dioctylfluorene-2,7-bis(trimethyleneborate] and reagents were purchased from Aldrich Canada Inc. unless otherwise stated. Dimethyl 2,5-bis(4-bromophenyl)terephthalate was synthesized by the procedure described in Chapter IV, and dimethyl 2,5-dibromoterephthalate was prepared as explained in Chapter II. All reagents were used as received without further purification. The same instruments were used as mentioned in Chapter IV (materials and measurements) to measure the IR, ^{1}H NMR and ^{13}C NMR, melting points, UV absorption and photoluminescence of the products. Decomposition temperature of the polymers were measured on Thermogravimetric Analyzer (TGA) on TGA 2950 CE Instrument at a heating rate of 20 °C/min, while the viscosity of polymers were measured by a Gallenkamp viscometer.

Synthesis of N-hexyl-4,4′-dibromodiphenylamine (V-1)

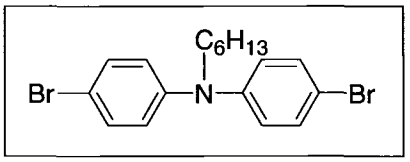

In a two-necked flask, 4,4′-dibromodiphenylamine (20.0 g, 61.2 mmol) and potassium *tert*-butoxide (10.0 g, 89.1 mmol) were placed and 360 mL of dry THF was added. After stirring for one hour at room temperature under argon atmosphere, 1-bromohexane (13.2 g, 80 mL) was added to solution and it was stirred for 24 hours at 60 °C. The progress of reaction was monitored by TLC. The reaction mixture was then cooled down to room temperature, poured in water and extracted with chloroform. The

combined organic layers were washed with water for few times, dried over $MgSO_4$ and the solvent was evaporated. The crude product was purified by column chromatography (silica, hexane/chloroform = 2:1, v/v) to give 24.1 g (96%). ^1H NMR ($CDCl_3$, 400 MHz) δ_H 7.33 (d, 4H, J=6.0 Hz), 6.80 (d, 4H, J=6.0 Hz), 3.60 (t, 2H, J=15.0 Hz), 1.60 (m, 2H), 1.32-1.27 (m, 6H), 0.87 (t, 3H). ^{13}C NMR ($CDCl_3$, 100 MHz) 146.74, 132.26, 122.56, 113.84, 52.45, 31.58, 27.21, 26.69, 22.63, 14.01.

Synthesis of 4,4′-bis(4,4,5,5-tetramethyl-1,3,2-dioxaborolane-2-yl)- N-hexyldiphenylamine (V-2)

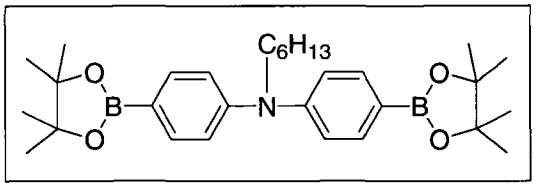

In a flame-dried, round-bottomed flask, N-hexyl-4,4′-dibromodiphenylamine (2.500 g, 6.1 mmol) was place and protected from humidity by argon. Dry THF (50 mL) was added via syringe and the mixture was cool down to –78 °C. To this reaction mixture, butyllithium (7 mL, 2.5 M in hexane) was added dropwise while the flask was under argon atmosphere all the time. After the mixture was stirred for 2 hours at –78 °C, 2-isopropoxy-4,4,5,5-tetramethyl-1,3,2-dioxaborolane (5.500 g, 29.5 mmol) was added to the solution, and the mixture was warmed up to room temperature and stirred overnight. The resulting milky yellowish mixture was poured in water, extracted with ether three times and then dried over $MgSO_4$. All the solvent was evaporated and the crude light yellow solid was recrystallized from hexane to provide the final product as bluish-white crystals (1.400 g, 45.6%). Mp: 164-166 °C; ^1H NMR ($CDCl_3$, 400 MHz) δ_H 7.72 (d, 4H,

J=6.0 Hz), 7.03 (d, 4H, J=9.0 Hz), 3.75 (t, 2H, J=15.0 Hz), 1.60 (m, 2H), 1.32 (s, 24H), 1.24 (m, 6H), 0.86 (t, 3H).

General Procedure for Polymerization

In a 25 mL, two-necked round-bottomed flask equipped with a condenser and an argon purge line, dibrominated monomer (1.0 mmol), diboronic acid monomer (1.0 mmol) and terakis(triphenylphosphine)palladium(0) (0.5 mol%, with the exception for polymer **V-3** which the amount of catalyst was 0.4 mol%) were placed and stirred under argon for few minutes. To this mixture, degassed toluene (20% of concentration) was added and the mixture was purged with argon for another 10 min, then heated slowly to 90-100 ^{o}C to dissolve all the starting materials. A solution of sodium carbonate (7.0 mmol in 1.5 mL of water) was then added followed by the addition of 2-3 drops of aliqute 336. The reaction mixture was heated at the same temperature for 24 hours while the light yellow solution turned to light green and viscous mixture. To terminate the reaction, phenyl boronic acid (10 mol %) was added as the first end-capping reagent and heating was continued at the same temperature for 5 more hours. Bromobenzene (10 mol %) was the second end-capping reagent added at the end and heating was continued for another 4 hours and stopped. After letting it cool, it was precipitated in methanol, filtered and dried.

Polymer V-3: Starting with 0.504 g (1.0 mmol) of dimethyl 2,5-bis(4-bromophenyl)terephthalate, 0.558 g (1.0 mmol) 9,9-dioctylfluorene-2,7-bis(trimethyleneborate) and 4.770 mg (0.4 mol%) catalyst, the polymer was prepared in

the presence of 0.739 g base in 4.2 mL solvent following the procedure outlined above. An off-white precipitate was obtained: 0.830 g; IR (KBr, cm^{-1}): 2925-2852 (C-H, aromatic and aliphatic), 1732 (C=O, ester), 1606 (C=C); ^1H NMR ($CDCl_3$, 400 MHz): δ_H 7.98 (s, 2H), 7.88-7.81 (m, 4H), 7.70 (s, 2H), 7.61-7.54 (m, 4H), 3.81 (s, 6H), 2.21-1.16 (m, 28H), 0.85 (t, 6H); ^{13}C NMR ($CDCl_3$, 100 MHz): δ_C 168.29, 151.82, 140.99, 140.28, 139.47, 133.13, 132.28, 128.88, 127.04, 126.09, 125.55, 121.50, 120.15, 77.47, 77.04, 76.62, 55.39, 52.46, 40.56, 31.82, 30.34, 30.09, 29.28, 23.91, 22.64, 14.12, 1.05.

Polymer V-4: The polymer was synthesized using the same procedure as outlined above but starting with dimethyl 2,5-bis(4-bromophenyl)terephthalate (0.504 g, 1.0 mmol), **V-2** (0.505 g, 1.0 mmol) and catalyst (0.5 mol%). The lime-green product was 0.612 g; IR (KBr, cm^{-1}): 3020-2851 (C-H, aromatic and aliphatic), 1724 (C=O, ester), 1604 (C=C); ^1H NMR ($CDCl_3$, 400 MHz): δ_H 7.91 (s, 2H), 7.69 (d, 2H, J=9.0 Hz), 7.63 (d, 2H, J=9.0 Hz), 7.47 (d, 2H, J=9.0 Hz), 7.17 (d, 2H, J=9.0 Hz), 3.74 (s, 6H), 1.79-1.64 (m, 10H), 1.37 (t, 3H); ^{13}C NMR ($CDCl_3$, 100 MHz): δ_C 168.50, 147.35, 140.72, 140.09, 138.09, 133.17, 132.08, 128.79, 127.87, 127.42, 126.95, 126.34, 121.15, 77.43, 77.01, 76.59, 52.34, 31.68, 26.81, 22.71, 14.07.

Polymer V-5: Starting with 0.352 g (1.0 mmol) of dimethyl 2,5-dibromoterephthalate, 0.575 g (1.0 mmol, 97% pure) of 9,9-dioctylfluorene-2,7-bis(trimethyleneborate) and 5.680 mg (0.5 mol%) of catalyst the light green polymer was obtained (0.600 g). IR (KBr, cm^{-1}): 2926-2852 (C-H, aromatic and aliphatic), 1735 (C=O, ester), 1604 (C=C);

^{1}H NMR ($CDCl_3$, 400 MHz): δ_H 7.94 (s, 2H), 7.84 (d, 2H, J=9.0 Hz), 7.44 (d, 2H, J=9.0 Hz), 7.35 (s, 2H), 3.68 (s, 6H), 2.02-1.13 (m, 28H), 0.85 (t, 6H).

Polymer V-6: The polymer was synthesized using the same procedure as outlined above but starting with dimethyl 2,5-dibromoterephthalate (0.352 g, 1.0 mmol), **V-2** (0.505 g, 1.0 mmol) and catalyst (0.5 mol%). The yellow product was 0.445 g; IR (KBr, cm^{-1}): 3032-2853 (C-H, aromatic and aliphatic), 1729 (C=O, ester), 1600 (C=C); ^{1}H NMR ($CDCl_3$, 400 MHz): δ_H 7.81 (s, 2H), 7.31 (d, 2H, J=9.0 Hz), 7.10 (d, 2HJ=9.0 Hz), 3.76 (s, 6H), 1.75-1.26 (m, 10H), 0.92 (t, 3H).

General Procedure for Cyclization

In a small test tube, the polymers **V-(3-6)** were placed and concentrated sulfuric acid was added and stirred over a period of time. The reaction time and temperature was different for the polymers. It was then poured into cold water, filtered and dried at 60 °C under vacuum.

Polymer V-7: Stirring at room temperature or 50 °C for over night resulted the partially cyclized polymer with the C=O peak at 1719 cm^{-1}. Higher degree of cyclization took place when the polymer **V-3** was stirred at room temperature for three days; IR (KBr, cm^{-1}): 1707 (C=O, ketone).

Polymer V-8: This polymer was obtained when the polymer **V-4** was stirred at 50 °C for over night; IR (KBr, cm^{-1}): 1710 (C=O, ketone). While stirring at room temperature for over night gave the partially closed polymer of **V-8** with the C=O peak at 1723 cm^{-1}.

Polymer V-9: Partially cyclized polymer was obtained **V-5** was stirred at room temperature for 6 hours or at 50 °C for 2 hours; IR (KBr, cm^{-1}): 1716 (C=O, ester and ketone). More ester groups in polymer **V-5** were converted to the ketones when stirred in concentrated H_2SO_4 at 50 °C for overnight; IR (KBr, cm^{-1}): 1707 (C=O, ketone).

Polymer V-10: This polymer was obtained with high degree of cyclization after the stirring at 50 °C for over night; IR (KBr, cm^{-1}): 1707 (C=O, ketone).

Synthesis of Polymer V-11 by Hydrolysis of Polymer V-3

Polymer **V-3** (0.150 g) was dissolved in dimethoxyethane (DME, 30 mL) and heated up to the 85 °C. A solution of NaOH (10%, 6 mL) was then added and the reaction mixture was stirred at the same temperature for 48 hours. The progress of the reaction was monitored by IR spectroscopy. When all the ester groups were converted to the sodium salt, the reaction was stopped, cooled down to the room temperature and poured in HCl (20%). The yellow solid was filtered, washed with water and dried over P_2O_5; Mp: 329 °C (DSC); IR (KBr): 1702 cm^{-1} (C=O, ketone of acid).

References

1. Gong, X.; Moses, D.; Heeger, A. J.; Xiao, S. *J. Phys. Chem.* **2004**, *108*, 8601.

2. Bliznyuk, V. N.; Carter, S. A.; Scott, J. C.; Klarner, C.; Miller, R. D.; Miller, D. C. *Macromolecules* **1999**, *32*, 361.

3. Gaal, M.; List, E. J. W.; Scherf, U. *Macromolecules* **2003**, *36*, 4236.

4. List, E. J. W.; Guentner, R.; de Freitas, P. S.; Scherf, U. *Adv. Mater.* **2002**, *14*, 374.

5. Uckert, F.; Tak, Y. H.; Mullen, K.; Bassler, H. *Adv. Mater.* **2000**, *12*, 905.

6. Wu, C.; Shan, J. *US Pat.* 6376590 B1, **2002**.

7. Yasuda, T.; Imase, T.; Yamamoto, T. *Macromolecules* **2005**, *38*, 7378.

8. Setayesh, S.; Marsitzky, D.; Mullen, K. *Macromolecules* **2000**, *33*, 2016.

9. Yang, X.; Yang, W.; Yuan, M.; Hou, Q.; Huang, J.; Zeng, X.; Cao, Y. *Synth. Met.* **2003**, *135*, 189.

10. Pavia, D. L.; Lampman, G. M.; Kriz, G. S. *Introduction to spectroscopy*. Third edition. Harcourt College Publishers, **2001.**

11. Justin Thomas, K. R.; Lin, J. T.; Velusamy, M.; Tao, Y. T.; Chuen, C. H. *Adv. Funct. Mater.* **2004**, *14*, 83.

12. Yang, R.; Tian, R.; Yan, J.; Zhang, Y.; Yang, J.; Hou, Q.; Yang, W.; Zhang, C.; Cao, Y. *Macromolecules* **2005**, *38*, 244.

13. Kitamura, C.; Tanaka, S.; Yamashita, Y. *Chem. Mater.* **1996**, *8*, 570.

14. de Leeuw, D. M.; Simenon, M. M. J.; Brown, A. R.; Einerhand, R. E. F. *Synth. Met.* **1997**, *87*, 53.